DISSERTATION

SEX DIFFERENCES IN CORTICAL-HYPOTHALAMIC CONTROL OF STRESS REACTIVITY AND CARDIOVASCULAR SUSCEPTIBILITY

Submitted by

Derek Schaeuble

Department of Biomedical Sciences

In partial fulfillment of the requirements

For the Degree of Doctor of Philosophy

Colorado State University

Fort Collins, Colorado

Spring 2023

Doctoral Committee:

Advisor: Brent Myers

Adam Chicco
Chris Gentile
Stu Tobet

ABSTRACT

SEX DIFFERENCES IN CORTICAL-HYPOTHALAMIC CONTROL OF STRESS REACTIVITY AND CARDIOVASCULAR SUSCEPTIBILITY

Major depressive disorder (MDD) is characterized by prolonged sadness and a loss of interest, and it impacts an estimated 21 million adults in the United States. The onset of MDD is multifactorial and rates of MDD have increased due to the psychosocial and economic factors associated COVID-19 pandemic. This poses a substantial threat to population health as MDD is projected to be the leading cause of disability by 2030. Even throughout the pandemic, cardiovascular disease (CVD) is still the highest mortality rate of any disease worldwide average of 17.9 million deaths per year. More importantly, MDD and CVD have devastating comorbidity that is poorly understood. MDD doubles the risk of developing cardiovascular disease and significantly increases the chance of morbidity following cardiovascular events. Thus, we need to address mental health disabilities and cardiovascular disease susceptibility. Interestingly, both diseases are exacerbated by chronic life stressors, which increase the prevalence of mood disorders and can alter sympathetic nervous activity increasing heart rate and blood pressure. Studying how stress affects the brain may yield important information on how to treat these two diseases.

In this series of experiments, I examine how the ventral medial prefrontal cortex (vmPFC) alters stress responding through its downstream connections to provide a mechanism for MDD and cardiovascular disease comorbidity. I will provide a brief background of the structure and function of the vmPFC and describe how neurons from this region can alter stress responding through synapses in the hypothalamus. Chapter 2 is the first of a series of experiments where I show decreased activity of the vmPFC interacts with chronic stress to predispose male rats to cardiovascular disease susceptibility. Because mood disorders are

more common in women and cardiovascular disease is more prevalent in post-menopausal women compared to men, chapter 3 examines whether activating vmPFC projection neurons is sufficient to influence behavior, stress responding, and cardiovascular activity in both sexes of rats. This work uncovered that output of vmPFC glutamate neurons has sexually divergent outcomes on neuroendocrine and autonomic cardiovascular responses to stress. Furthermore, it became evident that altered vmPFC activity predisposes males but not females to cardiovascular disease susceptibility. The vmPFC does not directly project to autonomic or neuroendocrine effector regions, so chapter 4 investigates whether the vmPFC is sufficient to control stress autonomic and neuroendocrine responding through downstream intermediary synapses. The intermediate region of interest is the posterior hypothalamus (PH) which can regulate endocrine and cardiovascular activity and receives dense innervation from the vmPFC. In chapter 5, I am exploring the necessity of this vmPFC-PH circuit to regulate cardiovascular activity and stress reactivity following chronic stress exposure. Altogether these data identify novel neurocircuitry linking stress exposure to cardiovascular disease risk.

ACKNOWLEDGEMENTS

Brent Myers: Thank you for being an excellent mentor and even better person. I truly admire how you run the lab and how you value everyone's health and happiness. You are always there to offer advice with all work or life-related issues no matter what was going on in your life. Your success not only comes from your intelligence and work ethic, but also because treat people like how you want to be treated.

Mom, Dad, Marty: I appreciate your support over the last 5+years of graduate school. Even though it may have been unclear of what I did day-to-day, you were all supporting regardless!

Bob and Iris Handa: Thank you both so much for providing me opportunity to pursue and succeed in research. You are both greatly missed.

Stu Tobet, Adam Chicco, and Chris Gentile: I couldn't have had a better committee! All three of you were very supportive in my research and were vital in helping me get my predoctoral fellowship funded and I cannot thank you enough for that.

Sebastian and Tyler: You have both been awesome co-workers throughout graduate school. I'm not sure how we all made it through the first few years of learning surgeries and behavior but we managed! I wish both of you success in whatever awaits!

Brandy Bratwurst: Acquiring a German Shepard was not one of my goals in graduate school but having you around made my life so much better.

TABLE OF CONTENTS

CHAPTER 1: INTRODUCTION[1]

Overview

The prevalence and severity of cardiovascular disease is exacerbated by chronic stress exposure. While stress-induced sympathetic predominance and elevated glucocorticoid secretion impair cardiovascular health, the mechanisms by which stress-responsive brain regions integrate autonomic and endocrine stress responses remains unclear. This review covers emerging literature on how specific cortical and hypothalamic nuclei regulate cardiovascular and neuroendocrine stress responses. We will also discuss the current understanding of the cellular and circuit mechanisms mediating physiological stress responses. Altogether, the reviewed literature highlights the current state of stress integration research, as well as unanswered questions about the brain basis of cardiovascular disease risk.

Introduction

Cardiovascular disease (CVD) is the leading cause of death worldwide. Although diet, exercise, and other lifestyle risk factors have been extensively characterized, less focus has been placed on the effects of prolonged mental stress to increase CVD morbidity and mortality (Barefoot et al., 1996; Chida & Steptoe, 2010). Notably, CVD risk more than doubles with chronic stress exposure (Steptoe & Kivimäki, 2012; Yusuf et al., 2004); yet, neurobiological mechanisms linking stress and cardiovascular health outcomes are only partially understood. However, recent methodological advances have enhanced the ability to specifically interrogate stress-responsive neurocircuitry and subsequent regulation of cardiovascular physiology.

[1] Funding: This work was supported by AHA Predoctoral Fellowship 827519 to DS and NIH R01 HL150559 to BM.
Author Contributions: Both authors contributed to the conceptualization of the review. Derek Schaeuble performed the initial literature search, wrote the first draft of the manuscript, and created the illustration in BioRender. Brent Myers contributed additional literature and revised the manuscript. Both authors approved the submitted version.

The physiological stress response is a conserved biological mechanism that promotes survival and adaptation in the presence of potential threats to homeostasis. In response to stressors, the brain activates both autonomic and endocrine output to mobilize energy resources (Myers et al., 2014). The immediate response is generated by the autonomic nervous system, composed of the sympathetic and parasympathetic branches. The sympathetic nervous system is governed by descending cortical and forebrain circuits that regulate the activity of pre-sympathetic neurons in the hypothalamus and brainstem which communicate with spinal pre-ganglionic sympathetic neurons (Ulrich-Lai & Herman, 2009). Postganglionic sympathetic neurons then promote fight-or-flight responses including elevations of epinephrine, glucose, heart rate, and blood pressure. The parasympathetic branch is regulated by descending cortical and forebrain innervation of brainstem pre-ganglionic nuclei which typically withdraw activity in response to stress. On a slower timescale, the neuroendocrine hypothalamic-pituitary-adrenocortical (HPA) axis is activated by paraventricular hypothalamic corticotropin releasing hormone (CRH) (Herman et al., 2016). CRH is secreted in the anterior pituitary gland and stimulates the release of adrenocorticotropic hormone (ACTH). Systemic ACTH then acts on the adrenal cortex to stimulate synthesis and release of glucocorticoids. Glucocorticoids (cortisol in humans and corticosterone in rodents) act throughout the body via glucocorticoid receptors (GR) and mineralocorticoid receptors (MR) (de Kloet et al., 2005). Importantly, corticolimbic circuits appraise context and prior experience to regulate autonomic activity, hormone secretion, and feedback through GR and MR signaling(Myers et al., 2012).

Although autonomic and endocrine stress responses are necessary for survival, exposure to traumatic or chronic stress can lead to autonomic imbalance, impaired negative feedback of the HPA axis, and illness(Herman et al., 2003; McEwen & Stellar, 1993). While the autonomic nervous system and HPA axis act through different mechanisms, central integration of both systems is necessary for appropriate physiological control. There is a limited collection of forebrain and brainstem structures that provide monosynaptic input to both autonomic

preganglionic neurons and HPA axis neurosecretory cells (Ulrich-Lai & Herman, 2009). In addition to the paraventricular hypothalamus (PVN), which houses both pre-autonomic and secretory cells (L. W. Swanson & Sawchenko, 1983), subsets of neurons in the bed nuclei of the stria terminalis, hypothalamus, and hindbrain (ventrolateral medulla and nucleus of the solitary tract) regulate neuroendocrine and autonomic outflow. Importantly, this stress regulation is modulated by descending corticolimbic inputs (Herman et al., 2003; Myers, 2017). The hierarchy of cortical inputs to subcortical regions that innervate stress effector cells is fundamental to translating cognitive and emotional processes into physiological activity. Accordingly, this review will focus on the rodent cortical-hypothalamic neurocircuitry that integrates neuroendocrine and autonomic activity. This review specifically focuses on stress-regulatory cortical regions and their targets in the hypothalamus. Although the brainstem has a pivotal role in stress integration, this topic has been reviewed elsewhere (Chaves et al., 2021; Herman et al., 2016; Lamotte et al., 2021; Maniscalco et al., 2017; Rinaman, 2011; Ulrich-Lai & Herman, 2009).

The current review focuses on the rodent prefrontal cortex, including a specific population of cells in the infralimbic cortex (IL) that is necessary for cardiovascular and endocrine responses to chronic stress. We also discuss the importance of prelimbic prefrontal cortex (PL) and highlight insular cortex effects on cardiovascular activity. Additionally, we discuss how these cortical regions may target the hypothalamus to trans-synaptically regulate autonomic and neuroendocrine effectors. The specific hypothalamic nuclei examined include the lateral hypothalamus (LH), dorsal medial hypothalamus (DMH), and posterior hypothalamus (PH), all of which innervate the paraventricular nucleus of the hypothalamus and regulate cardiovascular reactivity.

Cortical Stress Regulation

Medial Prefrontal Cortex

The medial prefrontal cortex (mPFC) is important for translating stress appraisal into adaptive behavioral and physiological responses through descending multi-synaptic circuits that target autonomic and HPA axis effectors. The mPFC is divided into dorsal and ventral subdivisions which have contrasting roles in acute and chronic stress reactivity (Jessica M. McKlveen et al., 2013; Radley et al., 2006). Dorsal mPFC, PL in rodents, inhibits heart rate reactivity to acute stress (Tavares et al., 2009). Additionally, PL disinhibition reduces HPA axis reactivity to acute psychological stressors (restraint), while enhancing responses to physiological stressors (hypoxia) (Jones et al., 2011). Further, GR signaling in the PL is necessary to inhibit corticosterone reactivity to acute restraint but not chronic variable stress (McKlveen et al., 2013). Although the circuitry underlying PL effects on the cardiovascular system has not been directly queried, the HPA axis regulatory effects are mediated by synaptic relays in the bed nuclei of the stria terminalis (Johnson et al., 2019; Radley et al., 2009). Ultimately, these data suggest that the PL limits cardiovascular and HPA axis responses to acute psychological stressors with little evidence for involvement in chronic stress integration.

Subregions of human ventral mPFC exhibit altered activity in mood disorders (Drevets et al., 1997, 2008) and have been targeted for deep brain stimulation in treatment-resistant depression (Mayberg et al., 2005). Further, growing evidence supports a role for rodent ventral mPFC (IL) in cardiovascular and HPA axis regulation during chronic stress. Anatomically, the IL is largely composed of pyramidal glutamate neurons with a smaller population of GABAergic interneurons that regulate local activity (J. M. McKlveen et al., 2015; Jessica M. McKlveen et al., 2019). Principal IL glutamate neurons have unique connectivity compared to other cortical regions and innervate stress-regulatory structures throughout the amygdala, hypothalamus, and brainstem (Vertes, 2004). Further, chronic stress exposure shifts IL excitatory/inhibitory balance toward increased inhibition (Ghosal et al., 2020; Gilabert-Juan et al., 2013; Nawreen et al., 2020).

Initial studies of IL effects on cardiovascular stress reactivity found that non-specific synaptic blockers attenuate heart rate and blood pressure responses to acute restraint and fear conditioning (Resstel et al., 2006; Tavares et al., 2009). In contrast, IL NMDA activation reduces cardiovascular responses to air-jet stress (Camargos et al., 2012). Additionally, IL lesions increase stress-induced PVN activation, especially in pre-autonomic cells (Radley et al., 2006). Taken together, these studies identify the importance of the IL for physiological stress responses but yield contrasting results on whether the region increases or decreases stress responding. The contradictory results may relate to a lack of cellular specificity with lesion, pharmacology, and synaptic blockade approaches. Subsequent studies employed viral-mediated gene transfer to specifically target glutamate release from pyramidal cells. Here, genetic knockdown of IL glutamate release increases tachycardic and pressor responses to acute restraint and elevates homecage arterial and pulse pressures during chronic variable stress (Schaeuble et al., 2019). Furthermore, decreased IL output during chronic stress increases vascular endothelial dysfunction, as well as histological indictors of cardiac and vascular hypertrophy. In terms of neuroendocrine regulation, IL glutamate knockdown increases HPA axis reactivity to acute restraint and exacerbates the effects of chronic stress on basal and stress-induced glucocorticoid hypersecretion (Myers et al., 2017). Altogether, these studies indicate that decreased IL glutamate release interacts with chronic stress to increase stress responding and promote susceptibility to cardiovascular pathologies.

Recent experiments utilizing optogenetic approaches to stimulate IL glutamate neurons in male and female rats revealed that activation of male IL pyramidal neurons restrains tachycardic and pressor reactivity to novel environment stress, as well as corticosterone and glucose responses to restraint (Wallace et al., 2021). Intriguingly, IL stimulation prior to chronic variable stress has protective effects on stress-induced ventricular remodeling. While the mechanisms underlying protection from subsequent stress exposure are unclear, prior IL stimulation decreases net cardiac sympathetic drive. These effects may be explained by the persistent

dendritic plasticity induced by optogenetic stimulation of IL glutamate neurons (Fuchikami et al., 2015). Although investigations of sex differences in cortical stress regulation are limited (Wallace & Myers, 2021), results from female IL glutamate neuron stimulation differ from males. In fact, female IL stimulation increases heart rate reactivity to novel environment and glucose responses to restraint. Collectively, these data indicate that IL glutamate neurons regulate cardiovascular and HPA axis responses to chronic stress in a sex-dependent manner. To investigate how IL output circuitry mediates autonomic-endocrine integration, IL presynaptic innervation and functional connectivity was quantified throughout the male forebrain (Wood et al., 2019). These data highlight IL inputs to key stress-integrative nuclei including the LH and DMH; however, significantly greater connectivity is evident in the PH. To date, the stress-regulatory effects of IL projections to specific hypothalamic nuclei have not been determined.

Insular Cortex

Human imaging studies reveal that insular cortex shifts autonomic activity, possibly leading to arrhythmias (S. Oppenheimer & Cechetto, 2016). Furthermore, both human and rodent studies include the insula in the central autonomic network(Clifford B. Saper, 1982; Shoemaker & Goswami, 2015). From rostral to caudal, insular cortex is divided into the anterior insula (AI), posterior insula (PI), and an overlapping intermediate insula. Additionally, dorsal to ventral differences in cytoarchitecture lead to disgranular, granular, and agranular subdivisions (Gogolla, 2017). Although the insula has widespread limbic and visceral connectivity, the anatomical size and complexity has limited research on insular stress regulation. However, numerous studies have investigated the effects of insular stimulation on cardiovascular parameters, identifying effects of both AI and PI (Allen et al., 1991; S. M. Oppenheimer et al., 1991; Yasui et al., 1991). Specifically, electrical stimulation elicits tachycardia and modest arterial pressure increases in anesthetized rats (Ruggiero et al., 1987). Further experiments stimulating multiple insular regions to pinpoint the origin of cardiac regulation found two distinct

regions of the rostral PI produce tachycardia and bradycardia (S. M. Oppenheimer & Cechetto, 1990). Systemic muscarinic and adrenergic antagonists indicate that insular chronotropic effects are mediated by either elevated (tachycardia) or decreased (bradycardia) sympathetic activity. This interpretation is further supported by recent findings that activation of rostral PI NMDA receptors inhibits brainstem pre-sympathetic regions causing bradycardia (Marins et al., 2016).

The results of functional studies align with monosynaptic anterograde tracing that indicates tachycardia-generating portions of the insula send efferents to pre-sympathetic regions including the LH, nucleus of the solitary tract, and parabrachial nucleus (Yasui et al., 1991). Efferents from bradycardic insular cortex have similar projection targets; although, connectivity with the pre-sympathetic regions is less dense. While anterograde tracing indicates that the LH is the primary hypothalamic target of insular cortex, retrograde tracing has identified projections to the DMH and PH (Abrahamson & Moore, 2001; Çavdar et al., 2001; Marins et al., 2020, 2021). In fact, recent reports specify that hemorrhagic stroke in the insula leads to disrupted cardiac sympathetic control and suggest that the DMH may be a downstream mediator (Marins et al., 2020, 2021). Altogether, decades of research have demonstrated that insular cortex influences cardiac autonomic activity, but the regional differentiation of the insula for stress integration remains unclear. Ultimately, more work is needed to understand the impact of insular subregions on stress adaptation and cardiovascular health.

While studies of insular cortex modulating cardiovascular or endocrine function during chronic stress have not been reported, recent work indicates chronic variable stress decreases expression of FosB/ΔFosB, a marker of long-term neural activity, throughout AI and PI (Pace et al., 2020). Interestingly, the long-term decrease in insular activity is dependent on the IL as knockdown of glutamate output from the IL prevents the effect. While insular FosB/ΔFosB-positive cells are glutamatergic, IL presynaptic terminals target both glutamatergic and GABAergic neurons in the AI and PI. These findings suggest that IL-insula communication

during chronic stress modulates long-term excitatory/inhibitory balance of the insular cortices, which may have significant implications for visceral regulation.

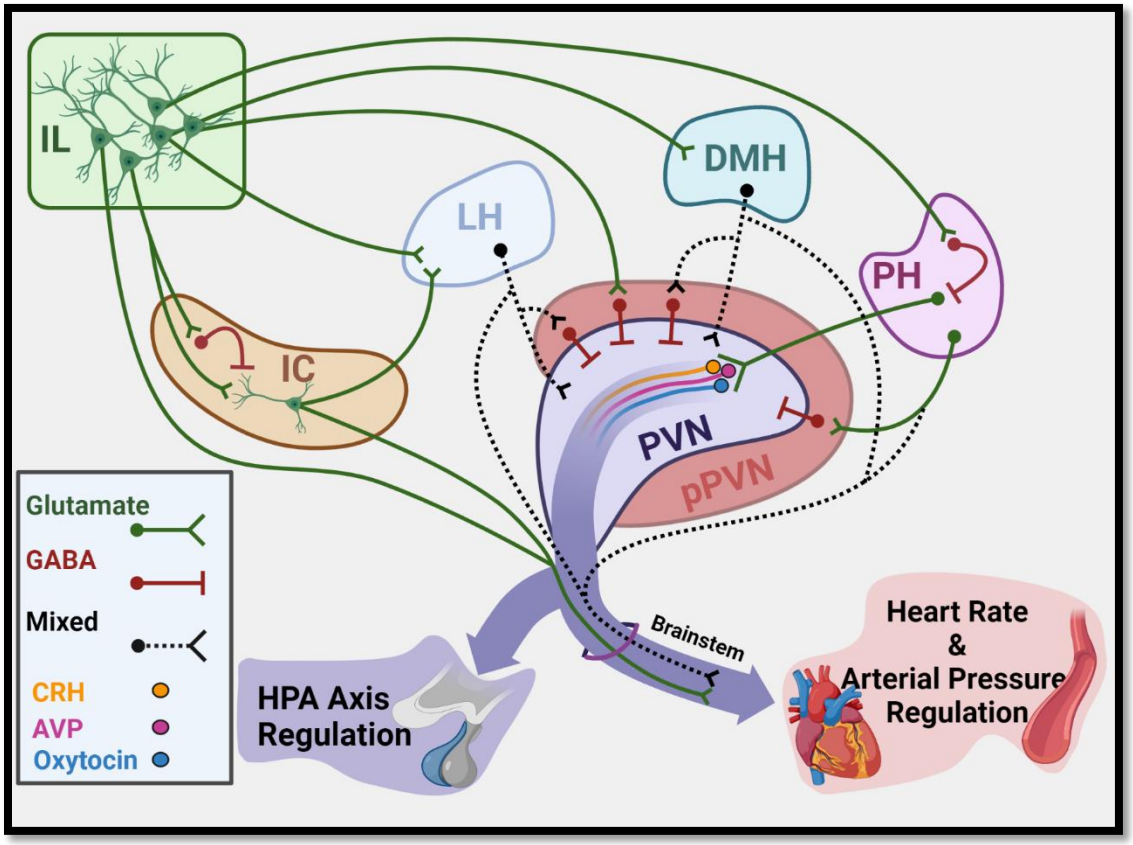

Figure 1.1 | Summary of cortical-hypothalamic circuits mediating stress integration. Graphical representation of the cortical and hypothalamic neurocircuitry that targets the PVN and/or brainstem to regulate neuroendocrine and cardiovascular reactivity to stress. Green represents glutamatergic neurons. Red represents GABAergic neurons. Black dashes represent mixed GABA and glutamate or neurochemically-undefined anatomical connections. Infralimbic cortex (IL), Insular cortex (IC), Lateral hypothalamus (LH), Dorsomedial hypothalamus (DMH), Posterior hypothalamus (PH), Paraventricular nucleus of the hypothalamus (PVN), Peri-paraventricular hypothalamus (pPVN), Corticotropin-releasing hormone (CRH), Arginine-vasopressin (AVP). Created with BioRender.com.

Effector Regions of the Hypothalamus

Paraventricular Hypothalamus

The PVN integrates hypothalamic and brainstem stress information to regulate both neuroendocrine and autonomic activity (L. W. Swanson & Kuypers, 1980). The region houses a

diverse population of neurons that synthesize peptides implicated in stress reactivity including CRH, arginine-vasopressin, and oxytocin. While PVN CRH release activates the HPA axis, multiple cell types give rise to brainstem and spinal projections to regulate sympathetic and parasympathetic balance (Ulrich-Lai & Herman, 2009). Notably, the descending cortical and limbic circuits that coordinate HPA axis and autonomic activity based on environmental context have limited direct innervation of the PVN (Roland & Sawchenko, 1993; Ulrich-Lai et al., 2011). However, numerous corticolimbic projections terminate in the GABAergic periphery of the PVN (peri-PVN) that surrounds neurosecretory cells (William E. Cullinan et al., 2008; Sunstrum & Inoue, 2019; Ulrich-Lai & Herman, 2009). Though direct assessment of stress regulation by specific inputs to peri-PVN has been difficult, combined anterograde and retrograde tracing studies have identified hypothalamic regions that provide direct input to the PVN. Glutamatergic projections arise from the LH, DMH, and PH, among others (Ulrich-Lai et al., 2011). These three hypothalamic nuclei are well-positioned based on connectivity to integrate descending limbic information (Ledoux et al., 1988). Furthermore, a portion of PVN-projecting neurons in the DMH and LH are GABAergic (Roland & Sawchenko, 1993), suggesting the nuclei may have bidirectional control over PVN neurons. Thus, cortical influences on HPA axis and cardiovascular reactivity are likely mediated trans-synaptically through innervation of hypothalamic regions that directly synapse in the PVN.

Lateral Hypothalamus

The prefrontal and insular cortices, among other limbic regions, target the LH (Vertes, 2004; Yasui et al., 1991). Moreover, the LH provides direct glutamate and GABA input to the PVN(Roland & Sawchenko, 1993; Ulrich-Lai et al., 2011) and innervates pre-ganglionic autonomic neurons in the parasympathetic dorsal motor nucleus of the vagus and sympathetic intermediolateral column (Hahn & Swanson, 2010; C.B. Saper et al., 1976; Sun & Guyenet, 1986). Additionally, swim and restraint stressors activate cells in the LH (W. E. Cullinan et al.,

1995); however, the phenotype of LH stress-responsive neurons has not been reported. The diversity of neurotransmitter and peptide messengers across the broad rostral to caudal breadth of the LH suggest a complex role in stress integration (Larry W. Swanson et al., 2005; Ulrich-Lai & Herman, 2009; Ziegler et al., 2002). For instance, LeDoux and colleagues found that LH lesions reduce pressor responses to conditioned fear (Ledoux et al., 1988). In contrast, NMDA signaling in the LH inhibits cardiovascular responses to restraint stress through parasympathetic activation (Deolindo et al., 2013). Moreover, recent studies found that LH $GABA_A$ and CRH receptor-1 antagonism decrease tachycardic responses to restraint stress (Barretto-de-Souza et al., 2021; Gomes-de-Souza et al., 2019). Together, these results suggest the LH may both increase and decrease cardiovascular reactivity. Despite direct PVN innervation, there are no reports to our knowledge of HPA axis modulation by the LH. However, it is worth noting that the LH more heavily targets the posterior PVN than the CRH-rich anterior PVN (Ulrich-Lai et al., 2011). Nevertheless, further analysis of LH stress integration is likely to elucidate specific subregional effects on sympathetic, parasympathetic, and neuroendocrine regulation.

Dorsomedial Hypothalamus

The DMH is another prominent limbic relay for stress regulation. The DMH receives glutamatergic input from cortical circuits as well as GABAergic innervation from sub-cortical regions such as the amygdala (Myers et al., 2014). Furthermore, the DMH robustly expresses immediately-early gene markers following swim and restraint stress (W. E. Cullinan et al., 1995). DMH efferents target the PVN as well as preganglionic sympathetic neurons (C.B. Saper et al., 1976), implying the region integrates stress-related processes (Ter Horst & Luiten, 1986, 1987; Thompson et al., 1996). The DMH projections to the PVN are both GABAergic and glutamatergic (Roland & Sawchenko, 1993; Ulrich-Lai et al., 2011), indicting the potential for bidirectional control of autonomic and endocrine stress responses. Seminal work by DiMicco and colleagues used pharmacological approaches to interrogate the functional role of DMH

neurotransmission in stress responding (Joseph A. DiMicco et al., 2002). Specifically, a series of studies in anesthetized rats found that $GABA_A$ receptor antagonism or activation of ionotropic glutamate receptors (NMDA, AMPA, and kainate) in the DMH increases heart rate and blood pressure (Soltis & DiMicco, 1991a, 1991b, 1992). Similar approaches in conscious rats found that DMH activation increased ACTH release, as well as stress-induced Fos in the PVN (Bailey & Dimicco, 2001; Morin et al., 2001). Moreover, $GABA_A$ agonists in the DMH reduce heart rate, blood pressure, and ACTH responses to stress (Stotz-Potter, Morin, et al., 1996; Stotz-Potter, Willis, et al., 1996). In all, this work suggests that tonic GABAergic inhibition of the DMH reduces acute cardiovascular and endocrine stress responding while glutamate-mediated DMH activation enhances stress reactivity at least partially through the PVN. Although, autonomic aspects of DMH modulation have been hypothesized to be mediated by brainstem circuits (Fontes et al., 2011). Interestingly, the DMH is activated by both repeated restraint and chronic variable stress (Flak et al., 2012), yet the stress-integrative role of the DMH under conditions of prolonged stress requires more investigation.

Posterior Hypothalamus

Cortical and limbic circuits also converge on the PH (Abrahamson & Moore, 2001; Çavdar et al., 2001) and the PH receives stress-activated inputs from multiple forebrain regions including the IL and PL (Myers et al., 2016). Although the PH is predominately glutamatergic, a portion of IL inputs appose PH GABA neurons, possibly regulating PH inhibition (Myers et al., 2016). Additionally, the PH sends glutamatergic projections to the PVN (Ulrich-Lai et al., 2011) and innervates preganglionic sympathetic neurons (C.B. Saper et al., 1976). Furthermore, stress-reactive neurons in the rostral PH innervate stress-activated cells in the medial parvicellular PVN and pre-autonomic raphe pallidus (Nyhuis et al., 2016). Ultimately, the stress-responsive upstream and downstream connectivity of the PH implies a prominent role in stress integration. Similar to the DMH, early studies by Dimicco and colleagues identified the PH as a regulator of

tachycardic and pressor responses under anesthesia (J. A. DiMicco et al., 1986). Specifically, both GABA release and GABA synthesis in the PH inhibit cardiovascular sympathetic activity (J. A. DiMicco & Abshire, 1987). In awake rodents, GABA modulation does not alter hemodynamics under basal conditions (Lisa et al., 1989). However, $GABA_A$ signaling reduces heart rate and blood pressure responses to acute stress. More recent work demonstrates that CRH-mediated excitation in the PH increases HR via pre-sympathetic neurons in the rostral ventrolateral and ventromedial medulla, without affecting vagal activity (Gao et al., 2016). Taken together, these data indicate that the PH is both necessary and sufficient for sympathetic cardiovascular stress responses.

Multiple lines of converging evidence also implicate the PH in HPA axis facilitation. $GABA_A$ agonists in the PH decrease ACTH during restraint (Myers et al., 2016) as well as corticosterone responses to restraint and audiogenic stress (Nyhuis et al., 2016). Additionally, GABA antagonist-mediated disinhibition of the PH increases PVN Fos and elevates ACTH and corticosterone reposnes to restraint (Myers et al., 2016). In addition to CRH neurons, PH projections also target vasopressin- and oxytocin-producing cells in the PVN (Myers et al., 2016), suggesting the potential for broad neuroendocrine regulation. Moreover, the PH exhibits long-term activation during chronic variable stress but not repeated restraint (Flak et al., 2012). Altogether, there is considerable evidence that PH excitatory/inhibitory balance is important for autonomic and neuroendocrine stress integration.

Conclusion

The widespread impact of stress on health-related quality of life and cardiovascular disease in particular makes understanding stress physiology a crucial issue. Here, we discussed the function and connectivity of cortical and hypothalamic brain regions that integrate cardiovascular and neuroendocrine responses to stressful stimuli (Figure 1). The aggregate literature reviewed

illustrates the hierarchal organization of descending cortical circuits that modulate stress-effector neurons through intermediary subcortical neurons. Cell-type specific approaches have contributed to our understanding of stress reactivity and have the potential to uncover the basis of excitatory/inhibitory balance as it relates to chronic stress-induced pathologies. While we are beginning to unravel the roles of these networks in specific stress responses, many questions remain regarding autonomic-endocrine stress integration. Chiefly, almost all the literature reviewed came from experiments with male subjects. Biological sex is an important factor for stress-related disease incidence and outcomes, yet the role of sex in stress integration across development and reproductive stages is largely unexplored. The experiments reviewed that included both sexes found markedly differences in neural regulation of endocrine and autonomic reactivity (Wallace et al., 2021). Moreover, there is increasing evidence for ovarian hormone regulation of cardiac and vascular outcomes after chronic stress (Finnell et al., 2018). Therefore, future studies examining the actions of sex steroids on cortical-hypothalamic circuits are vital for understanding the health burden of stress.

References

Abrahamson, E. E., & Moore, R. Y. (2001). The posterior hypothalamic area: chemoarchitecture and afferent connections. In *Brain Research* (Vol. 889). www.elsevier.com/locate/bres

Allen, G. V., Saper, C. B., Hurley, K. M., & Cechetto, D. F. (1991). Organization of visceral and limbic connections in the insular cortex of the rat. *Journal of Comparative Neurology*, *311*(1), 1–16. https://doi.org/10.1002/CNE.903110102

Bailey, T. W., & Dimicco, J. A. (2001). Chemical stimulation of the dorsomedial hypothalamus elevates plasma ACTH in conscious rats. *American Journal of Physiology - Regulatory Integrative and Comparative Physiology*, *280*(1 49-1). https://doi.org/10.1152/ajpregu.2001.280.1.r8

Barefoot, J. C., Helms, M. J., Mark, D. B., Blumenthal, J. A., Califf, R. M., Haney, T. L., O'Connor, C. M., Siegler, I. C., & Williams, R. B. (1996). Depression and Long-Term Mortality Risk in Patients With Coronary Artery Disease. *The American Journal of Cardiology*, *78*(6), 613–617. https://doi.org/10.1016/S0002-9149(96)00380-3

Barretto-de-Souza, L., Benini, R., Reis-Silva, L. L., & Crestani, C. C. (2021). Corticotropin-releasing factor neurotransmission in the lateral hypothalamus modulates the tachycardiac response during acute emotional stress in rats. *Brain Research Bulletin*, *166*, 102–109. https://doi.org/10.1016/J.BRAINRESBULL.2020.11.010

Camargos, F., Müller-Ribeiro, F., Zaretsky, D. V, Zaretskaia, M. V, Santos, R. A. S., Dimicco, J. A., Antônio, M., & Fontes, P. (2012). Contribution of infralimbic cortex in the cardiovascular response to acute stress. *Am J Physiol Regul Integr Comp Physiol*, *303*, 639–650. https://doi.org/10.1152/ajpregu.00573.2011.-The

Çavdar, S., ŞAN, T., AKER, R., ŞEHİRLİ, Ü., & ONAT, F. (2001). Cerebellar connections to the dorsomedial and posterior nuclei of the hypothalamus in the rat. *Journal of Anatomy*, *198*(1), 37–45. https://doi.org/10.1046/j.1469-7580.2001.19810037.x

Chaves, T., Fazekas, C. L., Horváth, K., Correia, P., Szabó, A., Török, B., Bánrévi, K., & Zelena,

D. (2021). Stress adaptation and the brainstem with focus on corticotropin-releasing hormone. *International Journal of Molecular Sciences*, *22*(16). https://doi.org/10.3390/ijms22169090

Chida, Y., & Steptoe, A. (2010). Greater Cardiovascular Responses to Laboratory Mental Stress Are Associated With Poor Subsequent Cardiovascular Risk Status. *Hypertension*, *55*(4), 1026–1032. https://doi.org/10.1161/HYPERTENSIONAHA.109.146621

Cullinan, W. E., Herman, J. P., Battaglia, D. F., Akil, H., & Watson, S. J. (1995). Pattern and time course of immediate early gene expression in rat brain following acute stress. *Neuroscience*, *64*(2), 477–505. https://doi.org/10.1016/0306-4522(94)00355-9

Cullinan, William E., Ziegler, D. R., & Herman, J. P. (2008). Functional role of local GABAergic influences on the HPA axis. *Brain Structure and Function 2008 213:1*, *213*(1), 63–72. https://doi.org/10.1007/S00429-008-0192-2

de Kloet, E. R., Joëls, M., & Holsboer, F. (2005). Stress and the brain: from adaptation to disease. *Nature Reviews Neuroscience*, *6*(6), 463–475. https://doi.org/10.1038/nrn1683

Deolindo, M. V., Reis, D. G., Crestani, C. C., Tavares, R. F., Resstel, L. B. M., & Corrêa, F. M. A. (2013). NMDA receptors in the lateral hypothalamus have an inhibitory influence on the tachycardiac response to acute restraint stress in rats. *European Journal of Neuroscience*, *38*(3), 2374–2381. https://doi.org/10.1111/ejn.12246

DiMicco, J. A., & Abshire, V. M. (1987). Evidence for GABAergic inhibition of a hypothalamic sympathoexcitatory mechanism in anesthetized rats. *Brain Research*, *402*(1), 1–10. https://doi.org/10.1016/0006-8993(87)91041-9

DiMicco, J. A., Abshire, V. M., Hankins, K. D., Sample, R. H. B., & Wible, J. H. (1986). Microinjection of GABA antagonists into posterior hypothalamus elevates heart rate in anesthetizes rats. *Neuropharmacology*, *25*(9), 1063–1066. https://doi.org/10.1016/0028-3908(86)90203-0

DiMicco, Joseph A., Samuels, B. C., Zaretskaia, M. V., & Zaretsky, D. V. (2002). The

dorsomedial hypothalamus and the response to stress: Part renaissance, part revolution. In *Pharmacology Biochemistry and Behavior* (Vol. 71, Issue 3). https://doi.org/10.1016/S0091-3057(01)00689-X

Drevets, W. C., Price, J. L., Simpson, J. R., Todd, R. D., Reich, T., Vannier, M., & Raichle, M. E. (1997). Subgenual prefrontal cortex abnormalities in mood disorders. *Nature*, *386*(6627), 824–827. https://doi.org/10.1038/386824a0

Drevets, W. C., Savitz, J., & Trimble, M. (2008). The subgenual anterior cingulate cortex in mood disorders. *CNS Spectrums*, *13*(8), 663–681. https://doi.org/10.1017/S1092852900013754

Finnell, J. E., Muniz, B. L., Padi, A. R., Lombard, C. M., Moffitt, C. M., Wood, C. S., Wilson, L. B., Reagan, L. P., Wilson, M. A., & Wood, S. K. (2018). Essential Role of Ovarian Hormones in Susceptibility to the Consequences of Witnessing Social Defeat in Female Rats. *Biological Psychiatry*. https://doi.org/10.1016/J.BIOPSYCH.2018.01.013

Flak, J. N., Solomon, M. B., Jankord, R., Krause, E. G., & Herman, J. P. (2012). Identification of chronic stress-activated regions reveals a potential recruited circuit in rat brain. *The European Journal of Neuroscience*, *36*(4), 2547–2555. https://doi.org/10.1111/j.1460-9568.2012.08161.x

Fontes, M. A. P., Xavier, C. H., de Menezes, R. C. A., & DiMicco, J. A. (2011). The dorsomedial hypothalamus and the central pathways involved in the cardiovascular response to emotional stress. *Neuroscience*, *184*, 64–74. https://doi.org/10.1016/J.NEUROSCIENCE.2011.03.018

Fuchikami, M., Thomas, A., Liu, R., Wohleb, E. S., Land, B. B., DiLeone, R. J., Aghajanian, G. K., & Duman, R. S. (2015). Optogenetic stimulation of infralimbic PFC reproduces ketamine's rapid and sustained antidepressant actions. *Proceedings of the National Academy of Sciences of the United States of America*, *112*(26), 8106–8111. https://doi.org/10.1073/pnas.1414728112

Gao, H. R., Zhuang, Q. X., Li, B., Li, H. Z., Chen, Z. P., Wang, J. J., & Zhu, J. N. (2016). Corticotropin releasing factor excites neurons of posterior hypothalamic nucleus to produce tachycardia in rats. *Scientific Reports*, *6*. https://doi.org/10.1038/srep20206

Ghosal, S., Duman, C. H., Liu, R. J., Wu, M., Terwilliger, R., Girgenti, M. J., Wohleb, E., Fogaca, M. V., Teichman, E. M., Hare, B., & Duman, R. S. (2020). Ketamine rapidly reverses stress-induced impairments in GABAergic transmission in the prefrontal cortex in male rodents. *Neurobiology of Disease*, *134*. https://doi.org/10.1016/j.nbd.2019.104669

Gilabert-Juan, J., Castillo-Gomez, E., Guirado, R., Moltó, M. D., & Nacher, J. (2013). Chronic stress alters inhibitory networks in the medial prefrontal cortex of adult mice. *Brain Structure and Function*, *218*(6), 1591–1605. https://doi.org/10.1007/s00429-012-0479-1

Gogolla, N. (2017). The insular cortex. *Current Biology*, *27*(12), R580–R586. https://doi.org/10.1016/j.cub.2017.05.010

Gomes-de-Souza, L., Benini, R., Costa-Ferreira, W., & Crestani, C. C. (2019). GABA A but not GABA B receptors in the lateral hypothalamus modulate the tachycardic response to emotional stress in rats. *European Neuropsychopharmacology*, *29*(5), 672–680. https://doi.org/10.1016/j.euroneuro.2019.03.001

Hahn, J. D., & Swanson, L. W. (2010). Distinct patterns of neuronal inputs and outputs of the juxtaparaventricular and suprafornical regions of the lateral hypothalamic area in the male rat. *Brain Research Reviews*, *64*(1), 14–103. https://doi.org/10.1016/j.brainresrev.2010.02.002

Herman, J. P., Figueiredo, H., Mueller, N. K., Ulrich-Lai, Y., Ostrander, M. M., Choi, D. C., & Cullinan, W. E. (2003). Central mechanisms of stress integration: Hierarchical circuitry controlling hypothalamo-pituitary-adrenocortical responsiveness. *Frontiers in Neuroendocrinology*, *24*(3), 151–180. https://doi.org/10.1016/j.yfrne.2003.07.001

Herman, J. P., McKlveen, J. M., Ghosal, S., Kopp, B., Wulsin, A., Makinson, R., Scheimann, J., & Myers, B. (2016). Regulation of the hypothalamic-pituitary- adrenocortical stress

response. *Comprehensive Physiology*, *6*(2), 603–621. https://doi.org/10.1002/cphy.c150015

Johnson, S. B., Emmons, E. B., Lingg, R. T., Anderson, R. M., Romig-Martin, S. A., Lalumiere, R. T., Narayanan, N. S., Viau, V., & Radley, J. J. (2019). Prefrontal–bed nucleus circuit modulation of a passive coping response set. *Journal of Neuroscience*, *39*(8), 1405–1419. https://doi.org/10.1523/JNEUROSCI.1421-18.2018

Jones, K. R., Myers, B., & Herman, J. P. (2011). Stimulation of the prelimbic cortex differentially modulates neuroendocrine responses to psychogenic and systemic stressors. *Physiology and Behavior*, *104*(2), 266–271. https://doi.org/10.1016/j.physbeh.2011.03.021

Lamotte, G., Shouman, K., & Benarroch, E. E. (2021). Stress and central autonomic network. *Autonomic Neuroscience: Basic and Clinical*, *235*. https://doi.org/10.1016/j.autneu.2021.102870

Ledoux, J. E., Iwata, J., Cicchetti, P., & Reis, D. J. (1988). Different Projections of the Central Amygdaloid Nucleus Mediate Autonomic and Behavioral Correlates of Conditioned Fear. *The Journal of Neuroscience*, *8*(7), 2517–2529.

Lisa, M., Marmo, E., Wible, J. H., & DiMicco, J. A. (1989). Injection of muscimol into posterior hypothalamus blocks stress-induced tachycardia. *American Journal of Physiology - Regulatory Integrative and Comparative Physiology*, *257*(1). https://doi.org/10.1152/ajpregu.1989.257.1.r246

Maniscalco, J. W., Rinaman, L., & Author, P. B. (2017). Interoceptive Modulation of Neuroendocrine, Emotional, and Hypophagic Responses to Stress HHS Public Access Author manuscript. *Physiol Behav*, *176*, 195–206. https://doi.org/10.1016/j.physbeh.2017.01.027

Marins, F. R., Limborço-Filho, M., D'Abreu, B. F., Machado de Almeida, P. W., Gavioli, M., Xavier, C. H., Oppenheimer, S. M., Guatimosim, S., & Fontes, M. A. P. (2020). Autonomic and cardiovascular consequences resulting from experimental hemorrhagic stroke in the

left or right intermediate insular cortex in rats. *Autonomic Neuroscience: Basic and Clinical*, *227*. https://doi.org/10.1016/j.autneu.2020.102695

Marins, F. R., Limborço-Filho, M., Iddings, J. A., Xavier, C. H., Biancardi, V. C., Stern, J. E., Ramiro Diaz, J., Oppenheimer, S. M., Filosa, J. A., & Peliky Fontes, M. A. (2021). Tachycardia evoked from insular stroke in rats is dependent on glutamatergic neurotransmission in the dorsomedial hypothalamus. *European Journal of Neurology*, *00*, 1–10. https://doi.org/10.1111/ene.14987

Marins, F. R., Limborço-Filho, M., Xavier, C. H., Biancardi, V. C., Vaz, G. C., Stern, J. E., Oppenheimer, S. M., & Fontes, M. A. P. (2016). Functional topography of cardiovascular regulation along the rostrocaudal axis of the rat posterior insular cortex. *Clinical and Experimental Pharmacology and Physiology*, *43*(4), 484–493. https://doi.org/10.1111/1440-1681.12542

Mayberg, H. S., Lozano, A. M., Voon, V., McNeely, H. E., Seminowicz, D., Hamani, C., Schwalb, J. M., & Kennedy, S. H. (2005). Deep Brain Stimulation for Treatment-Resistant Depression. *Neuron*, *45*(5), 651–660. https://doi.org/10.1016/J.NEURON.2005.02.014

McEwen, B. S., & Stellar, E. (1993). Stress and the Individual: Mechanisms Leading to Disease. *Archives of Internal Medicine*, *153*(18), 2093–2101. https://doi.org/10.1001/archinte.1993.00410180039004

McKlveen, J. M., Myers, B., & Herman, J. P. (2015). The Medial Prefrontal Cortex: Coordinator of Autonomic, Neuroendocrine and Behavioural Responses to Stress. *Journal of Neuroendocrinology*, *27*(6), 446–456. https://doi.org/10.1111/jne.12272

McKlveen, Jessica M., Moloney, R. D., Scheimann, J. R., Myers, B., & Herman, J. P. (2019). “Braking” the Prefrontal Cortex: The Role of Glucocorticoids and Interneurons in Stress Adaptation and Pathology. *Biological Psychiatry*, *86*(9), 669–681. https://doi.org/10.1016/j.biopsych.2019.04.032

McKlveen, Jessica M., Myers, B., Flak, J. N., Bundzikova, J., Solomon, M. B., Seroogy, K. B., &

Herman, J. P. (2013). Role of Prefrontal Cortex Glucocorticoid Receptors in Stress and Emotion. *Biological Psychiatry*, *74*(9), 672–679. https://doi.org/10.1016/J.BIOPSYCH.2013.03.024

Morin, S. M., Stotz-Potter, E. H., & Dimicco, J. A. (2001). Injection of muscimol in dorsomedial hypothalamus and stress-induced Fos expression in paraventricular nucleus. *Https://Doi.Org/10.1152/Ajpregu.2001.280.5.R1276*, *280*(5 49-5). https://doi.org/10.1152/AJPREGU.2001.280.5.R1276

Myers, B. (2017). Corticolimbic regulation of cardiovascular responses to stress. *Physiology and Behavior*, *172*, 49–59. https://doi.org/10.1016/j.physbeh.2016.10.015

Myers, B., Carvalho-Netto, E., Wick-Carlson, D., Wu, C., Naser, S., Solomon, M. B., Ulrich-Lai, Y. M., & Herman, J. P. (2016). GABAergic Signaling within a Limbic-Hypothalamic Circuit Integrates Social and Anxiety-Like Behavior with Stress Reactivity. *Neuropsychopharmacology*, *41*(6), 1530–1539. https://doi.org/10.1038/npp.2015.311

Myers, B., Mark Dolgas, C., Kasckow, J., Cullinan, W. E., & Herman, J. P. (2014). Central stress-integrative circuits: forebrain glutamatergic and GABAergic projections to the dorsomedial hypothalamus, medial preoptic area, and bed nucleus of the stria terminalis. *Brain Structure & Function*, *219*(4), 1287–1303. https://doi.org/10.1007/s00429-013-0566-y

Myers, B., McKlveen, J. M., & Herman, J. P. (2012). Neural regulation of the stress response: The many faces of feedback. *Cellular and Molecular Neurobiology*, *32*(5), 683–694. https://doi.org/10.1007/s10571-012-9801-y

Myers, B., McKlveen, J. M., Morano, R., Ulrich-Lai, Y. M., Solomon, M. B., Wilson, S. P., & Herman, J. P. (2017). Vesicular Glutamate Transporter 1 Knockdown in Infralimbic Prefrontal Cortex Augments Neuroendocrine Responses to Chronic Stress in Male Rats. *Endocrinology*, *158*(10), 3579–3591. https://doi.org/10.1210/en.2017-00426

Nawreen, N., Cotella, E. M., Morano, R., Mahbod, P., Dalal, K. S., Fitzgerald, M., Martelle, S., Packard, B. A., Franco-Villanueva, A., Moloney, R. D., & Herman, J. P. (2020).

Chemogenetic inhibition of infralimbic prefrontal cortex gabaergic parvalbumin interneurons attenuates the impact of chronic stress in male mice. *ENeuro*, *7*(5). https://doi.org/10.1523/ENEURO.0423-19.2020

Nyhuis, T. J., Masini, C. V., Day, H. E. W., & Campeau, S. (2016). Evidence for the integration of stress-related signals by the rostral posterior hypothalamic nucleus in the regulation of acute and repeated stress-evoked hypothalamo-pituitary-adrenal response in rat. *Journal of Neuroscience*, *36*(3), 773–784. https://doi.org/10.1523/JNEUROSCI.3413-15.2016

Oppenheimer, S., & Cechetto, D. (2016). The Insular Cortex and the Regulation of Cardiac Function. In *Comprehensive Physiology* (Vol. 6, Issue 2, pp. 1081–1133). John Wiley & Sons, Inc. https://doi.org/10.1002/cphy.c140076

Oppenheimer, S. M., & Cechetto, D. F. (1990). Cardiac chronotropic organization of the rat insular cortex. In *Brain Research*.

Oppenheimer, S. M., Wilson, J. X., Guiraudon, C., & Cechetto, D. F. (1991). Insular cortex stimulation produces lethal cardiac arrhythmias: a mechanism of sudden death? *Brain Research*, *550*(1), 115–121. https://doi.org/10.1016/0006-8993(91)90412-O

Pace, S. A., Christensen, C., Schackmuth, M. K., Wallace, T., McKlveen, J. M., Beischel, W., Morano, R., Scheimann, J. R., Wilson, S. P., Herman, J. P., & Myers, B. (2020). Infralimbic cortical glutamate output is necessary for the neural and behavioral consequences of chronic stress. *Neurobiology of Stress*, *13*, 100274. https://doi.org/10.1016/j.ynstr.2020.100274

Radley, J. J., Arias, C. M., & Sawchenko, P. E. (2006). Regional Differentiation of the Medial Prefrontal Cortex in Regulating Adaptive Responses to Acute Emotional Stress. *The Journal of Neuroscience*, *26*(50), 12967. https://doi.org/10.1523/JNEUROSCI.4297-06.2006

Radley, J. J., Gosselink, K. L., & Sawchenko, P. E. (2009). A discrete GABAergic relay mediates medial prefrontal cortical inhibition of the neuroendocrine stress response.

Journal of Neuroscience, *29*(22), 7330–7340. https://doi.org/10.1523/JNEUROSCI.5924-08.2009

Resstel, L. B. M., Joca, S. R. L., Guimarães, F. G., & Corrêa, F. M. A. (2006). Involvement of medial prefrontal cortex neurons in behavioral and cardiovascular responses to contextual fear conditioning. *Neuroscience*, *143*(2), 377–385. https://doi.org/10.1016/j.neuroscience.2006.08.002

Rinaman, L. (2011). Hindbrain noradrenergic A2 neurons: Diverse roles in autonomic, endocrine, cognitive, and behavioral functions. *American Journal of Physiology - Regulatory Integrative and Comparative Physiology*, *300*(2). https://doi.org/10.1152/ajpregu.00556.2010

Roland, B. L., & Sawchenko, P. E. (1993). Local origins of some GABAergic projections to the paraventricular and supraoptic nuclei of the hypothalamus in the rat. *Journal of Comparative Neurology*, *332*(1), 123–143. https://doi.org/10.1002/CNE.903320109

Ruggiero, D. A., Mraovitch, S., Granata, A. R., Anwar, M., & Reis, D. J. (1987). A role of insular cortex in cardiovascular function. *Journal of Comparative Neurology*, *257*(2), 189–207. https://doi.org/10.1002/CNE.902570206

Saper, C.B., Loewy, A. D., Swanson, L. W., & Cowan, W. M. (1976). Direct hypothalamo-autonomic connections. *Brain Research*, *117*(2), 305–312. https://doi.org/10.1016/0006-8993(76)90738-1

Saper, Clifford B. (1982). Convergence of autonomic and limbic connections in the insular cortex of the rat. *Journal of Comparative Neurology*, *210*(2), 163–173. https://doi.org/10.1002/CNE.902100207

Schaeuble, D., Packard, A. E. B., McKlveen, J. M., Morano, R., Fourman, S., Smith, B. L., Scheimann, J. R., Packard, B. A., Wilson, S. P., James, J., Hui, D. Y., Ulrich-Lai, Y. M., Herman, J. P., & Myers, B. (2019). Prefrontal Cortex Regulates Chronic Stress-Induced Cardiovascular Susceptibility. *Journal of the American Heart Association*, *8*(24), e014451.

https://doi.org/10.1161/JAHA.119.014451

Shoemaker, J. K., & Goswami, R. (2015). Forebrain neurocircuitry associated with human reflex cardiovascular control. *Frontiers in Physiology*, *6*(SEP). https://doi.org/10.3389/fphys.2015.00240

Soltis, R. P., & DiMicco, J. A. (1991a). GABA(A) and excitatory amino acid receptors in dorsomedial hypothalamus and heart rate in rats. *American Journal of Physiology - Regulatory Integrative and Comparative Physiology*, *260*(1 29-1). https://doi.org/10.1152/ajpregu.1991.260.1.r13

Soltis, R. P., & DiMicco, J. A. (1991b). Interaction of hypothalamic GABA(A) and excitatory amino acid receptors controlling heart rate in rats. *American Journal of Physiology - Regulatory Integrative and Comparative Physiology*, *261*(2 30-2). https://doi.org/10.1152/ajpregu.1991.261.2.r427

Soltis, R. P., & DiMicco, J. A. (1992). Hypothalamic excitatory amino acid receptors mediate stress-induced tachycardia in rats. *American Journal of Physiology - Regulatory Integrative and Comparative Physiology*, *262*(4 31-4). https://doi.org/10.1152/ajpregu.1992.262.4.r689

Steptoe, A., & Kivimäki, M. (2012). Stress and cardiovascular disease. *Nature Reviews. Cardiology*, *9*(6), 360–370. https://doi.org/10.1038/nrcardio.2012.45

Stotz-Potter, E. H., Morin, S. M., & DiMicco, J. A. (1996). Effect of microinjection of muscimol into the dorsomedial or paraventricular hypothalamic nucleus on air stress-induced neuroendocrine and cardiovascular changes in rats. *Brain Research*, *742*(1–2), 219–224. https://doi.org/10.1016/S0006-8993(96)01011-6

Stotz-Potter, E. H., Willis, L. R., & DiMicco, J. A. (1996). Muscimol acts in dorsomedial but not paraventricular hypothalamic nucleus to suppress cardiovascular effects of stress. *Journal of Neuroscience*, *16*(3), 1173–1179. https://doi.org/10.1523/jneurosci.16-03-01173.1996

Sun, M. K., & Guyenet, P. G. (1986). Hypothalamic glutamatergic input to medullary sympathoexcitatory neurons in rats. *American Journal of Physiology - Regulatory*

Integrative and Comparative Physiology, *251*(4 (20/4)). https://doi.org/10.1152/ajpregu.1986.251.4.r798

Sunstrum, J. K., & Inoue, W. (2019). Heterosynaptic modulation in the paraventricular nucleus of the hypothalamus. *Neuropharmacology*, *154*, 87–95. https://doi.org/10.1016/J.NEUROPHARM.2018.11.004

Swanson, L. W., & Kuypers, H. G. J. M. (1980). The paraventricular nucleus of the hypothalamus: Cytoarchitectonic subdivisions and organization of projections to the pituitary, dorsal vagal complex, and spinal cord as demonstrated by retrograde fluorescence double-labeling methods. *Journal of Comparative Neurology*, *194*(3), 555–570. https://doi.org/10.1002/cne.901940306

Swanson, L. W., & Sawchenko, P. E. (1983). Hypothalamic integration: Organization of the paraventricular and supraoptic nuclei. *Annual Review of Neuroscience*, *Vol. 6*, 269–324. https://doi.org/10.1146/annurev.ne.06.030183.001413

Swanson, Larry W., Sanchez-Watts, G., & Watts, A. G. (2005). Comparison of melanin-concentrating hormone and hypocretin/orexin mRNA expression patterns in a new parceling scheme of the lateral hypothalamic zone. *Neuroscience Letters*, *387*(2), 80–84. https://doi.org/10.1016/J.NEULET.2005.06.066

Tavares, R. F., Corrêa, F. M. A., & Resstel, L. B. M. (2009). Opposite role of infralimbic and prelimbic cortex in the tachycardiac response evoked by acute restraint stress in rats. *Journal of Neuroscience Research*, *87*(11), 2601–2607. https://doi.org/10.1002/jnr.22070

Ter Horst, G. J., & Luiten, P. G. M. (1986). The projections of the dorsomedial hypothalamic nucleus in the rat. *Brain Research Bulletin*, *16*(2), 231–248. https://doi.org/10.1016/0361-9230(86)90038-9

Ter Horst, G. J., & Luiten, P. G. M. (1987). Phaseolus vulgaris leuco-agglutinin tracing of intrahypothalamic connections of the lateral, ventromedial, dorsomedial and paraventricular hypothalamic nuclei in the rat. *Brain Research Bulletin*, *18*(2), 191–203.

https://doi.org/10.1016/0361-9230(87)90190-0

Thompson, R. H., Canteras, N. S., & Swanson, L. W. (1996). Organization of Projections From the Dorsomedial Nucleus of the Hypothalamus: A PHA-L Study in the Rat. *The Journal of Comparative Neurology*, *376*, 143–173. https://doi.org/10.1002/(SICI)1096-9861(19961202)376:1

Ulrich-Lai, Y. M., & Herman, J. P. (2009). Neural regulation of endocrine and autonomic stress responses. In *Nature Reviews Neuroscience* (Vol. 10, Issue 6, pp. 397–409). Nat Rev Neurosci. https://doi.org/10.1038/nrn2647

Ulrich-Lai, Y. M., Jones, K. R., Ziegler, D. R., Cullinan, W. E., & Herman, J. P. (2011). Forebrain origins of glutamatergic innervation to the rat paraventricular nucleus of the hypothalamus: Differential inputs to the anterior versus posterior subregions. *The Journal of Comparative Neurology*, *519*(7), 1301–1319. https://doi.org/10.1002/cne.22571

Vertes, R. P. (2004). Differential projections of the infralimbic and prelimbic cortex in the rat. *Synapse*, *51*(1), 32–58. https://doi.org/10.1002/syn.10279

Wallace, T., & Myers, B. (2021). Effects of Biological Sex and Stress Exposure on Ventromedial Prefrontal Regulation of Mood-Related Behaviors. *Frontiers in Behavioral Neuroscience*, *15*. https://doi.org/10.3389/fnbeh.2021.737960

Wallace, T., Schaeuble, D., Pace, S. A., Schackmuth, M. K., Hentges, S. T., Chicco, A. J., & Myers, B. (2021). Sexually divergent cortical control of affective-autonomic integration. *Psychoneuroendocrinology*, *129*, 105238. https://doi.org/10.1016/j.psyneuen.2021.105238

Wood, M., Adil, O., Wallace, T., Fourman, S., Wilson, S. P., Herman, J. P., & Myers, B. (2019). Infralimbic prefrontal cortex structural and functional connectivity with the limbic forebrain: a combined viral genetic and optogenetic analysis. *Brain Structure & Function*, *224*(1), 73–97. https://doi.org/10.1007/s00429-018-1762-6

Yasui, Y., Breder, C. D., Safer, C. B., & Cechetto, D. F. (1991). Autonomic responses and efferent pathways from the insular cortex in the rat. *Journal of Comparative Neurology*,

303(3), 355–374. https://doi.org/10.1002/CNE.903030303

Yusuf, S., Hawken, S., Ôunpuu, S., Dans, T., Avezum, A., Lanas, F., McQueen, M., Budaj, A., Pais, P., Varigos, J., & Lisheng, L. (2004). Effect of potentially modifiable risk factors associated with myocardial infarction in 52 countries (the INTERHEART study): case-control study. *The Lancet*, *364*(9438), 937–952. https://doi.org/10.1016/S0140-6736(04)17018-9

Ziegler, D. R., Cullinan, W. E., & Herman, J. P. (2002). Distribution of vesicular glutamate transporter mRNA in rat hypothalamus. *The Journal of Comparative Neurology*, *448*(3), 217–229. https://doi.org/10.1002/cne.10257

CHAPTER 2: PREFRONTAL CORTEX REGULATES CHRONIC STRESS-INDUCED CARDIOVASCULAR SUSCEPTIBILITY[1]

Preamble:

Overview

The medial prefrontal cortex is necessary for appropriate appraisal of stressful information, as well as coordinating visceral and behavioral processes. However, prolonged stress impairs medial prefrontal cortex function and prefrontal-dependent behaviors. Additionally, chronic stress induces sympathetic predominance, contributing to health detriments associated with autonomic imbalance. Previous studies identified a subregion of rodent prefrontal cortex, infralimbic cortex (IL), as a key regulator of neuroendocrine-autonomic integration after chronic stress, suggesting that IL output may prevent chronic stress-induced autonomic imbalance. In the current study, we tested the hypothesis that the IL regulates hemodynamic, vascular, and cardiac responses to chronic stress.

Introduction

Stress, a real or perceived threat to homeostasis or well-being, elicits behavioral and physiological responses to promote organismal adaptation (de Kloet et al., 2005; Myers, McKlveen, et al., 2014). However, prolonged stress exposure has deleterious effects on health, increasing susceptibility to cardiovascular, psychiatric, and metabolic disorders (Binder &

---

[1] The following material was published in a manuscript December 17th, 2019, in Journal of the American Heart Association under the title, 'Prefrontal Cortex Regulates Chronic Stress-Induced Cardiovascular Susceptibility'. Funding: This work was supported by NIH grants K99/R00 HL122454 to B. Myers and R01 MH049698 to J. P. Herman. Cincinnati Children's Hospital Medical Center Research Pathology Core carried out cardiac and vascular histological processing.
Disclosures: J. M. McKlveen contributed to this article in her personal capacity. The views expressed herein are those of the authors and do not necessarily represent the views of the National Institutes of Health, National Center for Complementary and Integrative Health, or the United States Government. All authors report no biomedical financial interests or potential conflicts of interest.

Nemeroff, 2010; Grippo & Johnson, 2009; Sgoifo et al., 2015; Wardle et al., 2011). In fact, chronic psychosocial stress predicts the incidence of cardiovascular disease, cardiac-related morbidity and mortality, and doubles the risk of myocardial infarction (Barefoot et al., 1996; Yusuf et al., 2004). Exaggerated heart rate (HR) reactivity to acute stress also predicts poor cardiovascular outcomes, including hypertension, ventricular hypertrophy, and atherosclerosis (Chida & Steptoe, 2010). Although the biological mechanisms mediating the relationship between stress and cardiovascular health are not completely understood, adverse outcomes likely result from prolonged exposure to neural and endocrine stress mediators.

The initial appraisal of psychological stressors largely occurs in the limbic system, a network of interconnected structures spanning the forebrain. The medial prefrontal cortex (mPFC) is a key limbic cortical structure mediating stress appraisal, emotion, and cognition (Damasio, 1996; J. M. McKlveen et al., 2015; Myers-Schulz & Koenigs, 2012; J. N. Wood & Grafman, 2003). Moreover, activity within a specific region of the ventral mPFC, the subgenual cingulate cortex (BA25), associates with sadness in healthy controls(Liotti et al., 2000), as well as pathological depression in treatment-resistant patients (Mayberg et al., 2005). Recent human neuroimaging studies have also identified the ventral mPFC as a component of the central autonomic network that responds to and coordinates visceral functions, including stress-evoked blood pressure reactivity (Beissner et al., 2013; Gianaros & Sheu, 2009; Gianaros & Wager, 2015; Shoemaker et al., 2015). The rodent homolog of BA25 is infralimbic cortex (IL) (Öngür et al., 2003; Uylings et al., 2003; Vertes, 2004). This subregion of ventral mPFC provides inputs to stress-integrative nuclei, including the posterior hypothalamus and brainstem autonomic centers(Gabbott et al., 2005; Myers et al., 2016; Myers, Mark Dolgas, et al., 2014; M. Wood et al., 2019). Our previous studies reduced glutamate outflow from the IL in rats undergoing chronic variable stress (CVS) and found hyperactivation of the hypothalamic-pituitary-adrenal axis (HPA) axis(Myers et al., 2017; Smith et al., 2017). As glutamate release from IL projections is a key regulator of acute and chronic neuroendocrine reactivity, we hypothesized that IL output

may prevent chronic stress-induced autonomic imbalance and associated cardiovascular susceptibility.

To address this hypothesis, a lentiviral-packaged small interfering RNA (siRNA) targeting vesicular glutamate transporter 1 (vGluT1) was injected in the IL. This approach selectively reduces vGluT1 expression in IL glutamate neurons, preventing the packaging and release of glutamate from presynaptic terminals(Myers et al., 2017; Schuske & Jorgensen, 2004; Wojcik et al., 2004). Animals were then exposed to CVS to examine interactions between chronic stress and hypo-functionality of ventral mPFC in terms of cardiovascular reactivity, arterial function, and remodeling of the vasculature and myocardium. These studies identified the necessity of the IL for reducing hemodynamic, vascular, and cardiac consequences of prolonged stress. Additionally, this work points toward a neurobiological mechanism mediating the relationship between stress and cardiovascular health.

Methods

The data that support the findings of this study are available from the corresponding author upon reasonable request.

Animals

Adult male Sprague-Dawley rats were obtained from Harlan (Indianapolis, IN) with weights ranging from 250-300 g. Rats were housed individually in shoebox cages in a temperature- and humidity-controlled room with a 12-hour light-dark cycle (lights on at 0600h, off at 1800h) and food and water *ad libitum*. All procedures and protocols were approved by the University of Cincinnati Institutional Animal Care and Use Committee (protocol: 04-08-03-01) and complied with the National Institutes of Health Guidelines for the Care and Use of Laboratory Animals. The cumulative sequence of procedures employed in the current experiments received veterinary consultation and all animals had daily welfare assessments by

veterinary and/or animal medical service staff. Signs of poor health and/or weight loss ≥ 20% of pre-surgical weight were *a priori* exclusion criteria. These criteria were not met by any animals in the current experiments.

Experiment 1

Design

For experiment 1, 32 rats (n = 8/group) were injected with either a lentiviral-packaged construct coding for vGluT1 siRNA or GFP as a control. After instrumentation with radiotelemetry devices, half of the animals were exposed to 14 days of CVS with the rest of the animals remaining as No CVS controls. All treatment assignments were randomized. Home cage cardiovascular parameters were continuously monitored in all rats throughout the 14-day period of CVS. On the morning of day 15, all rats were subject to an acute novel restraint to examine hemodynamic stress reactivity.

Viral construct

A lentivirus transfer vector, based on a third-generation, self-inactivating transfer vector was constructed as previously described (Myers et al., 2017; M. Wood et al., 2019). Briefly, a 363-bp piece of DNA from the rat vGluT1 complementary DNA was synthesized that included 151 bp of the 3' coding region and 212 bp of the 3' untranslated region. This corresponds to nucleotides 1656 to 2018 of GenBank accession no. NM_053859. This is a region of low homology with vGluT2 and vGluT3 and avoids all the putative transmembrane domains of the transporter. The fragment was cloned in antisense orientation into a lentivirus transfer vector that expressed an enhanced green fluorescent protein (GFP) reporter. This vector uses the phosphoglycerate kinase-1 promoter, which expresses well in rat brain and is primarily neuronal (Claudia A Grillo et al., 2015; Myers et al., 2017). A control virus was constructed similarly,

using a transfer vector with the phosphoglycerate kinase-1 promoter driving expression of enhanced GFP alone.

Stereotaxic surgery

Animals were anesthetized (90 mg/kg ketamine and 10 mg/kg xylazine, intraperitoneal) followed by analgesic (2 mg/kg butorphanol, subcutaneous) and antibiotic (5 mg/kg gentamicin, intramuscular) administration. Rats received bilateral 1 µL microinjections (5 x 10^6 tu/µL titer) into the IL (2.9 mm anterior to bregma, 0.6 mm lateral to midline, and 4.2 mm ventral from dura), as described previously(Jessica M. McKlveen et al., 2013; Myers et al., 2016, 2017), of either the vGluT1 siRNA virus or GFP control. All injections were carried out with a 25-gauge, 2-µL microsyringe (Hamilton, Reno, NV) using a microinjection unit (Kopf, Tujunga, CA) at a rate of 5 minutes/µL. To reduce tissue damage and allow diffusion, the needle was left in place for 5 minutes before and after injections. Animals recovered for 6 weeks before commencing experiments, corresponding to timeframes previously used for similar lentiviral systems (C.A. Grillo et al., 2007; Myers et al., 2017).

Telemetry

Four weeks after stereotaxic surgery, rats were implanted with radiotelemetry transmitters (PA-C40; Data Sciences International, St. Paul, MN) as previously described(Flak et al., 2011; Goodson et al., 2017). Briefly, animals were anesthetized with inhaled isoflurane anesthesia (1-5%). The descending aorta was exposed via an abdominal incision, allowing implantation of a catheter extending from the transmitter. The catheter was secured with tissue adhesive (Vetbond; 3M Animal Care Products, St. Paul, MN) and a cellulose patch. The transmitter body was then sutured to the abdominal musculature, followed by suturing of the abdominal musculature and closure of the skin with wound clips. Rats recovered for 2 weeks before wound clips were removed, and experiments began.

Chronic variable stress

CVS was comprised of twice daily (AM and PM) repeated and unpredictable stressors presented in a randomized manner, including exposure to a brightly-lit open field (1 m^2, 5 minutes), cold room (4°C, 1 hour), forced swim (23° to 27°C, 10 minutes), brightly-lit elevated platform (0.5 m, 5 minutes), shaker stress (100 rpm, 1 hour), and hypoxia (8% oxygen, 30 minutes). Additionally, overnight stressors were variably included, comprised of social crowding (6-8 rats/cage, 16 hours) and restricted housing (mouse cage, 16 hours). All animals went through the CVS paradigm concurrently. To prevent body weight differences between stress conditions, rats remaining unstressed in the home cage were food restricted in accordance with the reduced food intake induced by CVS(Flak et al., 2011, 2012). During the 2 weeks of CVS, unstressed animals received 80% of a food allotment prior to lights off and the other 20% after lights on to reduce the potential for fasting(Flak et al., 2011, 2012). On day 15, all rats were exposed to a novel acute restraint to directly compare the effects of vGluT1 knockdown on cardiovascular responses to acute and chronic stress.

Acute stress

The morning after completion of CVS (approximately 16 hours after the last stress exposure), all animals were subjected to a novel 40-minute restraint. Stress response assessment was initiated between 08:00 and 09:00 hours. Animals were placed in well-ventilated Plexiglass restraint tubes with baseline pressure and HR measurements collected in the one-hour period preceding restraint. After restraint, rats were returned to their home cage with pressure and HR recorded for 60 minutes after restraint.

Tissue collection

After acute restraint, all animals were euthanized with sodium pentobarbital (≥ 200 mg/kg, intraperitoneal) and transcardially perfused with 0.9% saline followed by 4% phosphate-buffered paraformaldehyde. Brains were postfixed in paraformaldehyde for 24 hours and then stored in 30% sucrose at 4°C. Brains were subsequently sectioned (30 µm-thick coronal sections) and processed for GFP immunohistochemistry to determine microinjection spread.

Immunohistochemistry

For single immunolabeling of GFP, tissue sections were washed in 50 mM KPBS and incubated in blocking buffer (50 mM KPBS, 0.1% bovine serum albumin, and 0.2% TritonX-100) for 1 hour at room temperature. Sections were placed in rabbit anti-GFP primary antibody (1:1000 in blocking buffer; Invitrogen, La Jolla, CA) overnight at 4°C. Following incubation, sections were rinsed and placed into Alexa488-conjugated donkey anti-rabbit immunoglobulin G (IgG; 1:500 in blocking buffer; Jackson Immunoresearch, West Grove, PA) for 30 minutes. Sections were rinsed, mounted onto slides, and cover slipped. Dual fluorescent immunolabeling was performed as described previously(Myers et al., 2017), with GFP labeled in sequence with vGluT1. vGluT1 was visualized with rabbit anti-vGluT1 primary antibody (1:1000; Synaptic Systems, Goettingen, Germany) followed by Cy3-conjugated donkey anti-rabbit IgG (1:500; Jackson ImmunoResearch, West Grove, PA).

Microscopy

For visualization of GFP and vGluT1 co-localization, digital images were captured from a 1-in-12 series with a Zeiss Axio Imager Z2 microscope using optical sectioning (63x objective) to permit co-localization within a given z-plane (0.5-□m thickness). Co-localizations were defined as white fluorescence from overlap between labeled GFP terminals and magenta-colored vGluT1. For each figure, brightness and contrast were enhanced uniformly using Adobe Photoshop (CC 14.2).

Data analysis

Data are expressed as mean +/- standard error of the mean (SEM). Quantification was conducted by experimenters blind to conditions. All analyses were conducted using GraphPad Prism (version 7.04) for 2-way ANOVA, R Studio (version 3.4.2) for 3-way repeated measures ANOVA, or Dataquest A.R.T. (version 4.3) for telemetry analysis. Over the course of CVS, activity, HR, arterial pressures, and pulse pressure were sampled in the home cage. Samples were collected during the light phase from 06:00-08:00 for AM measures (prior to the first stressor of the day) and during the dark phase from 19:00-21:00 for the PM period (at least 2 hours after the second stressor of the day). During each 2-hour time period, samples were averaged into 10-minute bins for analysis. Beginning the day before CVS, circadian curves were generated for each parameter over the 15-day period. Data over time (both CVS and acute restraint) were analyzed by 3-way repeated measures analysis of variance (ANOVA); with viral treatment, stress, and time (repeated) as factors. When significant main effects were reported, ANOVA was followed by Tukey post-hoc test to identify specific group differences. Area under the curve (AUC) for the 15 days of CVS or 100 minutes of acute stress was calculated by summing the average values acquired between two time points multiplied by the time elapsed [Σ(Time 1 + Time 2)/2)*Time elapsed]. Statistical significance for cumulative measures was determined by 2-way ANOVA with treatment and stress as factors. ANOVA was followed by Tukey post-hoc tests in the case of significant main effects. Values more than 2 standard deviations from the mean were removed as outliers. No animals were removed from the study as outliers but specific time points for telemetry recordings were identified as outliers based on deviation from the mean. These exclusion criteria were developed *a priori* and applied uniformly. The excluded data points were found to represent non-physiological parameters (e.g. HR < 200 beats/minute). Statistical significance was reported as ($p < 0.05$) for all tests.

Experiment 2

Design

Experiment 2 employed a similar design as experiment 1. Male rats (n = 7/group) received IL injections of lentiviral-packaged vGluT1 siRNA or GFP and experienced CVS or remained unstressed. All treatment assignments were randomized. On day 15, thoracic aorta was collected to examine vasoreactivity and histology. Additionally, hearts and brains were collected for histological analyses.

Chronic variable stress

For experiment 2, CVS was staggered based on the throughput of vascular function experiments. Seven cohorts (n = 4 animals/cohort, one animal for each treatment group) began the CVS paradigm one day apart so that each cohort of 4 would have tissue collected on successive days. All rats undergoing CVS in experiment 2 received the same stressors in the same sequence. The CVS paradigm was similar to experiment 1, except for the substitution of restraint (30 minutes) for crowding.

Tissue collection

The morning of day 15, approximately 16 hours after the last stress exposure, all animals were rapidly anesthetized with isoflurane (5%) and decapitated. Thoracic aorta was collected by dissecting 4 mm of aortic tissue proximal to the diaphragm for vascular function analysis. Additional aortic tissue was collected proximal to the initial sample and post-fixed in paraformaldehyde for histological analysis. Hearts were also collected and post-fixed in paraformaldehyde for histological analysis. Brains were post-fixed and subsequently sectioned and processed for GFP immunohistochemistry to determine microinjection spread as described for experiment 1.

Vascular function

Aortic tissue samples were processed for wire myographic vasoreactivity analyses as previously described (Basford et al., 2013). Briefly, vessels were kept in warm, oxygenated Krebs's solution with connective tissue and adipose removed under a dissecting microscope. Aortic rings were then placed on wires in organ baths (Radnoti, Covina, CA), equilibrated, and brought to tension. Vasoconstriction was assessed in response to increasing concentrations of the endothelial-dependent potassium chloride (KCl; 0 to 50 mM) and endothelial-independent phenylephrine ($1x10^{-6}$ to $1x10^{-2}$ mM). Vessels were then set to 80% of maximum phenylephrine-induced constriction and relaxation was determined in response to endothelial-dependent acetylcholine ($1x10^{-6}$ to $1x10^{-2}$ mM) and endothelial-independent sodium nitroprusside (SNP; $1x10^{-7}$ to $3x10^{-3}$ mM). At the end of the experiment, all vessels were weighed and measured (length, circumference, and area) to verify equal dimensions across all groups.

Histology and microscopy

Cardiac and aortic tissue was processed by the Cincinnati Children's Hospital Medical Center Research Pathology Core. Briefly, aortas were paraffin-embedded, sectioned (5 µm), and stained. Verhoeff-Van Gieson (VVG) was used to quantify elastin in the tunica media and Masson's Trichrome to quantify collagen in the tunica adventitia as previously described (Basford et al., 2013; Goodson et al., 2017). Paraffin-embedded hearts were oriented for four-chamber view, sectioned (5 µm), and stained with Masson's Trichrome to visualize collagen and wheat germ agglutinin (WGA) conjugated to Alexa488 to visualize myocyte cell membranes as previously described(Basford et al., 2013; Gupta et al., 2016). Vascular and heart tissue were imaged with a Zeiss AxioObserver microscope using a color camera and 10x objective.

Data analysis

Data are expressed as mean ± SEM. Quantification was conducted by experimenters blind to conditions. All analyses were conducted using GraphPad Prism (version 7.04) for 2-way

ANOVA, R Studio (version 3.4.2) for 3-way repeated measures ANOVA, or FIJI (version 1.51N) for histological quantification. Vasoreactivity data were analyzed by 3-way repeated measures ANOVA; with viral treatment, stress, and drug concentration (repeated) as factors. When significant main effects were reported, ANOVA was followed by Tukey post-hoc test to identify specific group differences. FIJI (version 1.51N) was used to quantify lumen and tunica media dimensions in VVG-stained aorta, as well as adventitia dimensions in Masson's Trichrome-stained tissue. FIJI was also used to quantify collagen density in hearts stained with Masson's Trichrome. For each animal, 6 sections of aorta or heart were quantified and averaged. To determine myocyte surface area, FIJI was used to binarize myocyte images. This technique produced dark cytoplasm and bright membranes in cardiomyocytes (Bensley et al., 2016). The dark cytoplasm was used to calculate surface areas of the myocytes in the apex and lateral wall of the left ventricle. For each animal, approximately 100 cells were counted from 6 heart sections and averaged. Statistical significance for histological measures was determined by 2-way ANOVA with treatment and stress as factors. ANOVA was followed by Tukey post-hoc tests in the case of significant main effects. Statistical significance was reported as ($p < 0.05$) for all tests.

Results

vGluT1 knockdown

Injections of a lentiviral-packaged construct expressing vGluT1 siRNA were targeted to the IL (Fig. 2.1A, 2.1B). Viral injections were largely limited to the deep layers of IL, with minimal spread to the prelimbic cortex (PL). We have previously shown that this approach reduces vGluT1 mRNA specifically in the IL, as well as vGluT1 protein co-localization with GFP-labeled terminals (Myers et al., 2017). In the current study, tissue from rats injected with a GFP control construct exhibited substantial co-localization with vGluT1 protein on cortico-cortical axonal

processes (Fig. 2.1C). IL projections transfected with the vGluT1 siRNA construct had reduced co-localization with vGluT1 protein (Fig. 2.1D).

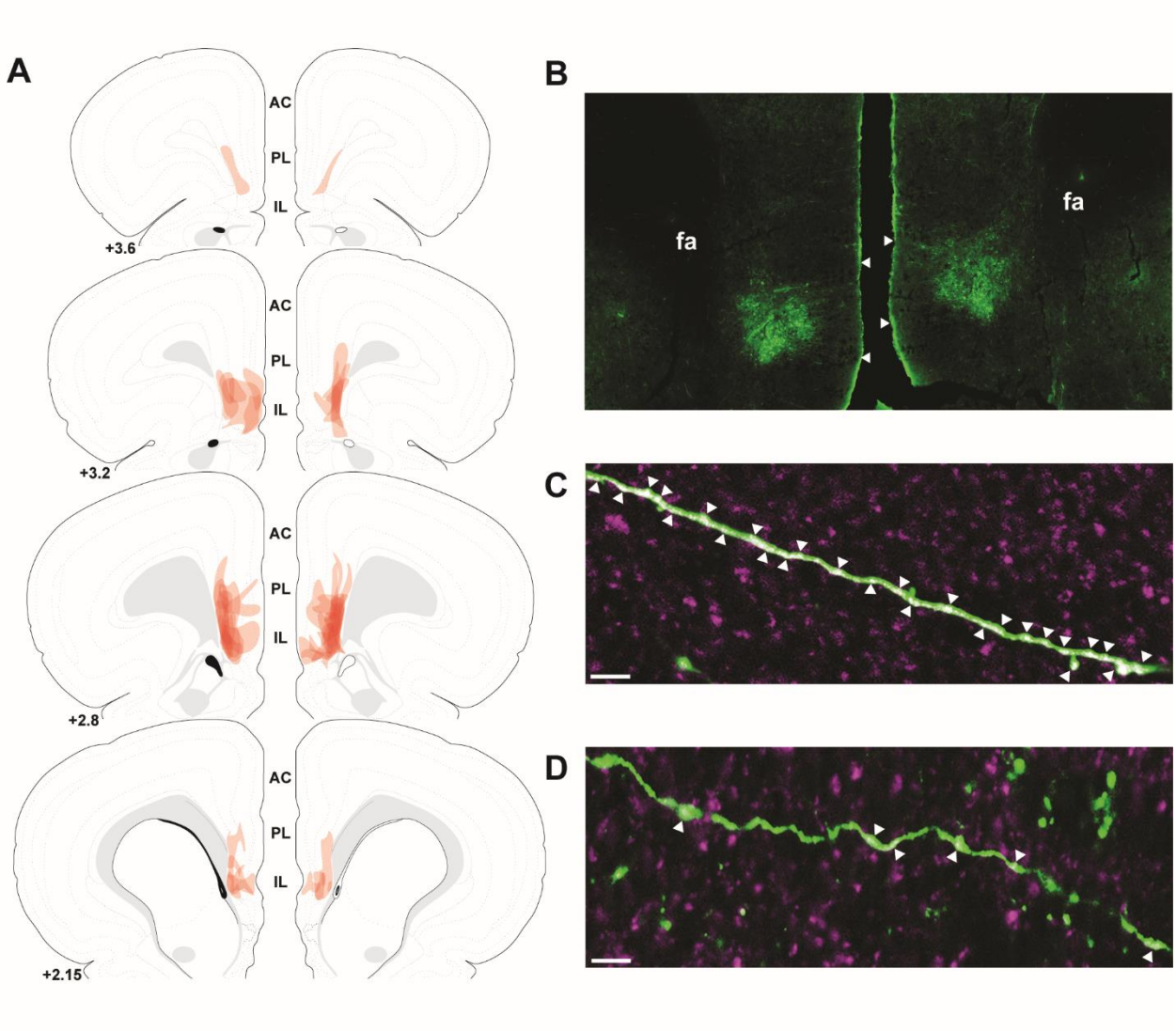

Figure 2.1. The spread of individual lentiviral injections was traced on photomicrographs and overlaid onto atlas templates from Swanson(Swanson, 2004) to depict the localization of vGluT1 knockdown in experiment 1 (A). Lentiviral injections targeted to the IL with minimal spread to the PL (B). White arrows indicate dorsal and ventral boundaries of the IL. Immunolabeling of GFP (green) and vGluT1 (magenta) indicated a high-degree of co-localization (white arrows) on IL projections in GFP controls (C). Knockdown of vGluT1 with siRNA treatment decreased vGluT1 co-localization with GFP on IL projections (D). Scale bars: (B) 100 µm, (C,D) 10 µm. Numbers indicate distance rostral to bregma in millimeters. AC: anterior cingulate, PL: prelimbic cortex, IL: infralimbic cortex, fa: anterior forceps of the corpus callosum.

Body weight and food intake

Chronic stress reduces food intake and body weight gain, leading to significant differences in body composition compared to control animals (Flak et al., 2011; Myers et al., 2017; Smith et al., 2017; Solomon et al., 2010). As this may confound results related to HR and blood pressure reactivity (Flak et al., 2011), animals in the No CVS groups for both experiments 1 and 2 received mild food restriction to match body weight with CVS rats (Table 2.1). In both experiments, there were no significant differences in body weight between groups. However, food restriction in experiment 1 led to food consumption that was significantly greater than the CVS groups [$F(1,28) = 31.24$, $p < 0.0001$]. In experiment 2, food restriction significantly decreased food intake compared to CVS groups [$F(1,24) = 33.25$, $p < 0.0001$].

Table 2.1. Body weight of animals at the beginning and end of CVS for experiments 1 and 2. In both experiments, CVS rats had *ad libitum* access to chow while No CVS animals received mild food restriction to prevent significant differences in body weight between chronically stressed animals and controls. $^{\#}p < 0.05$ CVS GFP vs. No CVS GFP, $^{\wedge}p < 0.05$ CVS siRNA vs. No CVS GFP, $^{\&}p < 0.05$ CVS siRNA vs. No CVS siRNA.

Table 2.1 Body weight and food intake throughout chronic variable stress

	Group	Body Weight CVS Day 1 (g)	Body Weight CVS Day 13 (g)	Daily Food Intake (g)
Experiment 1 n = 8/group	No CVS GFP	389.78 ± 6.21	405.06 ± 6.14	21.04 ± 0.36
	No CVS siRNA	389.84 ± 12.23	405.85 ± 12.13	21.68 ± 0.53
	CVS GFP	402.03 ± 7.45	404.19 ± 8.57	18.82 ± 0.30$^{\#}$
	CVS siRNA	417.16 ± 6.79	417.64 ± 6.25	18.89 ± 0.35$^{\wedge\&}$
Experiment 2 n = 7/group	No CVS GFP	372.83 ± 7.72	363.80 ± 7.15	15.08 ± 0.45
	No CVS siRNA	379.19 ± 5.03	368.00 ± 4.73	15.35 ± 0.29
	CVS GFP	381.44 ± 9.07	378.10 ± 9.33	17.44 ± 0.53$^{\#}$
	CVS siRNA	384.69 ± 5.10	379.49 ± 3.64	17.78 ± 0.35$^{\wedge\&}$

Experiment 1

Circadian behavioral activity

Home cage radiotelemetry data were analyzed for 15 days beginning the day before CVS. Throughout CVS, 3-way repeated-measures ANOVA of circadian activity (n = 7-8/group) revealed a main effect of time [$F(29, 930) = 21.38$, $p < 0.0001$] and interactions of stress x treatment [$F(1, 930) = 4.67$, $p = 0.031$] and stress x time [$F(29, 930) = 4.34$, $p < 0.0001$]. Post-hoc analysis indicated that, during the dark period of CVS day 2, rats that were subjected to an overnight crowding stressor exhibited more activity than No CVS controls (Fig. 2.2A). The CVS GFP rats had elevated activity compared to No CVS GFP controls ($p = 0.014$); furthermore, CVS siRNA animals were more active than CVS GFP rats ($p = 0.007$). In addition to overnight social crowding on day 2, rats experienced overnight housing in mouse cages days 6 and 10. Throughout the dark periods of days 6-9, CVS siRNA rats had decreased activity compared to No CVS animals ($p \leq 0.047$). Additionally, the CVS GFP rats were less active on the dark periods of days 9 ($p = 0.008$) and 14 ($p = 0.003$) compared to No CVS GFP. Also, on the dark period of Day 14, the CVS siRNA group was more active than CVS GFP ($p = 0.003$). Additional analysis was carried out on cumulative activity counts (No CVS GFP: 801.88 ± 1.04, No CVS siRNA: 819.29 ± 8.08, CVS GFP: 683.66 ±1.38, CVS siRNA: 860.81 ± 4.46). According to 2-way ANOVA, there were significant effects of treatment [$F(1,27) = 338.60$, $p < 0.0001$], stress [$F(1,27) = 60.38$, $p < 0.0001$], and a treatment x stress interaction [$F(1,27) = 261.9$, $p < 0.0001$]. Tukey post-hoc test indicated that total activity over 15 days was lower in CVS GFP rats compared to No CVS GFP ($p < 0.0001$). In contrast, cumulative activity was increased in CVS siRNA rats compared to all other groups ($p < 0.0001$).

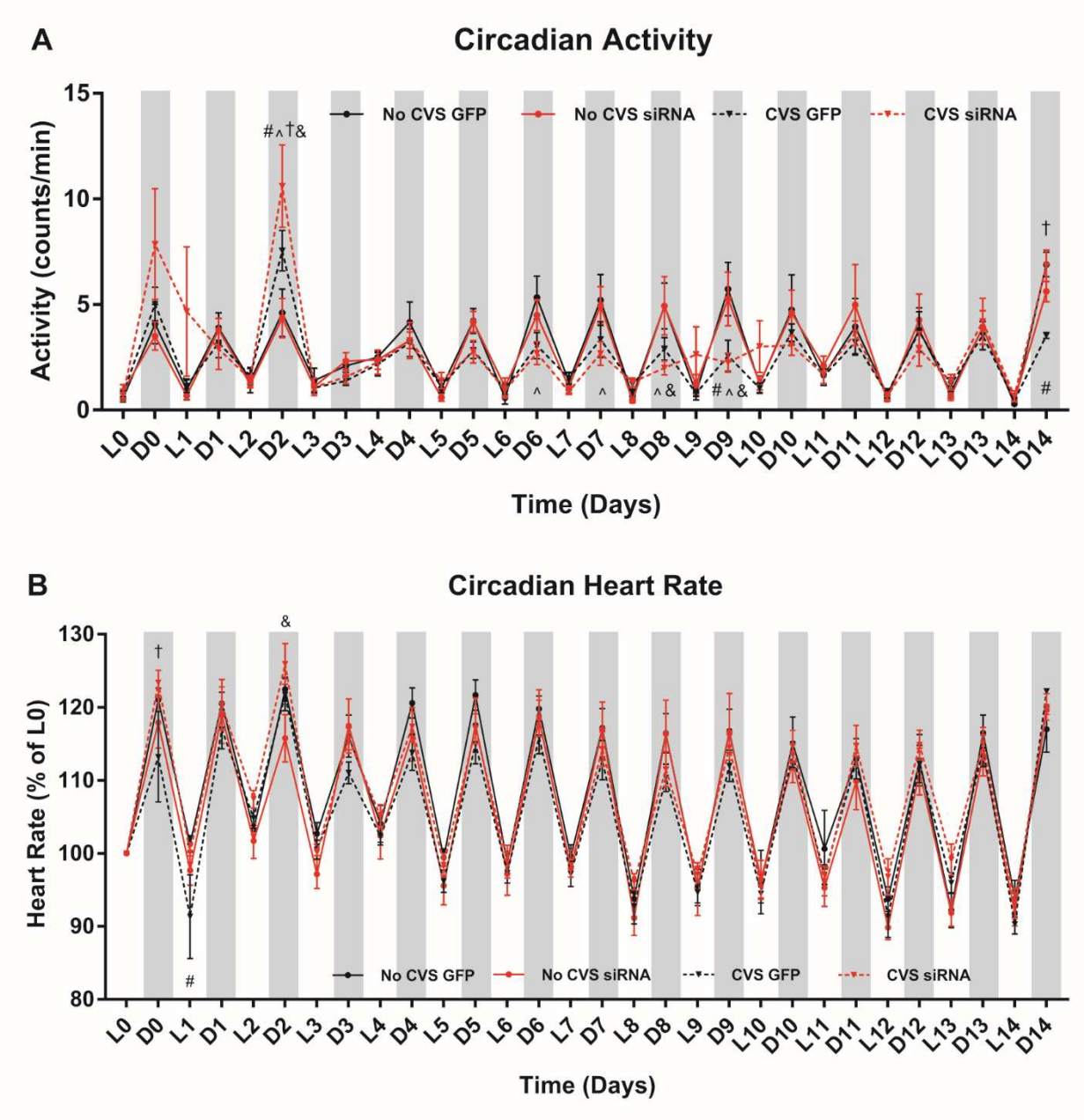

Figure 2.2. Chronically stressed rats had disrupted circadian behavioral rhythms evidenced by interactions of CVS and siRNA, as well as CVS and time (n = 7-8/group) (A). Circadian heart rate also exhibited a CVS x siRNA interaction (n = 8/group) leading to heart rate disruptions early in CVS (B). $^{\#}p < 0.05$ CVS GFP vs. No CVS GFP, $^{\wedge}p < 0.05$ CVS siRNA vs. No CVS GFP, $^{\dagger}p < 0.05$ CVS siRNA vs. CVS GFP, $^{\&}p < 0.05$ CVS siRNA vs. No CVS siRNA.

Circadian heart rate

Home cage HR (n = 8/group) was analyzed by 3-way repeated-measures ANOVA revealing a main effect of time, [$F(29, 960) = 72.64$, $p < 0.0001$] accompanied by a stress x

treatment interaction [$F(1, 960) = 28.71$, $p < 0.0001$]. Early in CVS (Fig. 2.2B), the CVS siRNA group had elevated dark phase HR compared to the CVS GFP group (Day 0, $p = 0.024$), as well as the No siRNA group during overnight social crowding (Day 2, $p = 0.024$). Also, on the first light period of CVS, the CVS GFP HR was decreased compared to No CVS GFP ($p = 0.028$).

Circadian and cumulative arterial pressures

In order to examine the effects of chronic stress and decreased IL output on long-term blood pressure regulation, home cage arterial pressures (n = 6-8/group) were continuously monitored. For mean arterial pressure (MAP), 3-way repeated-measures ANOVA found main effects of stress [$F(1, 900) = 15.33$, $p < 0.0001$] and time [$F(29, 900) = 13.91$, $p < 0.0001$], as well as an interaction of stress x treatment [$F(1, 900) = 14.41$, $p < 0.0001$]. In terms of time-specific effects, there was an increase in MAP in the CVS siRNA group compared to No CVS siRNA ($p = 0.022$, Fig. 2.3A) during the light period of CVS day 1. While few time point-specific circadian effects were identified, AUC analysis found that the CVS siRNA group experienced greater cumulative MAP ($p < 0.0001$, Fig. 2.3B) and systolic arterial pressure (SAP, $p < 0.0001$, Fig. 2.3B) than all other groups. Diastolic arterial pressure (DAP, $p < 0.0001$, Fig. 2.3D) was also elevated in the CVS siRNA animals compared to No CVS siRNA and CVS GFP. Between non-stressed rats, the siRNA treatment led to lower cumulative pressures (MAP, SAP, and DAP, $p < 0.0001$) relative to GFP.

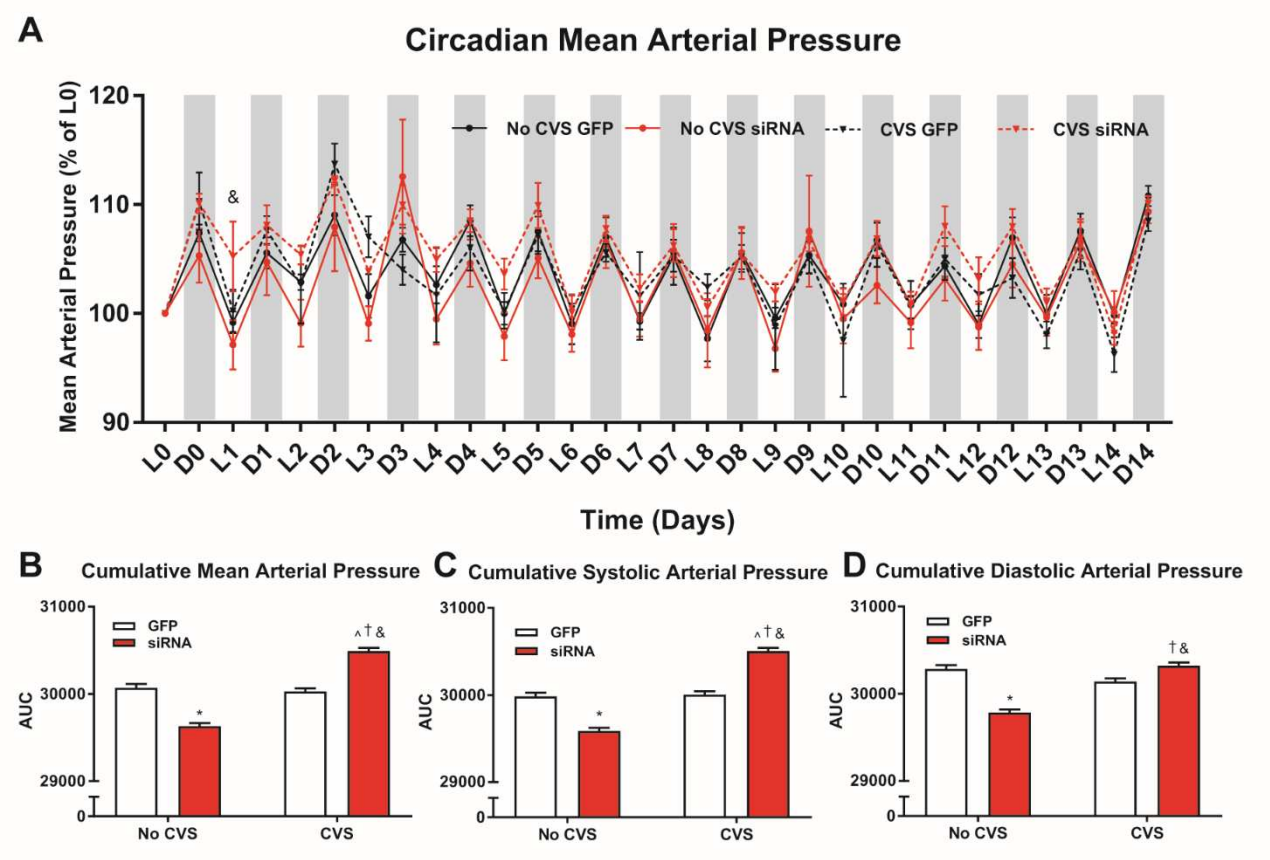

Figure 2.3. Chronic stress and siRNA treatment (n = 8/group) interacted leading to altered circadian arterial pressure (A). Analysis of cumulative arterial pressure indicated that CVS, only in siRNA-treated rats, increased chronic MAP (b), SAP (c), and DAP (d).
*p < 0.05 No CVS siRNA vs. No CVS GFP, ^p < 0.05 CVS siRNA vs. No CVS GFP, †p < 0.05 CVS siRNA vs. CVS GFP, &p < 0.05 CVS siRNA vs. No CVS siRNA.

Circadian and cumulative pulse pressure

Pulse pressure is a function of vascular stiffness and predicts heart disease independent of MAP(Franklin et al., 1999; Glasser et al., 2014). Three-way repeated-measures ANOVA identified a main effect of stress [F (1, 900) = 34.35, p < 0.0001] and an interaction of stress x treatment [F(29, 900 = 2.59, p < 0.0001] for circadian pulse pressure. Over the course of CVS, the only time-specific difference in circadian pulse pressure occurred during the dark phase of day 0 (Fig. 2.4A) where the CVS GFP pulse pressure was greater than No CVS GFP (p = 0.01, n = 6-8/group). Cumulative pulse pressure from AUC analysis was increased in both CVS

groups relative to No CVS ($p < 0.0001$, Fig 2.4b). Additionally, CVS siRNA cumulative pulse pressure was greater than all groups, including CVS GFP ($p < 0.0001$).

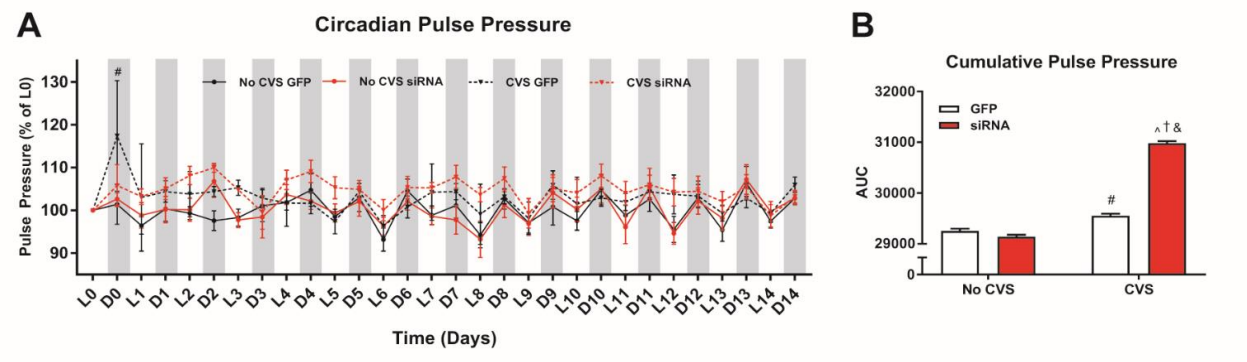

Figure 2.4. Chronic stress and siRNA treatment (n = 6-8/group) interacted to affect circadian pulse pressure (A). Cumulative pulse pressure was increased in CVS exposed rats with CVS siRNA rats experiencing the greatest chronic pulse pressure (B). $^{\#}p < 0.05$ CVS GFP vs. No CVS GFP, $^{\wedge}p < 0.05$ CVS siRNA vs. No CVS GFP, $^{\dagger}p < 0.05$ CVS siRNA vs. CVS GFP, $^{\&}p < 0.05$ CVS siRNA vs. No CVS siRNA.

Acute stress reactivity

In order to study the role of the IL in acute stress reactivity, MAP and HR reactivity were monitored during restraint (n = 8/group). During acute stress, 3-way repeated-measures ANOVA of HR reactivity found a main effect of time [$F(1, 84) = 53.99$, $p < 0.0001$] (Fig. 2.5A). Compared to No CVS GFP, vGluT1 siRNA elevated HR during restraint minutes 15-25 ($p \leq 0.040$). Both CVS GFP and CVS siRNA rats had elevated HR compared to No CVS GFP from 10-25 minutes of restraint ($p \leq 0.006$). Further, CVS siRNA rats had elevated HR during restraint at 35 and 40 minutes ($p \leq 0.008$). While recovering from stress in the home cage, HR remained elevated in the CVS siRNA group relative to No CVS GFP at minutes 45 and 95 ($p \leq 0.010$). Additionally, CVS GFP and No CVS siRNA had elevated HR on minutes 45 ($p = 0.0003$) and 95 ($p = 0.031$), respectively. Cumulative HR reactivity from AUC analysis of acute stress responses revealed that both No CVS siRNA and CVS GFP groups had elevated HR responses to acute restraint ($p < 0.0001$, Fig. 2.5B). Moreover, the CVS siRNA group experienced greater cumulative HR than all other groups ($p = 0.0006$).

Analysis of stress-evoked MAP by 3-way repeated-measures ANOVA identified a main effect of time [$F(1, 84) = 99.91$, $p < 0.0001$] (Fig. 2.5c). The CVS GFP group had greater MAP reactivity compared to No CVS GFP on minutes 5-15 of restraint ($p \leq 0.030$). The CVS siRNA animals had greater MAP than No CVS GFP at 15, 20, and 40 minutes ($p \leq 0.05$). During recovery, CVS GFP MAP remained elevated at 50, 75, and 80 minutes ($p \leq 0.04$); furthermore, CVS siRNA MAP was higher at minutes 75-90 ($p \leq 0.045$). AUC analysis by 2-way ANOVA found siRNA treatment increased cumulative MAP ($p < 0.0001$, Fig. 2.5D). CVS also increased MAP AUC as both CVS groups were higher than respective No CVS controls ($p < 0.0001$).

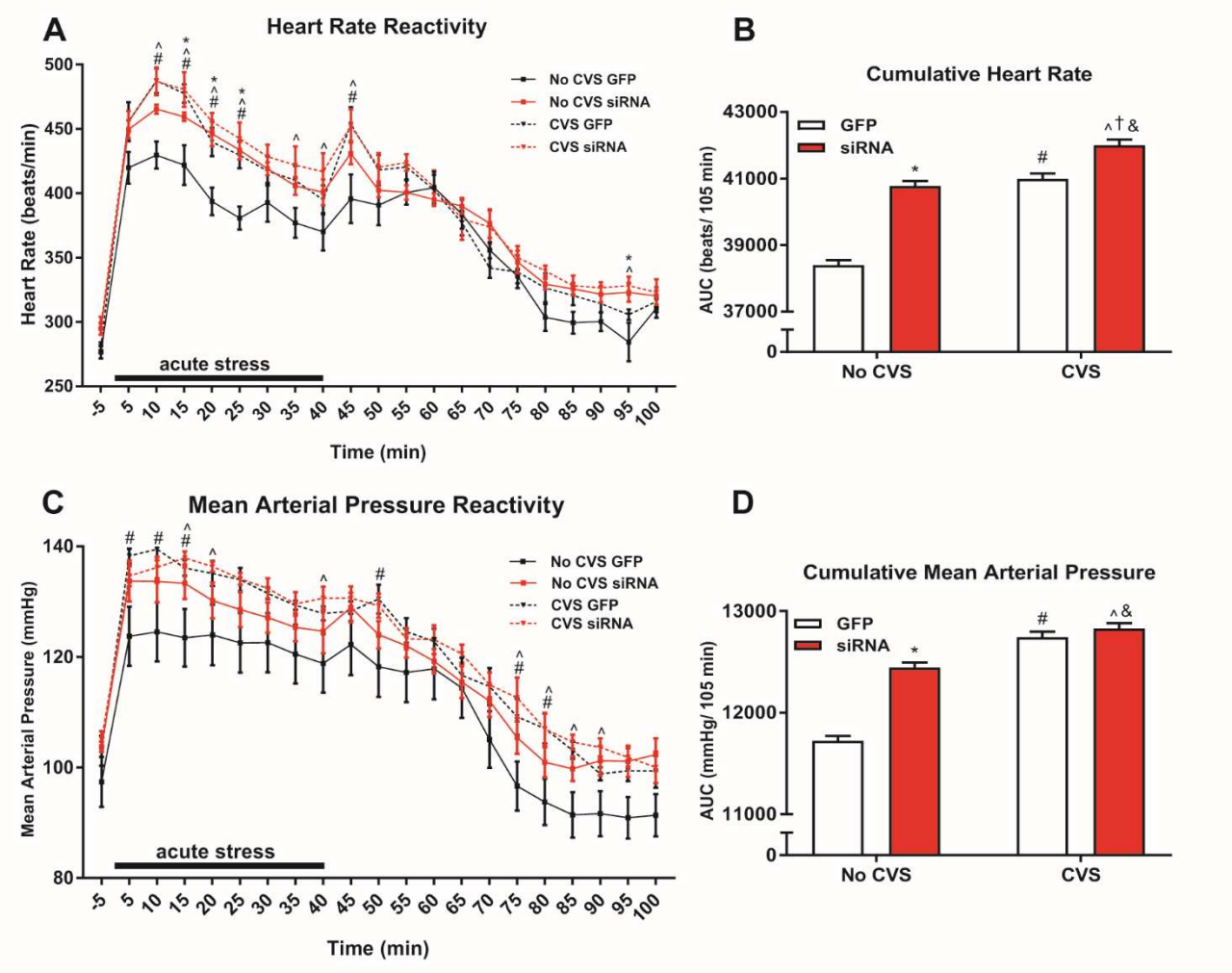

Figure 2.5. In response to acute restraint, both siRNA and CVS (n = 8/group) increased heart rate reactivity and impaired recovery (A). Cumulative acute heart rate responses were also elevated by siRNA and CVS but CVS siRNA rats had the greatest overall heart rate response (B). Chronically stressed rats, both GFP and siRNA treated, had increased MAP reactivity and

impaired recovery (C). Analysis of cumulative restraint-induced pressor responses indicated effects of both siRNA and CVS (D). *$p < 0.05$ No CVS siRNA vs. No CVS GFP, $^{\#}p < 0.05$ CVS GFP vs. No CVS GFP, ^$p < 0.05$ CVS siRNA vs. No CVS GFP, $^{\dagger}p < 0.05$ CVS siRNA vs. CVS GFP, $^{\&}p < 0.05$ CVS siRNA vs. No CVS siRNA.

Experiment 2

Injection placement

Similar to experiment 1, injections of lentiviral-packaged constructs were targeted to the IL with minimal spread to PL (Fig. 2.6). Although, injections from experiment 2 had greater spread into superficial layers of the IL. Additionally, some injections spread into the striatum caudally but this region does not exhibit vGluT1 expression(Ziegler et al., 2002).

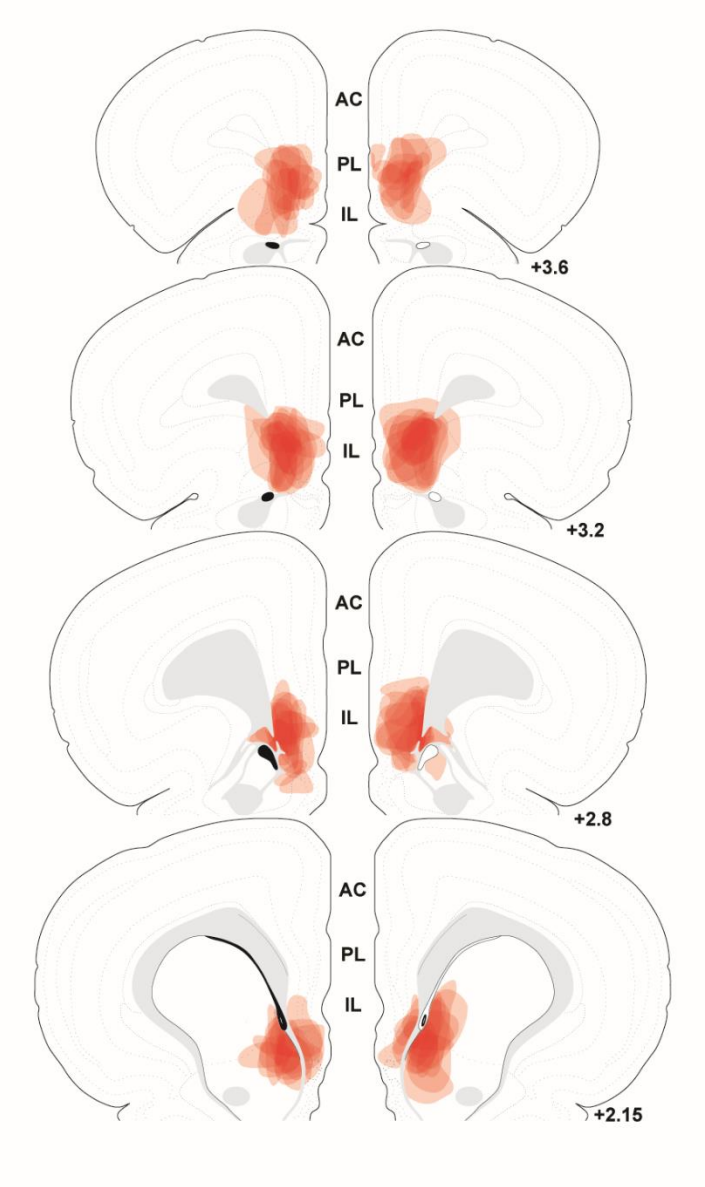

Figure 2.6. The spread of individual lentiviral injections was traced on photomicrographs and overlaid onto atlas templates from Swanson(Swanson, 2004) to depict the localization of vGluT1 knockdown in experiment 2. White arrows indicate dorsal and ventral boundaries of the IL. Numbers indicate distance rostral to bregma in millimeters. AC: anterior cingulate, PL: prelimbic cortex, IL: infralimbic cortex.

Vascular function

In order to assess the vascular consequences of prolonged stress, arterial function was monitored in response to endothelial-dependent and -independent agents *ex vivo*. In terms of endothelial-dependent vasoconstriction, 3-way repeated-measures ANOVA identified a main

effect of KCl concentration [$F(1,36) = 669.73$, $p < 0.0001$] and an interaction of drug concentration x viral treatment [$F(1,36) = 9.55$, $p = 0.004$] (Fig. 2.7A). As determined by post-hoc analyses, aortas of CVS siRNA animals constricted less than No CVS GFP at KCl concentrations above 25 mM ($p \leq 0.0006$). CVS siRNA also showed impaired constriction compared to CVS GFP at concentrations above 30 mM ($p \leq 0.006$). Compared to No CVS siRNA, CVS siRNA vasoreactivity was decreased at concentrations of 30 and 50 mM ($p \leq 0.042$). Within the No CVS groups, siRNA treatment decreased constriction at 40 mM ($p = 0.019$). Endothelium-independent vasoconstriction in response to phenylephrine showed a main effect of concentration [$F(1,40) = 31.62$, $p < 0.0001$] (Fig. 2.7B). Either siRNA or CVS alone impaired vasoreactivity at drug concentrations above 1 µM ($p < 0.05$). However, CVS siRNA animals had impaired vasoconstriction compared to all other groups at phenylephrine concentrations above 0.1 µM ($p < 0.05$).

Endothelial-dependent vasorelaxation to acetylcholine showed a main effect of drug concentration [$F(1,40) = 15.89$, $p = 0.0003$] by 3-way repeated-measures ANOVA (Fig. 2.7C). Post-test found that CVS siRNA vasorelaxation was decreased compared to all groups at acetylcholine concentrations above 1 µM ($p = 0.048$). Endothelial-independent vasorelaxation to SNP, as analyzed by 3-way repeated-measures ANOVA, showed a main effect of SNP concentration [$F(1,44) = 12.65$, $p = 0.0009$] (Fig. 2.7D). CVS siRNA tissue had impaired vasorelaxation compared to both No CVS groups at concentrations above of 0.03 µM ($p = 0.026$). Additionally, CVS alone impaired vasorelaxation in GFP rats at SNP concentrations above 0.3 µM ($p < 0.010$).

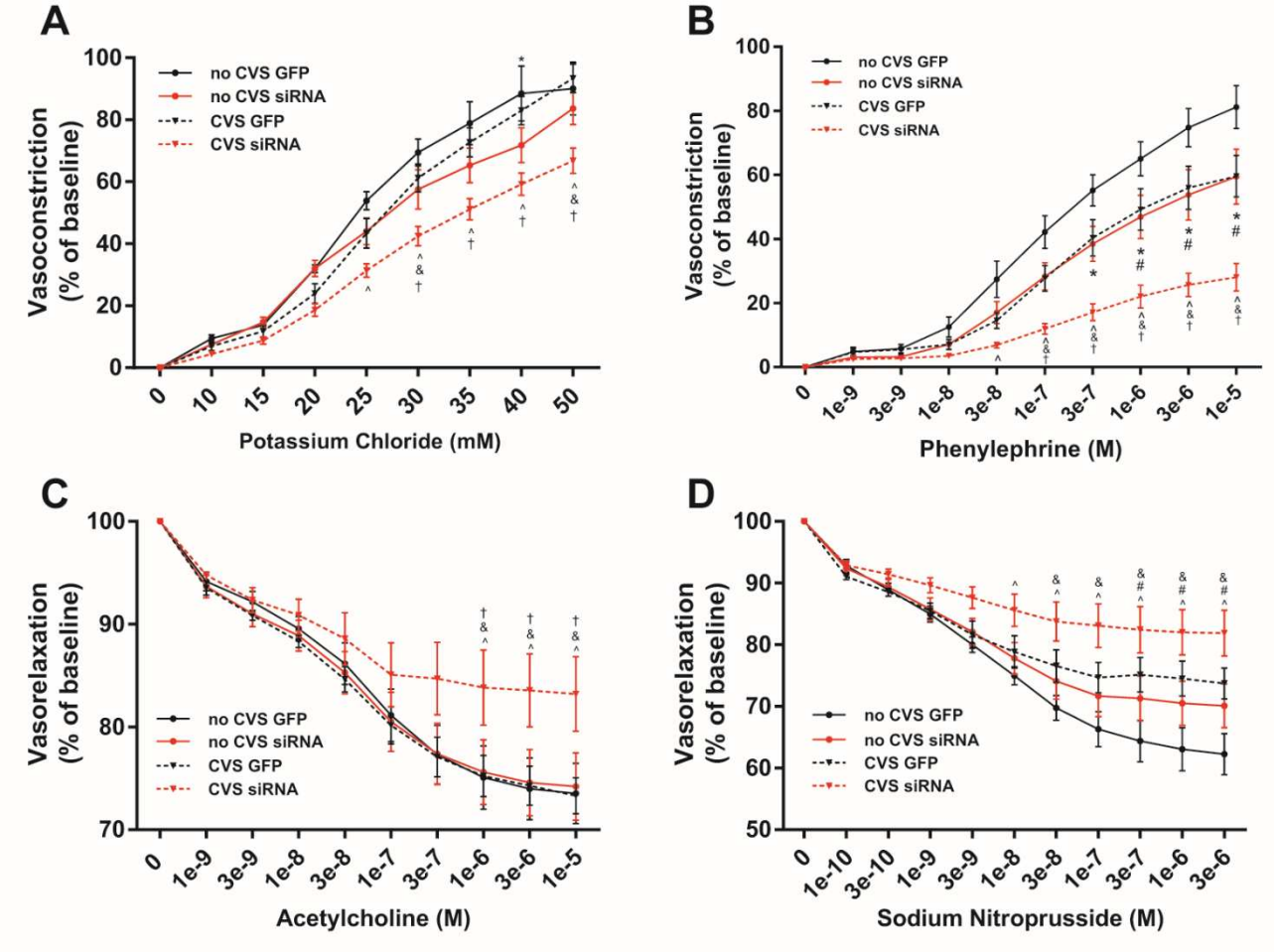

Figure 2.7. Aortic tissue from CVS siRNA animals (n = 7/group) had impaired endothelial-dependent vasoconstriction (A). Both CVS and siRNA impaired endothelial-independent vasoreactivity but the CVS siRNA group had the greatest impairment (B). Endothelial-dependent vasorelaxation was impaired only in the CVS siRNA group (C), while endothelial-independent relaxation was impaired in CVS GFP and CVS siRNA tissue (D). *$p < 0.05$ No CVS siRNA vs. No CVS GFP, $^{\#}p < 0.05$ CVS GFP vs. No CVS GFP, ^$p < 0.05$ CVS siRNA vs. No CVS GFP, $^{\dagger}p < 0.05$ CVS siRNA vs. CVS GFP, $^{\&}p < 0.05$ CVS siRNA vs. No CVS siRNA.

Vascular and cardiac histology

Histological analysis was carried out to investigate the effects of chronic stress and vGluT1 knockdown on markers of vascular and cardiac pathology (Table 2.2). In GFP-injected rats, CVS increased aortic tunica media thickness [$F(1,24) = 18.55$, $p = 0.0002$] and media:lumen area [$F(1,24) = 10.45$, $p < 0.004$]. Furthermore, CVS increased adventitial fibrosis in terms of increased collagen density [$F(1,24) = 4.944$, $p = 0.036$]. Chronic stress also affected

the myocardium by increasing heart weight [$F(1,24) = 7.028$, $p = 0.014$] and myocyte surface area [$F(1,23) = 5.084$, $p = 0.034$]. In animals with reduced vGluT1, CVS had greater effects on aortic remodeling. CVS siRNA rats had decreased luminal circumference [$F(1,24) = 8.217$, $p = 0.022$] and area [$F(1,24) = 8.142$, $p = 0.026$], increased media thickness [$F(1,24) = 18.55$, $p = 0.026$] and media:lumen area [$F(1,24) = 10.45$, $p < 0.0004$], increased collagen density [$F(1,24) = 4.944$, $p = 0.036$] and decreased adventitial thickness [$F(1,24) = 6.517$, $p = 0.031$] (Fig. 8A-D). Collectively, these results indicate that CVS interacts with decreased IL function to promote fibrosis and inward remodeling of vascular muscle leading to restricted luminal area, potentially accounting for impaired vasoreactivity and arterial stiffness. CVS siRNA rats also exhibited cardiac hypertrophy as these animals had increased heart weight [$F(1,24) = 7.028$, $p = 0.014$], heart weight relative to body weight [$F(1,24) = 17.09$, $p = 0.015$], and increased myocyte surface area [$F(1,23) = 5.084$, $p = 0.034$] (Fig. 8E, F), without affecting myocardial collagen deposition.

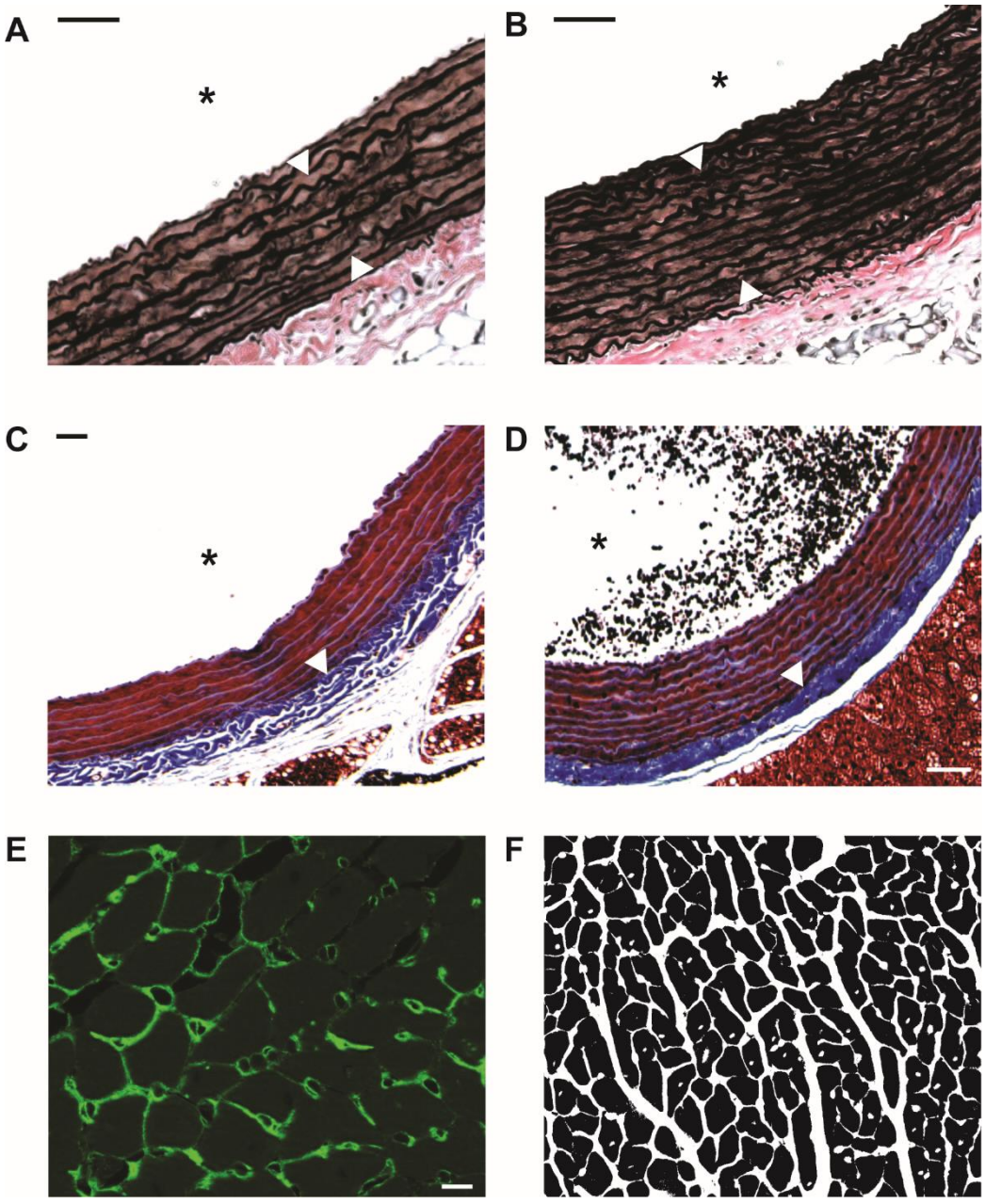

Figure 2.8. Verhoeff-van Gieson stain was used to visualize elastin (dark brown) in aortic tissue of No CVS GFP (A) and CVS siRNA (B) rats. Greater thickness of the tunica media is indicated by white arrows. Masson's Trichrome was used to stain collagen (blue) in aortic tissue of No CVS GFP (C) and CVS siRNA (D) animals. White arrows indicate increased collagen density in the tunica adventitia. Wheat germ agglutinin conjugated to Alexa 488 (green) was used to visualize cardiomyocyte membranes (E). Binarized myocyte images (F) were used to quantify myocyte surface area. Scale bars: (A-D) 50 µm, (E) 10 µm. * denotes the lumen.

Table 2.2. Histological quantification of vascular and myocardial structure. Dimensions of the lumen and media were quantified from elastin staining. Adventitial size and fibrosis were determined from collagen staining. Myocyte surface area was measured with membrane labeling and cardiac fibrosis was queried via collagen staining. There were no effects of siRNA alone. CVS increased media thickness, adventitial collagen, and myocyte size. In contrast, CVS siRNA tissue exhibited alterations in all structural endpoints assessed except myocardial fibrosis. $^{\#}p < 0.05$ CVS GFP vs. No CVS GFP, $^{\wedge}p < 0.05$ CVS siRNA vs. No CVS GFP, $^{\&}p < 0.05$ CVS siRNA vs. No CVS siRNA.

Table 2.2 Vascular and cardiac histological analysis

n = 7/group	No CVS GFP	No CVS siRNA	CVS GFP	CVS siRNA
Luminal Circumference (mm)	4.967 ± 0.058	5.135 ± 0.058	4.897 ± 0.069	4.893 ± 0.019$^{\&}$
Luminal Area (mm^2)	1.694 ± 0.035	1.786 ± 0.037	1.619 ± 0.037	1.550 ± 0.089$^{\&}$
Media Thickness (mm)	0.107 ± 0.001	0.108 ± 0.002	0.113 ± 0.001$^{\#}$	0.114 ± 0.001$^{\wedge\&}$
Media:Lumen Area	0.341 ± 0.009	0.335 ± 0.014	0.381 ± 0.005$^{\#}$	0.392 ± 0.024$^{\wedge\&}$
Adventitia Collagen (% area)	66.93 ± 1.320	66.82 ± 0.893	71.49 ± 2.313$^{\#}$	70.86 ± 2.659$^{\wedge\&}$
Adventitia Thickness	0.040 ± 0.001	0.037 ± 0.002	0.036 ± 0.002	0.034 ± 0.001$^{\wedge}$
Heart Weight (g)	1.264 ± 0.018	1.266 ± 0.038	1.321 ± 0.028$^{\#}$	1.365 ± 0.029$^{\wedge\&}$
Heart Weight/Body Weight (x100)	0.335 ± 0.005	0.340 ± 0.009	0.355 ± 0.007	0.366 ± 0.007$^{\wedge}$
Myocyte Surface Area (mm^2)	349.9 ± 18.70	352.1 ± 11.66	396.9 ± 18.84$^{\#}$	406.8 ± 28.53$^{\wedge\&}$
Myocardial Collagen (% area)	0.429 ± 0.013	0.449 ± 0.023	0.479 ± 0.042	0.459 ± 0.016

Discussion

In the current study, we utilized viral-mediated gene transfer to decrease IL glutamatergic output while simultaneously monitoring hemodynamic, vascular, and cardiac responses to chronic stress. We found that IL vGluT1 knockdown increased heart rate and arterial pressure reactivity to acute stress. Additionally, IL hypofunction during CVS increased chronic home cage arterial pressure. These changes were accompanied by both endothelial-independent and -dependent arterial dysfunction. Histological analysis revealed that animals experiencing CVS with decreased IL output also had inward vascular remodeling, fibrosis, and cardiac hypertrophy. Collectively, these results indicate that IL projection neurons are critical for reducing acute cardiovascular stress reactivity, long-term arterial pressure, and vascular

endothelial dysfunction. Furthermore, they identify a neurochemical mechanism linking stress appraisal and emotion with chronic stress-induced autonomic dysfunction.

Epidemiological evidence indicates that prolonged stress is a major risk factor for cardiovascular illness and mortality (Steptoe & Kivimäki, 2012; Yusuf et al., 2004). Additionally, numerous clinical studies point to enhanced stress reactivity as a marker of future cardiovascular pathology (Chida & Steptoe, 2010; Vogelzangs et al., 2010). Rodent studies employing repeated-stress models of depression (chronic variable stress, chronic mild stress, chronic social defeat, etc.) have found alterations in baroreflex function, decreased heart rate variability, and ventricular arrhythmias (Carnevali et al., 2013; Costoli et al., 2004; Crestani, 2016; Duarte et al., 2015; Grippo et al., 2002; Grippo & Johnson, 2009; S. K. Wood, 2014; S. K. Wood et al., 2012). Given the strong association between prolonged stress/emotional disorders and cardiovascular disease (Barton et al., 2007; Carney et al., 2001; Hausberg et al., 2007), it is important to identify the specific neural processes of stress appraisal and mood that impact cardiovascular function. Emerging evidence suggests that autonomic imbalance prolongs exposure to neural and endocrine stress mediators, generating risk for cardiovascular pathology (Johnson & Grippo, 2006; Thayer et al., 2012; Wulsin et al., 2015). Stress-associated molecules such as corticosteroids, corticotropin-releasing hormone, and neuropeptide Y, among others, have been shown to affect cardiovascular function in animal models (Costoli et al., 2005; Oakley et al., 2019; S. K. Wood et al., 2012). However, the neural circuits that integrate cognitive appraisal and autonomic balance remain to be determined.

The contribution of the current study relates to the site-specific genetic approach that reduces IL vGluT1 expression long-term (Myers et al., 2017). Given the decreased output from a critical cognitive/emotional region (The Medial Prefrontal Cortex: Coordinator of Autonomic, Neuroendocrine and Behavioural Responses to Stress, 2015; Jessica M. McKlveen et al., 2013), we monitored both stress-induced and resting parameters of heart rate and arterial pressure in otherwise unstressed rats, as well as rats experiencing the cumulative burden of

chronic stress exposure. This approach was followed by *ex vivo* analysis of arterial function and histological investigation of vascular and myocardial structure. These studies found several siRNA effects in animals that did not experience CVS (Table 2.3). The knockdown increased HR and MAP reactivity to acute restraint and impaired endothelial-independent vasoconstriction, suggesting hypo-function of IL primes for enhanced cardiovascular reactivity and impaired vasomotor function. Previous studies indicating that NMDA-mediated activation of the IL reduces tachycardic and pressor responses to acute air-jet stress further support the conclusion that IL glutamate output reduces acute cardiovascular reactivity (Müller-Ribeiro et al., 2012). Paradoxically, No CVS siRNA animals exhibited decreased resting home cage circadian arterial pressure. This effect may relate to the important role of IL molecular clocks in coordinating circadian physiological rhythms (Woodruff et al., 2016). In GFP-treated rats, CVS dampened home cage activity in the dark cycle, decreasing circadian rhythms of activity and potentially accounting for effects of CVS to decrease circadian HR. Interestingly, CVS did not alter chronic home cage MAP; however, CVS-exposed animals exhibited enhanced tachycardic and pressor responses to acute restraint. This was accompanied by impaired endothelial-independent vasorelaxation and constriction. Furthermore, CVS increased vascular smooth muscle thickness and fibrosis, as well as cardiomyocyte surface area.

Table 2.3. Integrative summary of all data reported in terms of siRNA effects, chronic stress effects, and the combination of siRNA and CVS.
Arrows indicate significant and/or CVS effects. HR: heart reate, MAP: mean arterial pressure, SAP: systolic arterial pressure, DAP: diastolic arterial pressure, ED: endothelial-dependent, EI: endothelial-independent. $^{*}p < 0.05$, vs. No CVS GFP, $^{\#}p < 0.05$ vs. No CVS siRNA, $^{\wedge}p < 0.05$ vs. CVS GFP

Table 2.3 Summary: siRNA and/or CVS effects from experiments 1 and 2

	siRNA	CVS	siRNA + CVS
Activity (15 days)	↔	↓*	↑*#^
HR (15 days)	↔	↓*	↑#^
MAP (15 days)	↓*	↔	↑*#^
SAP (15 days)	↓*	↔	↑*#^
DAP (15 days)	↓*	↔	↑*#
Pulse Pressure (15 days)	↔	↑*	↑*#^
HR (acute stress)	↑*	↑*	↑*#^
MAP (acute stress)	↑*	↑*	↑*#
Vasoconstriction (ED)	↔	↔	↓*#^
Vasoconstriction (EI)	↓*	↓*	↓*#^
Vasorelaxation (ED)	↔	↔	↓*#^
Vasorelaxation (EI)	↔	↓*	↓*#
Lumen Circumference	↔	↔	↓#
Luminal Area	↔	↔	↓#
Media Thickness	↔	↑*	↑*#
Media:Lumen Area	↔	↑*	↑*#
Adventitia Thickness	↔	↔	↓*
Adventitia Collagen	↔	↑*	↑*#
Heart Weight	↔	↑*	↑*#
Heart Weight/Body Weight	↔	↔	↑*
Myocardial Collagen	↔	↔	↔
Myocyte Surface Area	↔	↑*	↑*#

The effects of vGluT1 knockdown and CVS interacted to generate a phenotype of enhanced cardiovascular risk. All measures of HR and arterial pressure, both acute stress-induced and chronic home cage, were elevated. This group also had impairment of both endothelial-dependent and –independent vascular dilation and constriction. The overall risk

profile was further evident by inward remodeling of the vasculature due to hypertrophy and fibrosis that reduced luminal area, indicative of vascular stiffness. Additionally, these rats exhibited myocardial hypertrophy including increased myocyte size, heart weight, and body weight-corrected heart weight. It is worth noting that some effects in the CVS siRNA group result from comparisons to No CVS GFP. In the case of histological measures, there were no significant differences between CVS GFP and CVS siRNA animals. This suggests that the structural changes observed are not sufficient to fully account for vascular dysfunction in the CVS siRNA group relative to CVS GFP. Furthermore, home cage arterial pressure elevations were modest and not indicative of a hypertensive state. More likely, endothelial dysfunction after chronic stress in animals with impaired IL function results from the interaction of multiple factors, including enhanced HPA axis activity, elevated cardiovascular reactivity, increased resting arterial pressure, and vascular remodeling. Taken together, these results suggest that conditions associated with decreased ventral mPFC activity, including depression, anxiety, and post-traumatic stress disorder (Jessica M. McKlveen et al., 2013), may enhance vulnerability to the effects of prolonged stress on cardiovascular health.

The specific circuit mechanisms downstream of IL glutamate release that account for the current findings remain to be determined. Although the IL does not directly innervate either pre-ganglionic autonomic neurons or neurosecretory cells of the hypothalamus (Saper et al., 1976; Vertes, 2004), the region has widespread projections throughout the forebrain and brainstem (Vertes, 2004; M. Wood et al., 2019). Inputs to the posterior hypothalamus target local inhibitory cells (Myers et al., 2016), providing a potential pathway to inhibit stress reactivity(Lisa et al., 1989). Additionally, IL-targeted neurons of the PH innervate the paraventricular hypothalamus, a region important for vasomotor tone (Myers et al., 2016; Zhou et al., 2019). There are also IL projections to brainstem cardioregulatory centers including the nucleus of the solitary tract and the rostral and caudal regions of the ventrolateral medulla that may regulate autonomic outflow (Gabbott et al., 2005; Myers, 2017). Furthermore, there is a complex network of local cortical

circuitry, including interneurons in the IL, that mediates the overall activity of glutamatergic projection neurons (Jessica M. McKlveen et al., 2019). Based on the current findings, these local circuits would be expected to play a role in autonomic reactivity. Ultimately, projection-specific analyses are needed isolate the precise cell populations within IL glutamate neurons that reduce autonomic imbalance after chronic stress.

While these studies identified a novel frontal cortical node for preventing the deleterious cardiovascular effects of chronic stress, there are limitations worth discussing. First, the current studies were limited to males. As depression-cardiovascular co-morbidity has at least twice the prevalence in females (Möller-Leimkühler, 2007; Pimple et al., 2019; Tobet et al., 2013), it is important to consider sex-specific regulation. Interestingly, a recent study investigating vascular function in female rodents after chronic stress actually found that ovarian hormones protect against stress-induced arterial dysfunction (Brooks et al., 2018). Comparing the neural basis of pathological responses in males and females would likely yield a better understanding of the disproportionate female impact of mood disorder-cardiovascular co-morbidity. Another consideration is that the current vasoreactivity experiments were carried out in thoracic aorta. Although the results identified impaired function and indicators of stiffness, the aorta is a conductive artery and future experiments with resistance arterioles might yield differing results. Indeed, these studies could show greater effects as resistance arteries receive more sympathetic innervation (Brown et al., 2018; Hao et al., 2005). Furthermore, investigating vascular resistance could yield data with significant relevance for stress-related hypertension.

In conclusion, the current findings highlight IL glutamatergic neurons as a node of integration that links stress appraisal with hemodynamic reactivity, long-term arterial pressure control, and vascular endothelial function. These results also indicate that, in the context of chronic stress, cortical cells mediating cognition and behavior can impact the structure and function of the heart and vasculature. Future research investigating the mechanisms that regulate IL projection neuron activity and the downstream post-synaptic events activated by IL

glutamate release may yield insight into novel targets to prevent or reduce the burden of cardiovascular disease.

References

Barefoot, J. C., Helms, M. J., Mark, D. B., Blumenthal, J. A., Califf, R. M., Haney, T. L., O'Connor, C. M., Siegler, I. C., & Williams, R. B. (1996). Depression and Long-Term Mortality Risk in Patients With Coronary Artery Disease. *The American Journal of Cardiology*, *78*(6), 613–617. https://doi.org/10.1016/S0002-9149(96)00380-3

Barton, D. A., Dawood, T., Lambert, E. A., Esler, M. D., Haikerwal, D., Brenchley, C., Socratous, F., Kaye, D. M., Schlaich, M. P., Hickie, I., & Lambert, G. W. (2007). Sympathetic activity in major depressive disorder: identifying those at increased cardiac risk? *Journal of Hypertension*, *25*(10), 2117–2124. https://doi.org/10.1097/HJH.0b013e32829baae7

Basford, J. E., Koch, S., Anjak, A., Singh, V. P., Krause, E. G., Robbins, N., Weintraub, N. L., Hui, D. Y., & Rubinstein, J. (2013). Smooth muscle LDL receptor-related protein-1 deletion induces aortic insufficiency and promotes vascular cardiomyopathy in mice. *PloS One*, *8*(11), e82026. https://doi.org/10.1371/journal.pone.0082026

Beissner, F., Meissner, K., Bär, K.-J., & Napadow, V. (2013). The Autonomic Brain: An Activation Likelihood Estimation Meta-Analysis for Central Processing of Autonomic Function. *Journal of Neuroscience*, *33*(25), 10503–10511. https://doi.org/10.1523/JNEUROSCI.1103-13.2013

Bensley, J. G., De Matteo, R., Harding, R., & Black, M. J. (2016). Three-dimensional direct measurement of cardiomyocyte volume, nuclearity, and ploidy in thick histological sections. *Scientific Reports*, *6*(1), 23756. https://doi.org/10.1038/srep23756

Binder, E. B., & Nemeroff, C. B. (2010). The CRF system, stress, depression and anxiety—insights from human genetic studies. *Molecular Psychiatry*, *15*(6), 574–588. https://doi.org/10.1038/mp.2009.141

Brooks, S. D., Hileman, S. M., Chantler, P. D., Milde, S. A., Lemaster, K. A., Frisbee, S. J., Shoemaker, J. K., Jackson, D. N., & Frisbee, J. C. (2018). Protection from vascular dysfunction in female rats with chronic stress and depressive symptoms. *American Journal*

of Physiology-Heart and Circulatory Physiology, *314*(5), H1070–H1084. https://doi.org/10.1152/ajpheart.00647.2017

Brown, I. A. M., Diederich, L., Good, M. E., DeLalio, L. J., Murphy, S. A., Cortese-Krott, M. M., Hall, J. L., Le, T. H., & Isakson, B. E. (2018). Vascular Smooth Muscle Remodeling in Conductive and Resistance Arteries in Hypertension. *Arteriosclerosis, Thrombosis, and Vascular Biology*, *38*(9), 1969–1985. https://doi.org/10.1161/ATVBAHA.118.311229

Carnevali, L., Trombini, M., Rossi, S., Graiani, G., Manghi, M., Koolhaas, J. M., Quaini, F., Macchi, E., Nalivaiko, E., & Sgoifo, A. (2013). Structural and Electrical Myocardial Remodeling in a Rodent Model of Depression. *Psychosomatic Medicine*, *75*(1), 42–51. https://doi.org/10.1097/PSY.0b013e318276cb0d

Carney, R. M., Blumenthal, J. A., Stein, P. K., Watkins, L., Catellier, D., Berkman, L. F., Czajkowski, S. M., O'Connor, C., Stone, P. H., & Freedland, K. E. (2001). Depression, Heart Rate Variability, and Acute Myocardial Infarction. *Circulation*, *104*(17), 2024–2028. https://doi.org/10.1161/hc4201.097834

Chida, Y., & Steptoe, A. (2010). Greater Cardiovascular Responses to Laboratory Mental Stress Are Associated With Poor Subsequent Cardiovascular Risk Status. *Hypertension*, *55*(4), 1026–1032. https://doi.org/10.1161/HYPERTENSIONAHA.109.146621

Costoli, T., Bartolomucci, A., Graiani, G., Stilli, D., Laviola, G., & Sgoifo, A. (2004). Effects of chronic psychosocial stress on cardiac autonomic responsiveness and myocardial structure in mice. *American Journal of Physiology - Heart and Circulatory Physiology*, *286*(6 55-6), H2133–H2140. https://doi.org/10.1152/ajpheart.00869.2003

Costoli, T., Sgoifo, A., Stilli, D., Flugge, G., Adriani, W., Laviola, G., Fuchs, E., Pedrazzini, T., & Musso, E. (2005). Behavioural, neural and cardiovascular adaptations in mice lacking the NPY Y1 receptor. *Neuroscience & Biobehavioral Reviews*, *29*(1), 113–123. https://doi.org/10.1016/J.NEUBIOREV.2004.09.016

Crestani, C. C. (2016). Emotional Stress and Cardiovascular Complications in Animal Models: A

Review of the Influence of Stress Type. *Frontiers in Physiology*, *7*, 251. https://doi.org/10.3389/fphys.2016.00251

Damasio, A. R. (1996). The somatic marker hypothesis and the possible functions of the prefrontal cortex. *Philosophical Transactions of the Royal Society of London. Series B, Biological Sciences*, *351*(1346), 1413–1420. https://doi.org/10.1098/rstb.1996.0125

de Kloet, E. R., Joëls, M., & Holsboer, F. (2005). Stress and the brain: from adaptation to disease. *Nature Reviews Neuroscience*, *6*(6), 463–475. https://doi.org/10.1038/nrn1683

Duarte, J. O., Planeta, C. S., & Crestani, C. C. (2015). Immediate and long-term effects of psychological stress during adolescence in cardiovascular function: Comparison of homotypic vs heterotypic stress regimens. *International Journal of Developmental Neuroscience*, *40*, 52–59. https://doi.org/10.1016/J.IJDEVNEU.2014.11.004

Flak, J. N., Jankord, R., Solomon, M. B., Krause, E. G., & Herman, J. P. (2011). Opposing effects of chronic stress and weight restriction on cardiovascular, neuroendocrine and metabolic function. *Physiology & Behavior*, *104*(2), 228–234. https://doi.org/10.1016/J.PHYSBEH.2011.03.002

Flak, J. N., Solomon, M. B., Jankord, R., Krause, E. G., & Herman, J. P. (2012). Identification of chronic stress-activated regions reveals a potential recruited circuit in rat brain. *The European Journal of Neuroscience*, *36*(4), 2547–2555. https://doi.org/10.1111/j.1460-9568.2012.08161.x

Franklin, S. S., Khan, S. A., Wong, N. D., Larson, M. G., & Levy, D. (1999). Is pulse pressure useful in predicting risk for coronary heart Disease? The Framingham heart study. *Circulation*, *100*(4), 354–360. http://www.ncbi.nlm.nih.gov/pubmed/10421594

Gabbott, P. L. A., Warner, T. A., Jays, P. R. L., Salway, P., & Busby, S. J. (2005). Prefrontal cortex in the rat: Projections to subcortical autonomic, motor, and limbic centers. *The Journal of Comparative Neurology*, *492*(2), 145–177. https://doi.org/10.1002/cne.20738

Gianaros, P. J., & Sheu, L. K. (2009). A review of neuroimaging studies of stressor-evoked

blood pressure reactivity: emerging evidence for a brain-body pathway to coronary heart disease risk. *NeuroImage*, *47*(3), 922–936. https://doi.org/10.1016/j.neuroimage.2009.04.073

Gianaros, P. J., & Wager, T. D. (2015). Brain-Body Pathways Linking Psychological Stress and Physical Health. *Current Directions in Psychological Science*, *24*(4), 313–321. https://doi.org/10.1177/0963721415581476

Glasser, S. P., Halberg, D. L., Sands, C., Gamboa, C. M., Muntner, P., & Safford, M. (2014). Is Pulse Pressure an Independent Risk Factor for Incident Acute Coronary Heart Disease Events? The REGARDS Study. *American Journal of Hypertension*, *27*(4), 555–563. https://doi.org/10.1093/ajh/hpt168

Goodson, M. L., Packard, A. E. B., Buesing, D. R., Maney, M., Myers, B., Fang, Y., Basford, J. E., Hui, D. Y., Ulrich-Lai, Y. M., Herman, J. P., & Ryan, K. K. (2017). Chronic stress and Rosiglitazone increase indices of vascular stiffness in male rats. *Physiology & Behavior*, *172*, 16–23. https://doi.org/10.1016/J.PHYSBEH.2016.03.031

Grillo, C.A., Tamashiro, K. L., Piroli, G. G., Melhorn, S., Gass, J. T., Newsom, R. J., Reznikov, L. R., Smith, A., Wilson, S. P., Sakai, R. R., & Reagan, L. P. (2007). Lentivirus-mediated downregulation of hypothalamic insulin receptor expression. *Physiology & Behavior*, *92*(4), 691–701. https://doi.org/10.1016/J.PHYSBEH.2007.05.043

Grillo, Claudia A, Piroli, G. G., Lawrence, R. C., Wrighten, S. A., Green, A. J., Wilson, S. P., Sakai, R. R., Kelly, S. J., Wilson, M. A., Mott, D. D., & Reagan, L. P. (2015). Hippocampal Insulin Resistance Impairs Spatial Learning and Synaptic Plasticity. *Diabetes*, *64*(11), 3927–3936. https://doi.org/10.2337/db15-0596

Grippo, A. J., & Johnson, A. K. (2009). Stress, depression and cardiovascular dysregulation: a review of neurobiological mechanisms and the integration of research from preclinical disease models. *Stress (Amsterdam, Netherlands)*, *12*(1), 1–21. https://doi.org/10.1080/10253890802046281

Grippo, A. J., Moffitt, J. A., & Johnson, A. K. (2002). Cardiovascular alterations and autonomic imbalance in an experimental model of depression. *American Journal of Physiology-Regulatory, Integrative and Comparative Physiology*, *282*(5), R1333–R1341. https://doi.org/10.1152/ajpregu.00614.2001

Gupta, M. K., McLendon, P. M., Gulick, J., James, J., Khalili, K., & Robbins, J. (2016). UBC9-Mediated Sumoylation Favorably Impacts Cardiac Function in Compromised Hearts. *Circulation Research*, *118*(12), 1894–1905. https://doi.org/10.1161/CIRCRESAHA.115.308268

Hao, Z., Jiang, X., Sharafeih, R., SHEN, S., Hand, A. R., Cone, R. E., & O'Rourke, J. (2005). Stimulated release of tissue plasminogen activator from artery wall sympathetic nerves: Implications for stress-associated wall damage. *Stress*, *8*(2), 141–149. https://doi.org/10.1080/10253890500168098

Hausberg, M., Hillebrand, U., & Kisters, K. (2007). Addressing sympathetic overactivity in major depressive disorder. *Journal of Hypertension*, *25*(10), 2004–2005. https://doi.org/10.1097/HJH.0b013e3282ef9819

Johnson, A. K., & Grippo, A. J. (2006). Sadness and broken hearts: Neurohumoral mechanisms and co-morbidity of ischemic heart disease and psychological depression. *Journal of Physiology and Pharmacology*, *57*(SUPPL. 11), 5–29. www.jpp.krakow.pl

Liotti, M., Mayberg, H. S., Brannan, S. K., McGinnis, S., Jerabek, P., & Fox, P. T. (2000). Differential limbic–cortical correlates of sadness and anxiety in healthy subjects: implications for affective disorders. *Biological Psychiatry*, *48*(1), 30–42. https://doi.org/10.1016/S0006-3223(00)00874-X

Lisa, M., Marmo, E., Wible, J. H., & DiMicco, J. A. (1989). Injection of muscimol into posterior hypothalamus blocks stress-induced tachycardia. *The American Journal of Physiology*, *257*(1 Pt 2), R246-51. https://doi.org/10.1152/ajpregu.1989.257.1.R246

Mayberg, H. S., Lozano, A. M., Voon, V., McNeely, H. E., Seminowicz, D., Hamani, C.,

Schwalb, J. M., & Kennedy, S. H. (2005). Deep Brain Stimulation for Treatment-Resistant Depression. *Neuron*, *45*(5), 651–660. https://doi.org/10.1016/J.NEURON.2005.02.014

The Medial Prefrontal Cortex: Coordinator of Autonomic, Neuroendocrine and Behavioural Responses to Stress, 27 Journal of Neuroendocrinology 446 (2015). https://doi.org/10.1111/jne.12272

McKlveen, J. M., Myers, B., & Herman, J. P. (2015). The Medial Prefrontal Cortex: Coordinator of Autonomic, Neuroendocrine and Behavioural Responses to Stress. *Journal of Neuroendocrinology*, *27*(6), 446–456. https://doi.org/10.1111/jne.12272

McKlveen, Jessica M., Moloney, R. D., Scheimann, J. R., Myers, B., & Herman, J. P. (2019). “Braking” the Prefrontal Cortex: The Role of Glucocorticoids and Interneurons in Stress Adaptation and Pathology. *Biological Psychiatry*, *86*(9), 669–681. https://doi.org/10.1016/j.biopsych.2019.04.032

McKlveen, Jessica M., Myers, B., Flak, J. N., Bundzikova, J., Solomon, M. B., Seroogy, K. B., & Herman, J. P. (2013). Role of Prefrontal Cortex Glucocorticoid Receptors in Stress and Emotion. *Biological Psychiatry*, *74*(9), 672–679. https://doi.org/10.1016/J.BIOPSYCH.2013.03.024

Möller-Leimkühler, A. M. (2007). Gender differences in cardiovascular disease and comorbid depression. *Dialogues in Clinical Neuroscience*, *9*(1), 71–83. http://www.ncbi.nlm.nih.gov/pubmed/17506227

Müller-Ribeiro, F. C. de F., Zaretsky, D. V, Zaretskaia, M. V, Santos, R. A. S., DiMicco, J. A., & Fontes, M. A. P. (2012). Contribution of infralimbic cortex in the cardiovascular response to acute stress. *American Journal of Physiology. Regulatory, Integrative and Comparative Physiology*, *303*(6), R639-50. https://doi.org/10.1152/ajpregu.00573.2011

Myers-Schulz, B., & Koenigs, M. (2012). Functional anatomy of ventromedial prefrontal cortex: implications for mood and anxiety disorders. *Molecular Psychiatry*, *17*(2), 132–141. https://doi.org/10.1038/mp.2011.88

Myers, B. (2017). Corticolimbic regulation of cardiovascular responses to stress. *Physiology and Behavior*, *172*, 49–59. https://doi.org/10.1016/j.physbeh.2016.10.015

Myers, B., Carvalho-Netto, E., Wick-Carlson, D., Wu, C., Naser, S., Solomon, M. B., Ulrich-Lai, Y. M., & Herman, J. P. (2016). GABAergic Signaling within a Limbic-Hypothalamic Circuit Integrates Social and Anxiety-Like Behavior with Stress Reactivity. *Neuropsychopharmacology*, *41*(6), 1530–1539. https://doi.org/10.1038/npp.2015.311

Myers, B., Mark Dolgas, C., Kasckow, J., Cullinan, W. E., & Herman, J. P. (2014). Central stress-integrative circuits: forebrain glutamatergic and GABAergic projections to the dorsomedial hypothalamus, medial preoptic area, and bed nucleus of the stria terminalis. *Brain Structure & Function*, *219*(4), 1287–1303. https://doi.org/10.1007/s00429-013-0566-y

Myers, B., McKlveen, J. M., & Herman, J. P. (2014). Glucocorticoid actions on synapses, circuits, and behavior: Implications for the energetics of stress. *Frontiers in Neuroendocrinology*, *35*(2), 180–196. https://doi.org/10.1016/J.YFRNE.2013.12.003

Myers, B., McKlveen, J. M., Morano, R., Ulrich-Lai, Y. M., Solomon, M. B., Wilson, S. P., & Herman, J. P. (2017). Vesicular Glutamate Transporter 1 Knockdown in Infralimbic Prefrontal Cortex Augments Neuroendocrine Responses to Chronic Stress in Male Rats. *Endocrinology*, *158*(10), 3579–3591. https://doi.org/10.1210/en.2017-00426

Oakley, R. H., Cruz-Topete, D., He, B., Foley, J. F., Myers, P. H., Xu, X., Gomez-Sanchez, C. E., Chambon, P., Willis, M. S., & Cidlowski, J. A. (2019). Cardiomyocyte glucocorticoid and mineralocorticoid receptors directly and antagonistically regulate heart disease in mice. *Science Signaling*, *12*(577), eaau9685. https://doi.org/10.1126/scisignal.aau9685

Öngür, D., Ferry, A. T., & Price, J. L. (2003). Architectonic subdivision of the human orbital and medial prefrontal cortex. *The Journal of Comparative Neurology*, *460*(3), 425–449. https://doi.org/10.1002/cne.10609

Pimple, P., Lima, B. B., Hammadah, M., Wilmot, K., Ramadan, R., Levantsevych, O., Sullivan, S., Kim, J. H., Kaseer, B., Shah, A. J., Ward, L., Raggi, P., Bremner, J. D., Hanfelt, J.,

Lewis, T., Quyyumi, A. A., & Vaccarino, V. (2019). Psychological Distress and Subsequent Cardiovascular Events in Individuals With Coronary Artery Disease. *Journal of the American Heart Association*, *8*(9), e011866. https://doi.org/10.1161/JAHA.118.011866

Saper, C. B., Loewy, A. D., Swanson, L. W., & Cowan, W. M. (1976). Direct hypothalamo-autonomic connections. *Brain Research*, *117*(2), 305–312. https://doi.org/10.1016/0006-8993(76)90738-1

Schuske, K., & Jorgensen, E. M. (2004). Vesicular glutamate transporter--shooting blanks. *Science (New York, N.Y.)*, *304*(5678), 1750–1752. https://doi.org/10.1126/science.1100475

Sgoifo, A., Carnevali, L., Pico Alfonso, M. D. L. A., & Amore, M. (2015). Autonomic dysfunction and heart rate variability in depression. *Stress*, *18*(3), 343–352. https://doi.org/10.3109/10253890.2015.1045868

Shoemaker, J. K., Badrov, M. B., Al-Khazraji, B. K., & Jackson, D. N. (2015). Neural Control of Vascular Function in Skeletal Muscle. In *Comprehensive Physiology* (pp. 303–329). John Wiley & Sons, Inc. https://doi.org/10.1002/cphy.c150004

Smith, B. L., Lyons, C. E., Correa, F. G., Benoit, S. C., Myers, B., Solomon, M. B., & Herman, J. P. (2017). Behavioral and physiological consequences of enrichment loss in rats. *Psychoneuroendocrinology*, *77*, 37–46. https://doi.org/10.1016/j.psyneuen.2016.11.040

Solomon, M. B., Jones, K., Packard, B. A., & Herman, J. P. (2010). The medial amygdala modulates body weight but not neuroendocrine responses to chronic stress. *Journal of Neuroendocrinology*, *22*(1), 13–23. https://doi.org/10.1111/j.1365-2826.2009.01933.x

Steptoe, A., & Kivimäki, M. (2012). Stress and cardiovascular disease. *Nature Reviews Cardiology*, *9*(6), 360–370. https://doi.org/10.1038/nrcardio.2012.45

Swanson, L. W. (2004). *Brain Maps: Structure of the Rat Brain* (Third Ed.). Academic Press.

Thayer, J. F., Åhs, F., Fredrikson, M., Sollers, J. J., & Wager, T. D. (2012). A meta-analysis of heart rate variability and neuroimaging studies: Implications for heart rate variability as a marker of stress and health. *Neuroscience & Biobehavioral Reviews*, *36*(2), 747–756.

https://doi.org/10.1016/J.NEUBIOREV.2011.11.009

Tobet, S. A., Handa, R. J., & Goldstein, J. M. (2013). Sex-dependent pathophysiology as predictors of comorbidity of major depressive disorder and cardiovascular disease. *Pflügers Archiv - European Journal of Physiology*, *465*(5), 585–594. https://doi.org/10.1007/s00424-013-1248-6

Uylings, H. B. M., Groenewegen, H. J., & Kolb, B. (2003). Do rats have a prefrontal cortex? *Behavioural Brain Research*, *146*(1–2), 3–17. https://doi.org/10.1016/J.BBR.2003.09.028

Vertes, R. P. (2004). Differential projections of the infralimbic and prelimbic cortex in the rat. *Synapse*, *51*(1), 32–58. https://doi.org/10.1002/syn.10279

Vogelzangs, N., Beekman, A. T. F., Milaneschi, Y., Bandinelli, S., Ferrucci, L., & Penninx, B. W. J. H. (2010). Urinary Cortisol and Six-Year Risk of All-Cause and Cardiovascular Mortality. *The Journal of Clinical Endocrinology & Metabolism*, *95*(11), 4959–4964. https://doi.org/10.1210/jc.2010-0192

Wardle, J., Chida, Y., Gibson, E. L., Whitaker, K. L., & Steptoe, A. (2011). Stress and Adiposity: A Meta-Analysis of Longitudinal Studies. *Obesity*, *19*(4), 771–778. https://doi.org/10.1038/oby.2010.241

Wojcik, S. M., Rhee, J. S., Herzog, E., Sigler, A., Jahn, R., Takamori, S., Brose, N., & Rosenmund, C. (2004). An essential role for vesicular glutamate transporter 1 (VGLUT1) in postnatal development and control of quantal size. *Proceedings of the National Academy of Sciences of the United States of America*, *101*(18), 7158–7163. https://doi.org/10.1073/pnas.0401764101

Wood, J. N., & Grafman, J. (2003). Human prefrontal cortex: processing and representational perspectives. *Nature Reviews Neuroscience*, *4*(2), 139–147. https://doi.org/10.1038/nrn1033

Wood, M., Adil, O., Wallace, T., Fourman, S., Wilson, S. P., Herman, J. P., & Myers, B. (2019). Infralimbic prefrontal cortex structural and functional connectivity with the limbic forebrain: a

combined viral genetic and optogenetic analysis. *Brain Structure & Function*, *224*(1), 73–97. https://doi.org/10.1007/s00429-018-1762-6

Wood, S. K. (2014). Cardiac autonomic imbalance by social stress in rodents: understanding putative biomarkers. *Frontiers in Psychology*, *5*, 950. https://doi.org/10.3389/fpsyg.2014.00950

Wood, S. K., McFadden, K. V., Grigoriadis, D., Bhatnagar, S., & Valentino, R. J. (2012). Depressive and cardiovascular disease comorbidity in a rat model of social stress: a putative role for corticotropin-releasing factor. *Psychopharmacology*, *222*(2), 325–336. https://doi.org/10.1007/s00213-012-2648-6

Woodruff, E. R., Chun, L. E., Hinds, L. R., & Spencer, R. L. (2016). Diurnal Corticosterone Presence and Phase Modulate Clock Gene Expression in the Male Rat Prefrontal Cortex. *Endocrinology*, *157*(4), 1522–1534. https://doi.org/10.1210/en.2015-1884

Wulsin, L. R., Horn, P. S., Perry, J. L., Massaro, J. M., & D'Agostino, R. B. (2015). Autonomic Imbalance as a Predictor of Metabolic Risks, Cardiovascular Disease, Diabetes, and Mortality. *The Journal of Clinical Endocrinology & Metabolism*, *100*(6), 2443–2448. https://doi.org/10.1210/jc.2015-1748

Yusuf, S., Hawken, S., Ôunpuu, S., Dans, T., Avezum, A., Lanas, F., McQueen, M., Budaj, A., Pais, P., Varigos, J., & Lisheng, L. (2004). Effect of potentially modifiable risk factors associated with myocardial infarction in 52 countries (the INTERHEART study): case-control study. *The Lancet*, *364*(9438), 937–952. https://doi.org/10.1016/S0140-6736(04)17018-9

Zhou, J. J., Ma, H. J., Shao, J., Wei, Y., Zhang, X., Zhang, Y., & Li, D. P. (2019). Downregulation of orexin receptor in hypothalamic paraventricular nucleus decreases blood pressure in obese zucker rats. *Journal of the American Heart Association*, *8*(13). https://doi.org/10.1161/JAHA.118.011434

Ziegler, D. R., Cullinan, W. E., & Herman, J. P. (2002). Distribution of vesicular glutamate

transporter mRNA in rat hypothalamus. *The Journal of Comparative Neurology*, *448*(3), 217–229. https://doi.org/10.1002/cne.10257

CHAPTER 3: SEXUALLY DIVERGENT CORTICAL CONTROL OF AFFECTIVE-AUTONOMIC INTEGRATION[1]

Overview

Depression and cardiovascular disease reduce quality of life and increase mortality risk. These conditions commonly co-occur with sex-based differences in incidence and severity. However, the biological mechanisms linking the disorders are poorly understood. In the current study, we hypothesized that the infralimbic (IL) prefrontal cortex integrates mood-related behaviors with the cardiovascular burden of chronic stress. In a rodent model, we utilized optogenetics during behavior and *in vivo* physiological monitoring to examine how the IL regulates affect, social motivation, neuroendocrine-autonomic stress reactivity, and the cardiac consequences of chronic stress. Our results indicate that IL glutamate neurons increase socio-motivational behaviors specifically in males. IL activation also reduced endocrine and cardiovascular stress responses in males, while increasing reactivity in females. Moreover, prior IL stimulation protected males from subsequent chronic stress-induced sympatho-vagal imbalance and cardiac hypertrophy. Our findings suggest that cortical regulation of behavior, physiological stress responses, and cardiovascular outcomes fundamentally differ between sexes.

Introduction

Major depressive disorder (MDD) and cardio-metabolic conditions including hypertension, glucose intolerance, and heart failure significantly contribute to global disease burden. Epidemiological evidence implicates life stressors as a risk factor for both MDD and

[1] The following material was adapted from a manuscript published July 2021 in Psychoneuroendocrinology under the title, “Sexually Divergent Cortical Control of Affective-Autonomic Integration”. The data presented here were a part of a larger collaborative experiment that also examined behavior.
Funding: This work was supported by NIH grants R00 HL122454 and R01 HL150559 to Brent Myers. Data generated by the University of Cincinnati Mouse Metabolic Phenotyping Core were supported by NIH grant U2C DK059630.

cardiovascular disease (CVD) (Binder & Nemeroff, 2010; Grippo & Johnson, 2009; Myers, McKlveen, et al., 2014; Sgoifo et al., 2015). Furthermore, sex differences in the incidence of MDD, CVD, and MDD-CVD co-morbidity suggest that sex-specific factors contribute to outcomes (Goldstein et al., 2019). However, the biological basis for stress effects on health, particularly the integration of affective and physiological systems, is poorly understood. Human brain imaging studies indicate that ventral medial prefrontal cortex (vmPFC) activity associates with sadness and blood pressure reactivity, suggesting that top-down cortical control may integrate diverse aspects of mood and systemic physiology.

The vmPFC is involved in numerous cognitive and emotional processes (J. M. McKlveen et al., 2015; Myers-Schulz & Koenigs, 2012; J. N. Wood & Grafman, 2003). A subregion of the vmPFC, the subgenual cingulate cortex (BA25), is activated by sadness-provoking stimuli, responds to social isolation, and has reduced volume in MDD patients (Beckmann et al., 2009; Liotti et al., 2000; Vijayakumar et al., 2017). BA25 is also targeted for deep brain stimulation in patients with treatment-resistant depression, where larger volumes predict better treatment outcomes (Mayberg et al., 2005; Sankar et al., 2019). Although, broader investigation of BA25 activity in mood disorders has yielded mixed results with reports of both hyper- (Hamani et al., 2011; Mayberg et al., 2005) and hypo-activity (Drevets et al., 1997, 2008). Subgenual regions of vmPFC have also been identified as components of a central autonomic network monitoring visceral functions (Beissner et al., 2013; Gianaros & Sheu, 2009; Gianaros & Wager, 2015; Myers, 2016; Shoemaker et al., 2016). Furthermore, recent pharmacological studies employing glutamate uptake inhibitors in non-human primates have implicated BA25 activity in reduced reward motivation (Alexander et al., 2019) and enhanced threat-related autonomic responses (Alexander et al., 2020). The rodent putative anatomical homolog of BA25, the infralimbic cortex (IL) (Öngür et al., 2003; Roberts & Clarke, 2019; Uylings et al., 2003; Vertes, 2004), innervates limbic and stress-regulatory nuclei including the amygdala, thalamus, and hypothalamus (Gabbott et al., 2005; Myers et al., 2016; Myers, Mark Dolgas, et al., 2014; M. Wood et al.,

2018). Moreover, knockdown of IL glutamatergic output exacerbates chronic stress effects on hypothalamic-pituitary-adrenal (HPA) axis reactivity and vascular function (Myers et al., 2017; Schaeuble et al., 2019). However, the potential sex-specific roles of IL activity to integrate socio-motivational behaviors with physiological stress reactivity and the cardiac outcomes of chronic stress remain to be determined.

To identify how the male and female vmPFC coordinates mood-related behaviors and cardiovascular outcomes, genetically-identified vmPFC projection neurons received temporally-specific stimulation in an *in vivo* rodent model. Specifically, channelrhodopsin-2 (ChR2) was expressed under the calcium/calmodulin-dependent protein kinase type II α (CaMKIIα) promoter in the IL to permit optogenetic activation of IL pyramidal neurons in both male and female rats (M. Wood et al., 2018). This approach was combined with measures of place preference and social behavior to examine affective valence and sociability. Behavioral assessment was followed by measures of physiological stress reactivity, including radiotelemetry and echocardiography over the course of chronic variable stress (CVS). Ultimately, these findings identify the IL as an affective-autonomic integrator that links motivation and stress responding divergently in males and females.

Methods

Animals

Age-matched adult male and female Sprague-Dawley rats were obtained from Envigo (Denver, CO) with male rat weight ranging from 250-300 g and female from 150-200 g. After stereotaxic surgery, rats were housed individually in shoebox cages with cardboard tubes for enrichment in a temperature- and humidity-controlled room with a 12-hour light-dark cycle (lights on at 07:00h, off at 19:00h) and food and water *ad libitum*. In accordance with ARRIVE guidelines, all treatments were randomized, and experimenters blinded. All procedures and protocols were approved by the Colorado State University Institutional Animal Care and Use

Committee (protocol: 16-6871A) and complied with the National Institutes of Health Guidelines for the Care and Use of Laboratory Animals. Signs of poor health and/or weight loss ≥ 20% of pre-surgical weight were *a priori* exclusion criteria. These criteria were not met by any animals in the current experiments; however, animals were removed from experimentation if fiber optic or radiotelemetry devices failed.

Microinjections

Rats were anesthetized with isoflurane (1-5%) and administered analgesic (0.6 mg/kg buprenorphine-SR, subcutaneous). Rats received bilateral microinjections (Males 1.5 - 2 µL, Females 0.75 – 1.25 µL) of adeno-associated virus (AAV) into the IL (males: 2.7 mm anterior to bregma, 0.6 mm lateral to midline, and 4.2 mm ventral from dura, females: 2.3 mm anterior to bregma, 0.5 mm lateral to midline, and 4 mm ventral from dura). These volumes correspond with prior studies utilizing viral vector transduction in rat vmPFC (Ferenczi et al., 2016; Ji & Neugebauer, 2012; M. Wood et al., 2018). AAV5-packaged constructs (University of North Carolina Vector Core, Chapel Hill, NC) either expressed yellow fluorescent protein (YFP) or ChR2 conjugated to YFP under the CaMKIIα promoter to achieve pyramidal cell-predominant expression (M. Wood et al., 2018). All microinjections were carried out with a 25-gauge, 2-µL microsyringe (Hamilton, Reno, NV) using a microinjection unit (Kopf, Tujunga, CA) at a rate of 5 minutes/µL. The needle was left in place for 5 minutes before and after injections to reduce tissue damage and allow diffusion. Skin was closed with wound clips that were removed 2 weeks after injections and animals were allowed at least 6 weeks for recovery and ChR2 expression.

Electrophysiology

Adult male rats (n = 8) were injected with AAV constructs as described above and, after 8-12 weeks, exposed to 5% isoflurane prior to decapitation and brain removal. As previously

described (Rau & Hentges, 2017), brains and sections were collected in ice-cold artificial CSF (aCSF) consisting of the following (in mM): 126 NaCl, 2.5 KCl, 1.2 $MgCl_2$ Λ $6H_2O$, 2.4 $CaCl_2$ Λ $2H_2O$, 1.2 NaH_2PO_4, 11.1 glucose, and 21.4 $NaHCO_3$, bubbled with 95% O_2 and 5% CO_2. Coronal slices containing the IL were cut at a thickness of 240 µm using a model VT1200S vibratome (Leica Microsystems, Buffalo Grove, IL). After resting 1 hr at 37°C in aCSF, slices were transferred to the recording chamber and perfused with oxygenated 37° C aCSF at a 2 ml/min flow rate. For whole-cell recordings, the internal recording solution contained the following (in mM): KCL 57.5, K-methyl sulfate 57.5, NaCl 20, $MgCl_2$ 1.5, HEPES 5; EGTA 0.1; ATP 2; GTP 0.5, and phosphocreatine 10. The pH was adjusted to 7.3. Recording electrodes had a resistance of 2 – 4 MΩ when filled with this solution. IL pyramidal neurons were identified for recording based on the expression of ChR2-YFP under the control of CaMKIIα. Whole-cell patch-clamp recordings were acquired in voltage-clamp at a holding potential of -60 mV using an Axopatch 200B Amplifier (Molecular Devices, San Jose, CA). Current-clamp recordings were acquired while holding current at 0 pA. Electrophysiological data were collected and analyzed using Axograph X software on a Mac OS X operating system (Apple, Cupertino, CA). Light activation of IL neurons expressing ChR2 occurred via 473 nm LED (Thorlabs, Newton, NJ) 1.1 mW light pulse driven by a LEDD1B driver (Thorlabs, Newton, NJ) triggered through the TTL output on an ITC-18 computer interface board (HEKA Instruments, Holliston, MA). Current-clamp experiments utilized 5, 10, and 20 Hz stimulation frequencies for 5 min bouts. Recordings were excluded if access resistance exceeded 10 Ω during recording.

Radiotelemetry implantation

A subset of rats was instrumented with ECG-enabled radiotelemetry transmitters (HD-S11 F0, Data Sciences International, St. Paul, MN) as previously described (Flak et al., 2011; Goodson et al., 2017; Schaeuble et al., 2019). Briefly, rats were anesthetized with inhaled isoflurane anesthesia (1-5%) and given a subcutaneous injection of analgesic (0.6 mg/kg

Buprenorphine-SR) and an intramuscular injection of antibiotic (5 mg/kg gentamicin). The descending aorta was exposed via an abdominal incision, allowing implantation of a catheter extending from the transmitter. The catheter was secured with tissue adhesive (Vetbond; 3M Animal Care Products, St. Paul, MN) applied over a cellulose patch. ECG leads were passed through abdominal musculature and sutured subcutaneously above the rib cage and pectoral muscles. The transmitter body was then sutured to the abdominal musculature, followed by closure of the abdominal and skin with suture and wound clips, respectively. Rats then recovered for 2 weeks before wound clips were removed.

Fiber optic cannulas

Rats were anesthetized with isoflurane (1-5%) followed by analgesic (0.6 mg/kg buprenorphine-SR, subcutaneous) and antibiotic (5 mg/kg gentamicin, intramuscular) administration. Bilateral fiber-optic cannulas (flat tip 400/430 μm, NA = 0.66, 1.1 mm pitch with 4.5 mm protrusion for males and 4.2 mm protrusion for females; Doric Lenses, Québec, Canada) were aligned with the IL injection sites and lowered to the ventral PL/dorsal IL approximately 1 mm dorsal to the injection to enable optic stimulation of the IL. Cannulas were secured to the skull with metal screws (Plastics One) and dental cement (Stoelting, Wood Dale, IL). Skin was sutured and, following 1 week of recovery, rats were handled daily and acclimated to the stimulation procedure for another week before experiments began. Rat handling and cannula habituation continued daily throughout experiments.

Optogenetic stimulation

Light pulses (1.0 - 1.3 mW, 5 ms pulses, 10 or 20 Hz) were delivered through a fiber-optic patch cord (240 μm core diameter, NA = 0.63; Doric Lenses) connected to a 473 nm LED driver (Doric Lenses). Optic power was measured with a photodiode sensor (PM160, Thorlabs Inc, Newton, NJ) at the cannula fiber tip. Initial male experiments used

20 Hz stimulation but, following the results of slice electrophysiology experiments, all subsequent studies used 10 Hz stimulation. Rats received a single 20-minute session of stimulation (1 min on/1 min off) in their homecage the week prior to stress exposure. In total, rats received self-determined stimulation in the stimulation zone of RTPP day 2, throughout the social behavior assay, and during acute stress exposure (restraint and novel environment), all prior to CVS. Immediately before and after CVS, ultrasound measures were conducted with optics both off and on to isolate long-term structural changes and acute functional changes. Further optic details are elaborated in the specified sections below.

Estrous cycle cytology

All female rats went through experiment 3 simultaneously, housed in the same room and randomly cycling. Immediately following data collection, vaginal cytology was examined to approximate the estrous cycle stage. A damp (deionized water) cotton swab was used to collect cells from the vaginal canal and place them onto a glass slide. When dried, slides were viewed under a 10x objective light microscope by a minimum of two blind observers and were categorized as proestrus, estrus, metestrus, or diestrus (Cora et al., 2015; Smith et al., 2018; Solomon et al., 2015).

Novel environment

In rats with radiotelemetry implants, baseline cardiovascular measurements were collected the weekend prior to novel environment stress. Rats were then exposed to a 30-minute novel environment stressor to assess acute cardiovascular reactivity. During novel environment, rats were connected to fiber-optic patch cords for stimulation and placed into a brightly-lit semi-transparent arena. Radiotelemetry receiver pads (Data Sciences International, St. Paul, MN) were arrayed under the arena with 10 Hz optic stimulation during the stressor to

record hemodynamics and activity in 1-minute bins. Heart rate (HR), mean arterial pressure (MAP), systolic arterial pressure (SAP), and diastolic arterial pressure (DAP) were collected and analyzed with Ponemah software (Version:6.4x Data Sciences International).

Restraint stress

Restraint was used to examine neuroendocrine responses to acute stress. Rats were placed in plastic film decapicones (Braintree Scientific, Braintree, MA) and connected to fiber-optic patch cords for optic stimulation throughout the 30-minute restraint. Blood samples (approximately 250 µL) were collected by tail clip at the initiation of restraint with additional samples taken 15 and 30 min after (Vahl et al., 2005). At the conclusion of restraint, patch cords were disconnected, and rats returned to their homecage with recovery blood samples collected at 60 and 90 min after the initiation of restraint. Blood glucose was determined with Contour Next EZ glucometers (Bayer, Parsippany, NJ) and 2 independent readings for each time point were averaged. Blood samples were centrifuged at 3000 X g for 15 minutes at 4° C and plasma was stored at –20° C until radioimmunoassay (RIA). Plasma corticosterone levels were measured with an ^{125}I RIA kit (MP Biomedicals, Orangeburg, NY) as previously described (Myers et al., 2017). All samples for each sex were run in duplicate and all time points were run in the same assay. RIA intra-assay coefficient of variation was 8.6% and interassay 13.6%.

Chronic variable stress

Chronic variable stress was comprised of twice daily (AM and PM) repeated and unpredictable stressors presented in a randomized manner including: exposure to a brightly-lit open field (28.5 x 18'' 13'' deep, 1 hour), cold room (4° C, 1 hour), cage tilt (45°, 1 hour), forced swim (23° to 27° C, 10 minutes), predator odor (fox or coyote urine, 1 hour), restraint (1 hour), and shaker stress (100 rpm, 1 hour). Additionally, overnight stressors were variably included,

comprised of damp bedding (400 mL water) and overnight light. During the 2 weeks of CVS, rats were weighed every 3-4 days to monitor body weight.

Spectral analysis of heart rate variability

Throughout CVS, resting homecage recordings of heart rate variability (HRV) were collected and analyzed using Ponemah software (Version:6.4x Data Sciences International, St. Paul, MN). Using guidelines for heart rate variance (Electrophysiology, 1996) in the frequency domain, low (LF) and high frequency (HF) components were collected during two-hour periods in the AM and PM and averaged within treatment groups. Recordings were sampled at least one hour after stressors and did not follow overnight stressors, swim, or restraint. Spectral analysis is used to measure autonomic balance as LF predominantly represents sympathetic and HF predominantly parasympathetic contributions to HRV (Electrophysiology, 1996; Sgoifo et al., 2015). Accordingly, LF/HF represents net cardiac sympathetic drive.

Echocardiography

Left ventricle structure and function were assessed before and after CVS via echocardiography. In preparation, rats were anesthetized with inhaled isoflurane (5% induction, 2% maintenance), connected to fiber optic patch cord, and shaved over the ventral thorax. A 12-mHz pediatric transducer connected to a Phillips XD11 ultrasound system was used to image the heart in transverse (parasternal short axis) and 4-chamber angles. M-mode echocardiograms were utilized to measure left ventricular end-systolic and end-diastolic chamber dimensions and anterior/posterior wall thickness (Chicco et al., 2008; Le et al., 2014). Once the measurements were taken for a rat, optics were turned on (1.3 mW, 5 ms pulses, 10 Hz) and a second exam was conducted to investigate acute stimulation-induced changes. Total exam time for each trial was approximately 5 minutes with approximately 2 minutes of optic stimulation.

Tissue collection

At the conclusion of experiments, rats were given an overdose of sodium pentobarbital and perfused transcardially with 0.9% saline followed by 4.0% paraformaldehyde in 0.1 M PBS. Brains were removed and post-fixed in 4.0% paraformaldehyde for 24 h at room temperature, followed by storage in 30% sucrose in PBS at 4 °C. Coronal sections were made on a freezing microtome at 30 µm thickness and then stored in cryoprotectant solution at −20 °C until processing. A subset of rats received optogenetic stimulation prior to tissue collection. Rats were tethered to a fiber optic patch cord and received 5 minutes of optic stimulation (1 mW, 5 ms pulses, 10 Hz) followed by 90 minutes of recovery for immediate-early gene (c-Fos) expression prior to euthanasia, as described above.

Immunohistochemistry and microscopy

For fluorescent labeling of c-Fos, coronal brain sections were removed from cryoprotectant and rinsed in PBS (5 x 5 min) at room temperature. Sections were then placed in blocking solution (PBS, 0.1% bovine serum albumin, and 0.2% Triton X-100) for 1 hour. Next, sections were incubated overnight in rabbit anti-c-Fos primary antibody (1:200 in blocking solution, Cell Signaling Technologies, Ab #2250). Following overnight incubation in primary antibody, sections were rinsed in PBS (5 x 5 min) and incubated in donkey anti-rabbit Cy5 secondary (1:1000 in PBS, Jackson ImmunoResearch, AB_2340607) for 1 hour. The tissue was then washed (5 x 5 min in PBS), mounted with polyvinyl medium, and cover slipped for imaging. For chromogen labeling of c-Fos positive nuclei, sections were first rinsed in PBS (5 x 5 min) at room temperature. Sections were then incubated in 1% hydrogen peroxide in PBS for 10 minutes followed by a second PBS (5 x 5 min) wash. Sections were then placed in blocking solution for 1 hour. Following blocking, sections were incubated overnight in rabbit anti-c-Fos primary antibody (1:2000 in blocking solution, Abcam, ab190289). Sections were then rinsed in

PBS (5 x 5 min) followed by a 1-hour incubation in biotinylated goat anti-rabbit secondary (1:500 in PBS, Vector Laboratories, BA-1000). Sections were rinsed in PBS (5 x 5 min) followed by a 1-hour incubation in Vectastain ABC Solution (1:1,000; Vector Laboratories). Sections were rinsed again prior to incubation in diaminobenzidine and hydrogen peroxide (0.02% diaminobenzidine/0.09% hydrogen peroxide in KPBS) for 10 min. Following incubation, slices were rinsed, slide mounted, dehydrated in graded ethanol, and cover slipped.

To determine injection placement, YFP was imaged with a Zeiss Axio Imager Z2 microscope using the 10x objective, while YFP and c-Fos dual fluorescence were acquired as tiled 20x objective images. For quantification of c-Fos positive cells, slides were imaged in brightfield with the 10x objective.

Quantification of c-Fos

To quantify the number of c-Fos positive cells, 3-4 IL micrographs adjacent to visible cannula tracts were imaged and positive cells within a half-width 10x frame were hand-counted by a treatment-blind observer.

Experimental design

Timelines for experiments are outlined in figure 3.1. Experiment 1 was comprised of 2 cohorts of male rats (n = 13-14 each) to yield 10 YFP and 17 ChR2. For this experiment, real-time place preference and social behavior were assessed prior to restraint stress with 20 Hz used for all stimulation. A parallel group of injected male rats (n = 8) were used for slice electrophysiology. Experiment 2 consisted of 3 cohorts of male rats (n = 7-8 each) for a total of 12 YFP and 10 ChR2. A subset of these rats was equipped with radiotelemetry transmitters (YFP n = 7, ChR2 n = 8) and all underwent real-time place preference and social behavior prior to novel environment with 10 Hz stimulation. Afterward, rats in experiment 2 underwent echocardiography before and after CVS. Experiment 3 was designed as a single cohort of

female rats (n = 29) with 12 YFP and 17 ChR2. A subset of these rats was equipped with radiotelemeters (YFP n = 7, ChR2 n = 8). Real-time place preference and social motivation were followed by novel environment and restraint with 10 Hz stimulation for all measures. Female rats also underwent echocardiography before and after CVS. A subset of rats in experiments 2 and 3 (n = 6-7/group/sex) received optic stimulation prior to tissue collection to verify neuronal activation.

Data analysis

Data are expressed as mean ± standard error of the mean. Data were analyzed using Prism 8 (GraphPad, San Diego, CA), with statistical significance set at $p < 0.05$ for rejection of null hypotheses. Stimulation induced c-Fos was analyzed with Welch's unpaired t-test comparing virus groups. Stress responses over time (corticosterone, glucose, HR, MAP, SAP, DAP, and HRV spectra) were analyzed using mixed-effects analysis with virus and time (repeated) as factors, followed by Fisher's post-hoc if significant main or interaction effects were present. Baseline HR and MAP, as well as mean activity during novel environment, were assessed with Mann-Whitney U non-parametric test comparing virus groups. Fractional shortening and ventricular structure were assessed with paired Wilcoxon signed-rank tests comparing pre- and post-CVS or optic status within virus groups.

Results

Validation and design

AAV viral vectors were targeted to the IL for expression of membrane-targeted ChR2-YFP or cytosolic YFP under the pyramidal neuron promoter, CaMKIIα. Fiber optic cannulas implanted in the IL permitted selective stimulation of IL glutamatergic neurons as previously reported (Fuchikami et al., 2015; M. Wood et al., 2018). Whole-cell patch-clamp recordings in slice demonstrated light-evoked depolarizing current in male IL neurons expressing ChR2 (Fig.

3.1B). Further, 10 Hz stimulation led to high-fidelity action potential generation. 20-Hz light pulses induced action potential firing, but also increased resting membrane potential (Fig. 3.1C). These results, combined with our previous studies quantifying increased immediate-early gene expression after 20 Hz stimulation (M. Wood et al., 2018), suggest that both 10 Hz and 20 Hz stimulation activate IL CaMKIIα-positive neurons. Although, 10 Hz stimulation is more in line with the reported 4-10 Hz intrinsic firing rate of IL pyramidal neurons (Homayoun & Moghaddam, 2007; Ji & Neugebauer, 2012). The experimental design (Fig. 3.1D) is detailed in the methods. Male and female rats received optogenetic stimulation during behavioral and physiological measures in separate experiments. At the conclusion of all experiments, the placement of viral injections and fiber optics was determined. Only animals with cannula placement verified to be within or immediately (within 0.5 mm) dorsal to the IL were included in analyses (Fig. 3.1E).

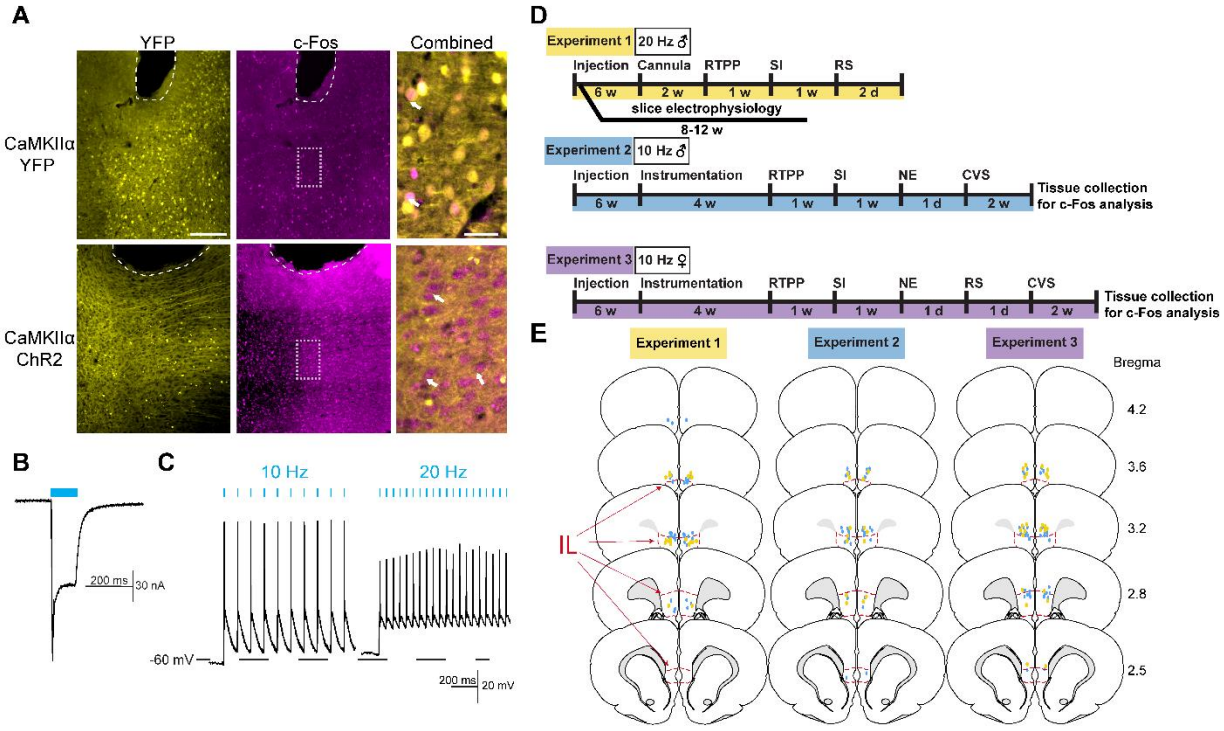

Figure 3.1: Approach validation and experimental design. (A) Injection of AAV-packaged constructs led to expression of cytosolic YFP or membrane-targeted ChR2-YFP under the CaMKIIα promoter. Blue light stimulation in ChR2 females (1 mW, 10 Hz, 5 ms pulses for 5 min) led to robust expression of the immediate-early gene marker c-Fos. Bregma +2.8mm. White arrows indicate representative c-Fos-positive nuclei. Dashed white lines indicate fiber tip. Scale bar: 200 µm and 40 µm for combined. (B) Voltage-clamp recordings from male IL-containing slices illustrated light-evoked (1.1 mW, 100 ms pulse) depolarizing current. (C) Current-clamp recordings found stimulation-locked spiking with 10 and 20 Hz stimulation (1.1 mW, 5 ms pulse). (D) Experimental timelines. RTPP: real-time place preference, SI: social interaction, RS: restraint stress, NE: novel environment, CVS: chronic variable stress. (E) Optic fiber placements (YFP: yellow, ChR2: blue) were mapped within or immediately dorsal to the IL (red outline). Coronal sections adapted from Swanson Rat Brain Atlas (3rd edition).

Endocrine reactivity

To determine the effect of stimulating IL pyramidal neurons on neuroendocrine responses, blood glucose and plasma corticosterone were monitored during restraint stress. In males, optic stimulation decreased corticosterone (n = 10-17/group, mixed-effects: time $F_{(4,81)}$ = 139.4, p < 0.0001, ChR2 $F_{(1,25)} = 8.93$, $p < 0.01$) at the 30-minute timepoint (Fig. 3.2A; $p < 0.01$). Additionally, corticosterone was decreased post-stimulation in the ChR2 group during stress recovery (90 min; $p < 0.05$). Stimulation also decreased blood glucose (mixed-effects: time $F_{(4,90)}$ = 62.86, $p < 0.0001$, time x ChR2 $F_{(4,90)} = 3.43$, $p < 0.05$) in male rats during restraint (Fig. 3.2B; 15 min, $p < 0.01$; 30 min, $p < 0.05$). In contrast, stimulation did not alter plasma corticosterone in female rats (Fig. 3.2C; n = 10-17/group, mixed-effects: time $F_{(4,93)} = 62.94$, $p < 0.0001$) with effects of time limited to within treatment. Additionally, stimulation increased glucose responses to stress in female rats (n = 10-17/group, mixed effects: time $F_{(4,90)} = 24.96$, $p < 0.0001$) specifically at the 15-min timepoint (Fig. 3.2D; $p < 0.05$). Collectively, these results suggest that IL activity in males reduces HPA axis activation as well as glucose mobilization. In females, IL activity does not appear to alter HPA axis response to stress. However, IL stimulation in females increases glucose, possibly through sympathetic mobilization of epinephrine and/or glucagon.

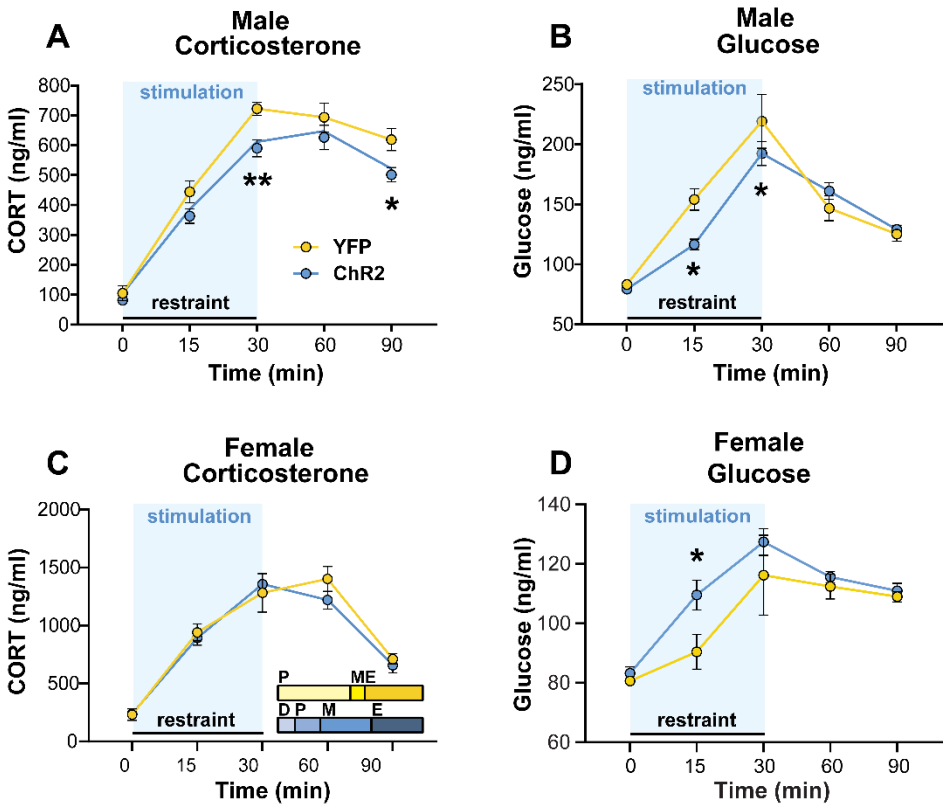

Figure 3.2: IL activation during acute restraint stress attenuated endocrine responses in males but increased female stress reactivity. Stimulation (blue shading) during restraint lowered plasma corticosterone (A) and blood glucose (B) in ChR2 males. (C) Stimulation in females did not alter corticosterone responses. Inset: portion of rats in each estrous cycle phase. D: diestrus, P: proestrus, M: metestrus, E: estrous. (D) IL stimulation during restraint increased glucose mobilization in ChR2 females. n = 10-17/group, * $p < 0.05$, ** $p < 0.01$ vs. YFP.

Cardiovascular reactivity

Baseline hemodynamic measures were recorded in the homecage prior to handling. Animals were connected to fiber optic patch cords and exposed to a brightly lit novel environment as a psychogenic stimulus to examine IL glutamatergic effects on cardiovascular reactivity. Over the course of the stressor, there were no differences in activity between male YFP (n = 7) and ChR2 (n = 8) rats (Fig. 3.3A; Mann-Whitney: U = 407, $p = 0.53$). In terms of hemodynamic responses, stimulation decreased HR reactivity in male ChR2 rats (mixed-effects: time $F_{(30,280)} = 19.61$, $p < 0.0001$, time x ChR2 $F_{(30,280)} = 2.06$, $p < 0.01$), an interaction present at the 8-minute timepoint (Fig. 3.3B; $p < 0.05$). After the first minute of stimulation, arterial

pressures including mean (mixed-effects: time $F_{(30,172)} = 25.99$, $p < 0.0001$, time x ChR2 $F(30,172) = 1.86$, $p < 0.01$), systolic (mixed-effects: time $F_{(30,213)} = 27.61$, $p < 0.0001$), and diastolic (mixed-effects: time $F_{(30,189)} = 20.56$, $p < 0.0001$, ChR2 $F_{(1,12)} = 8.05$, $p < 0.05$, time x ChR2 $F_{(30,189)} = 2.38$, $p < 0.01$) were decreased in male ChR2 rats. Post-hoc analysis indicated these effects were present across multiple timepoints (Fig. 3.3C-E; 7-28 minutes; $p < 0.05$). In contrast, stimulation increased MAP and DAP in minute 1 ($p < 0.05$). For females, there was no effect of ChR2 on activity in the novel environment (Fig. 3.3F; n = 7-8, Mann-Whitney: ChR2 vs YFP $U = 352$, $p = 0.15$). However, IL activation increased female HR responses (mixed effects: time $F_{(30,390)} = 25.83$, $p < 0.0001$) early in the stressor (Fig. 3.3G; 1-9 min; $p < 0.05$) as well as at 25 min ($p < 0.05$). Mixed effects analysis of arterial pressure found main effects of time for MAP (Fig. 3.3H; time $F_{(30,390)} = 31.96$, $p < 0.0001$) and SAP (Fig. 3.3I; time $F_{(30,390)} = 35.01$, $p < 0.0001$) without virus-specific effects. Taken together, these results indicate activation of male IL glutamate neurons decreases HR and arterial pressure responses to psychological stress. In contrast, activation in females increases HR.

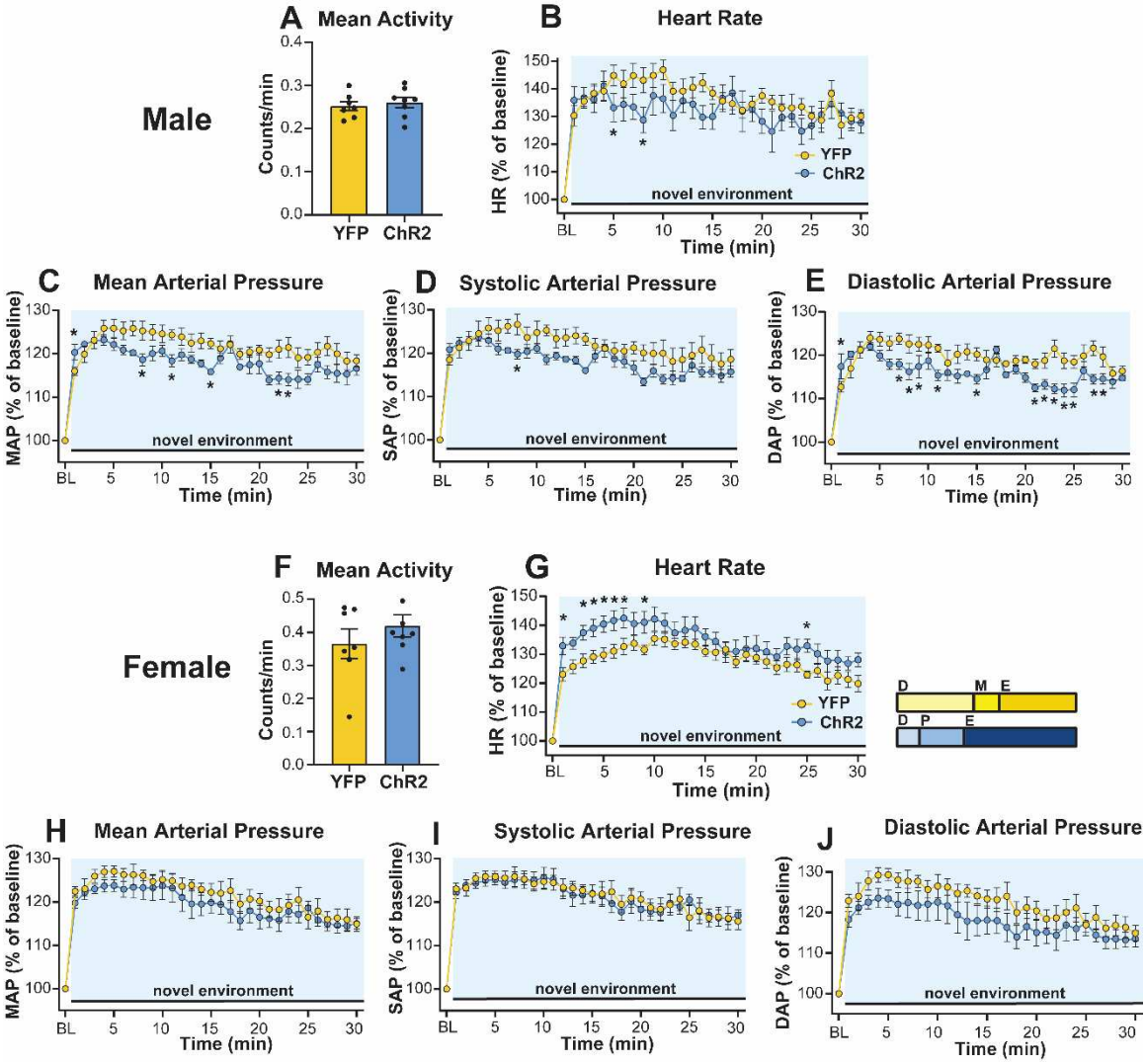

Figure 3: Activation of glutamatergic IL neurons during novel environment exposure reduced male cardiovascular stress responses but increased female HR reactivity. (A) Male IL activation did not affect mean activity in the novel environment. Despite an increase in MAP and DAP during the first minute of stimulation (blue shading) and stress, all recorded hemodynamic responses were decreased in ChR2 males (B-E). (F) Stimulation did not alter activity in females. (G) Female IL stimulation elevated HR reactivity compared to YFP controls but did not affect arterial pressures (H-J). Inset: portion of rats in each estrous cycle phase. D: diestrus, P: proestrus, M: metestrus, E: estrous. n = 7-8/group, * $p < 0.05$ vs. YFP.

3.6 Effects of chronic stress on cardiac function

Resting homecage LF/HF of HRV was recorded via radiotelemetry to assess how prior optic stimulation affected circadian autonomic balance and net cardiac sympathetic drive during CVS. In the absence of ongoing stimulation, ChR2 (n = 8) males had lower LF/HF than YFP (n

= 7) rats (Fig. 3.4A; mixed-effects: time $F_{(5,62)} = 4.45$, $p < 0.01$, ChR2 $F_{(1,13)} = 5.33$, $p < 0.05$). In the AM the day prior to CVS, ChR2 males had lower baseline LF/HF ($p < 0.05$) leading to decreased sympathetic drive the morning of CVS day 14 ($p < 0.05$). In females, there were circadian effects on LF/HF (Fig. 3.4B; n = 5-6/group, mixed-effects: time $F_{(5,45)} = 5.98$, $p < 0.01$) but no differences due to virus (mixed-effects: ChR2 $F_{(1,9)} = 1.28$, $p > 0.05$).

Left ventricle echocardiography was performed before and after CVS to examine the *in vivo* cardiac consequences of chronic stress and the effects of IL stimulation on cardiac contractility. Fractional shortening (FS) was measured as the portion of diastolic dimension lost in systole. In male rats treated with YFP (n = 8), CVS increased FS (Fig. 3.4C; Wilcoxon: Post vs Pre W = 30.0, $p < 0.05$). In contrast, there was no effect of CVS on FS in ChR2 (n = 8) males (Wilcoxon: Post vs Pre W = -4.0, $p = 0.84$). To determine whether post-CVS FS was affected by acute stimulation, measurements were taken with optics off and then on (Fig. 4D). Here, a cohort of males showed no effect of acute optic status on FS (n = 3-4/group, Wilcoxon: YFP On vs Off W = 4.0, $p = 0.13$; ChR2 On vs Off W = 2.0, $p = 0.75$). In females there was no effect of CVS on FS (Fig. 4E; n = 10, YFP Post vs Pre W = -21.0, $p = 0.25$; n = 17, ChR2 Post vs Pre W = 53.0, $p = 0.07$). However, optic stimulation increased post-CVS FS in ChR2 animals (Fig. 4F; Wilcoxon: On vs Off W = 87.0, $p < 0.01$). In aggregate, these findings indicate that a history of IL stimulation limits net cardiac sympathetic drive during chronic stress in males, an effect that may protect against CVS-increased FS. Conversely, neither CVS nor prior IL stimulation affected autonomic balance or cardiac function in females. However, acute IL stimulation after CVS increased female cardiac contractility.

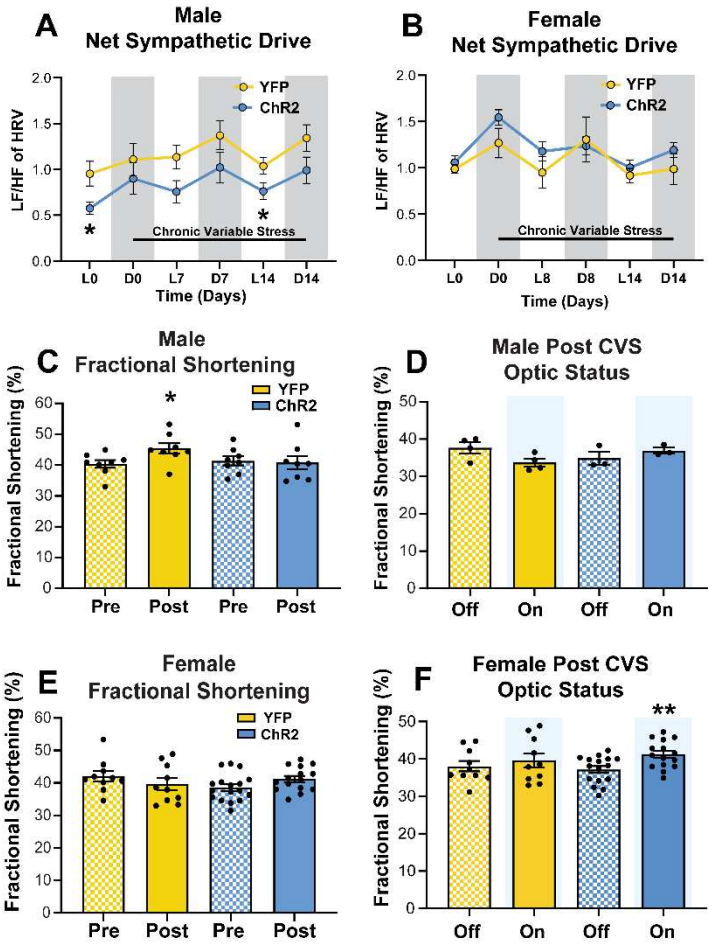

Figure 3.4: The effects of chronic stress and IL activity on cardiac function. (A) The ratio of LF to HF components of HRV were reduced in ChR2 males at baseline and the end of CVS. (B) Females had no treatment-based effects on net sympathetic drive. L: light phase, D: dark phase, LF: low frequency, HF: high frequency, HRV: heart rate variability. (C) CVS increased FS in YFP but not ChR2 males. (D) Acute optic status (On vs. Off) did not affect FS in males. (E) Females showed no changes in FS after CVS. (F) However, acute optogenetic activation (blue shading) increased female FS after CVS. * $p < 0.05$ vs YFP or Pre CVS YFP, ** $p < 0.01$ vs. ChR2 Off.

Chronic stress effects on cardiac structure

Left ventricular morphological analysis was carried out to examine potential structural contributions to altered function. In YFP males (Fig. 3.5A; n = 8), CVS increased wall thickness of the posterior wall in systole (Fig 3.5B; Wilcoxon: Post vs Pre W = 28, $p < 0.05$) and the anterior wall in both systole (Wilcoxon: Post vs Pre W = 36, $p < 0.01$) and diastole (Wilcoxon: Post vs Pre W = 28, $p < 0.05$). Furthermore, increased wall thickness was sufficient to decrease

ventricle size in systole (Fig. 3.5C; Wilcoxon: Post vs Pre W = -30, $p < 0.05$). Critically, male rats that had previously received IL stimulation (ChR2, n = 8) were protected from the effects of CVS on cardiac hypertrophy (Fig 3.5D-E; Wilcoxon: Post vs Pre W = -9 to 20, $p > 0.05$). In contrast to males, female rats (Fig. 3.5F) showed minimal effects of CVS on cardiac remodeling as YFP rats (n = 10) had decreased posterior wall thickness in diastole (Fig. 3.5G; Wilcoxon: Post vs Pre W = -37.0, $p < 0.05$) with no other structural changes (Fig. 3.5H; $p > 0.05$). Additionally, there were no significant changes in cardiac structure in the female ChR2 group (Fig. 3.5I-J; n = 16, Wilcoxon: Post vs Pre W = -45 to 25, $p > 0.05$). Overall, CVS-induced inward hypertrophic remodeling was prevented by prior IL activation in males. In contrast, female rats were generally resistant to the hypertrophic effects of chronic stress.

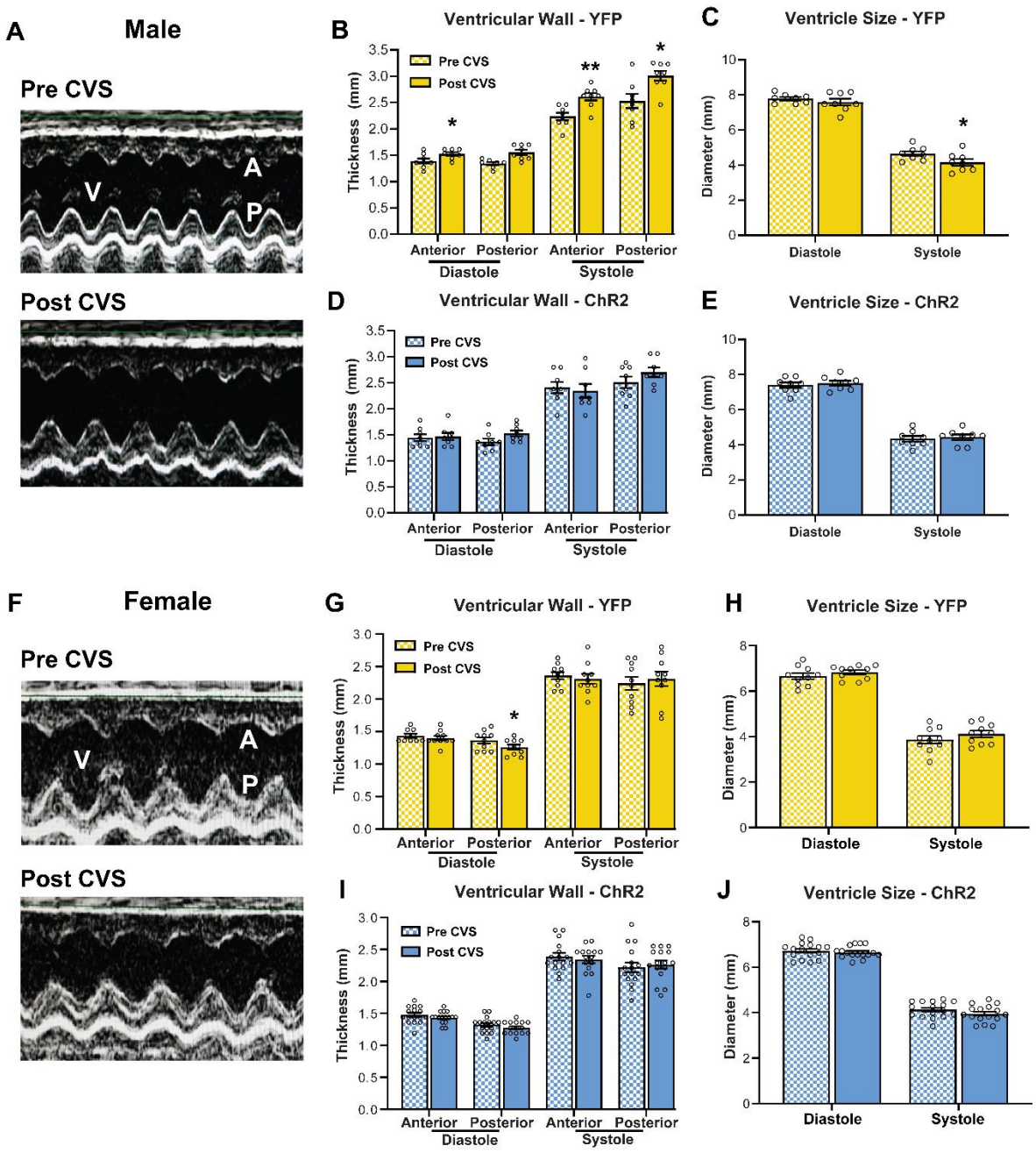

Figure 3.5: Effects of chronic stress and prior IL stimulation on cardiac structure.
(A) Representative echocardiographic images of the left ventricle in bisected m-mode view before and after CVS in YFP males. V: ventricle, A: anterior wall, P: posterior wall. (B) CVS increased wall thickness in diastole and systole in YFP males, (C) reducing ventricle size. (D, E) ChR2 males that received prior stimulation were protected from the cardiac consequences of CVS. (F) Representative m-mode view of the left ventricle in YFP females before and after CVS. (G, H) Females did not exhibit ventricular hypertrophy after CVS as posterior wall thickness in diastole was decreased. (I, J) No myocardial structural changes were evident in ChR2 females. n = 8-16/group, * $p < 0.05$, ** $p < 0.01$ vs. Pre CVS YFP.

4. Discussion

In the current study, optogenetic stimulation of glutamatergic IL pyramidal neurons was combined with behavioral, endocrine, and cardiovascular assessments. Our results show that, in males, IL pyramidal neuron activity was preferred, increased social motivation, and reduced acute physiological stress reactivity. Intriguingly, prior IL activation lowered net cardiac sympathetic drive and protected against subsequent myocardial remodeling after chronic stress. However, IL activity had fundamentally different regulatory effects in females. Stimulation did not have motivational valence or alter social behavior but increased acute physiological stress reactivity and cardiac contractility following chronic stress. Collectively, these findings identify sexual divergence in the cortical integration of affective and physiological systems, suggesting that vmPFC output signaling may differentially impact health outcomes in males and females.

The comorbidity of CVD and MDD shows sexual divergence with females at twice the risk (Goldstein et al., 2019; Möller-Leimkühler, 2007; Naqvi et al., 2005). Given the interactions between stress, mood disorders, and CVD, stress-reactive neural populations are well positioned to regulate affective and cardiovascular outcomes. Importantly, chronic stress exposure in male rats reduces IL pyramidal neuron dendritic arborization and increases local GABAergic signaling, suggesting reduced glutamatergic output (Jessica M. McKlveen et al., 2019; Jessica M McKlveen et al., 2016; Radley et al., 2008). Further, long-term reduction of male IL glutamatergic output increases HPA axis activity and impairs vascular function (Myers et al., 2017; Schaeuble et al., 2019). Collectively, IL output neurons represent a target for modulating behavioral and physiological responses to stress. Thus, we sought to test this hypothesis through real-time *in vivo* assessments of behavior, physiology, and organ function. Altogether, we found that the neurobiology of emotional behaviors, endocrine-autonomic integration, and cardiovascular outcomes differed substantially between sexes.

Activation of IL glutamatergic neurons also reduced male glucose and corticosterone responses to stress. Conversely, female IL glutamatergic stimulation increased glucose mobilization without affecting corticosterone, suggesting a role in sympatho-excitation. Female IL activity also increased tachycardic responses to stress, while male IL stimulation reduced cardiovascular stress responses including HR and arterial pressures. These experiments indicate that IL activity has opposing effects on endocrine-autonomic integration in males and females whereby male glutamatergic IL neurons cause widespread inhibition of the stress response and female IL neurons facilitate sympathetic responses.

Chronic stress exposure induced ventricular hypertrophy and increased endocardial FS in males, suggesting that increased wall thickness likely accounted for the increase in FS. This effect was prevented by a history of IL stimulation in males, likely arising from a reduction in symaptho-vagal imbalance throughout CVS. In fact, previous IL stimulation limited resting net sympathetic drive, a major risk for CVD (Thayer et al., 2012; Wulsin et al., 2015). Given that rats received no optic stimulation during CVS and that acute optic status did not impact male FS, this effect was likely driven by stimulation-induced IL plasticity. IL stimulation has been shown to induce persistent morphological changes in males including increased excitatory synapses onto pyramidal neurons, suggesting a prolonged state of enhanced excitability (Fuchikami et al., 2015; Moda-Sava et al., 2019). Thus, lower resting net sympathetic tone and/or reduced sympathetic activity during stressors may have prevented the consequences of chronic stress to induce inward hypertrophic remodeling of the myocardium. These effects were not present in females as hypertrophic remodeling was not evident and acute stimulation increased FS. Collectively, these results indicate that prior male IL glutamatergic activity is sufficient to restrain responses to chronic stress while female IL activity increases cardiac contractility independent of structural changes.

Physiological responses to stress are critical for survival, tightly defended, and limited in maximum capacity; accordingly, our manipulations only caused moderate changes in response

magnitude to acute challenges. However, our findings suggest that the interaction of altered stress responding with chronic stressors is sufficient to account for differences in cardiac structure and function. It is also worth noting that prior studies on the role of vmPFC in stress responding have yielded equivocal results. Specifically, lesions studies in male rats have observed both increased (Diorio et al., 1993; Figueiredo et al., 2003) and decreased (Radley et al., 2006) neuroendocrine stress responding. Similarly, pharmacological studies found that male vmPFC both reduces (Müller-Ribeiro et al., 2012) and enhances (Tavares et al., 2009) cardiovascular stress responses. These discrepancies are not limited to rodents as pharmacological studies in non-human primates suggest that vmPFC increases cardiovascular stress responding (Alexander et al., 2020), while electrical stimulation in humans causes hypotension (Lacuey et al., 2018). Although it is possible that variations in acute stressors, selectivity of cortical subregion targeting, and/or species may account for these divergent findings, all of the described studies used non-specific blockade or stimulation. Given the complexity of cortical circuitry and the numerous local inhibitory mechanisms (Jessica M. McKlveen et al., 2019), cell-type specific targeting has the ability to isolate the precise contribution of vmPFC principal cells independent of afferents, interneurons, and glia. To address this issue, our prior studies developed anatomical and cell-type specific approaches to reduce glutamate outflow from IL pyramidal neurons. Genetic knockdown of IL glutamate release in males increased neuroendocrine and cardiovascular responses to both acute and chronic stress (Myers et al., 2017; Schaeuble et al., 2019), demonstrating the necessity of IL output for inhibiting physiological stress responses. The current cell-type specific optogenetic targeting adds further temporal specificity and identifies the sufficiency of male IL glutamate neurons for stress inhibition. Albeit with opposing effects in females.

The IL does not directly innervate the neurons that govern endocrine and autonomic stress responses. Accordingly, downstream glutamate signaling from IL synaptic terminals requires intermediary synapses. The exact circuits engaged by IL pyramidal cells to bring about

the observed effects remain to be determined. However, anterograde mapping studies indicate that IL projections widely innervate the forebrain and brainstem (Vertes, 2004; M. Wood et al., 2018). We previously found that, in males, stress-activated IL neurons innervate local inhibitory GABAergic neurons in the posterior hypothalamus (PH) (Myers et al., 2016). Furthermore, blocking GABAergic tone in the PH reduces social behavior and increases HPA axis reactivity suggesting inhibition of the PH may be important for limiting behavioral and physiological stress responses (Myers et al., 2016). Additionally, IL inputs to the amygdala are critical for fear extinction and reducing anxiety-like behavior (Adhikari et al., 2015; Sierra-Mercado et al., 2011). Interestingly, amygdala-projecting IL neurons are both resistant to stress-induced dendritic retraction as well as sensitive to estrogen (Shansky et al., 2009, 2010). Thus, the IL-amygdala circuit could play a key role in sex differences in behavioral regulation. Although the downstream mechanisms of IL cardiovascular regulation are unknown, male IL projections target pre-autonomic cell groups in the brainstem and give rise to multi-synaptic pathways that innervate the adrenal medulla (Dum et al., 2019; Gabbott et al., 2005). Further sex-specific analysis of IL synaptic signaling in forebrain and brainstem nuclei is necessary to determine the basis of divergent behavioral and physiological integration.

While ovarian hormones have far-reaching effects on behavior and physiological systems, we did not control for estrous cycle phase. Instead, we used randomly cycling females. Cycle phase was reported for each treatment, but statistical power was insufficient to examine phase as a factor. It remains to be determined how gonadal hormones might contribute to the sexually divergent effects observed. Estrogen receptor (ER) α, β, and the g-protein coupled ER are expressed in pyramidal and non-pyramidal PFC neurons in both sexes (Almey et al., 2014; Montague et al., 2008). Further, ER localized to PFC dendritic spines regulates synaptic morphology and ionotropic glutamate receptor ubiquitination/degradation following repeated stress (Hao et al., 2006; Wei et al., 2014; Yuen et al., 2016). These protective effects are dependent on PFC ERα and estradiol-synthesizing aromatase (Wei et al., 2014), indicating a

role for extra-ovarian estrogen synthesis. In addition, ER expressed in axons and axonal terminals rapidly alters pre-synaptic transmission in pyramidal cells (Almey et al., 2014). Although studies have described multiple interactions between ER and cortical glutamate signaling (Galvin & Ninan, 2014; Hara et al., 2018), much less is known about PFC progesterone signaling. Progesterone receptors are expressed in frontal cortex (Guerra-Araiza et al., 2003) but progesterone derivatives also signal through $GABA_A$ receptors and regulate GABA subunit expression (Andrade et al., 2012). Moreover, sex differences in IL regulation of behavior and physiology could arise from the actions of androgens. Androgen receptors (AR) are expressed in PFC neurons and glia (Finley & Kritzer, 1999). AR is also enriched in VTA-projecting PFC neurons that influence extracellular dopamine in PFC through downstream VTA glutamate signaling (Aubele & Kritzer, 2012). It is particularly interesting that androgens and estrogens act in opposition to modify PFC dopamine, norepinephrine, and serotonin metabolism during novel environment stress (Handa et al., 1997). Thus, gonadal steroids and locally synthesized modulators affect PFC cellular processes and projection activity, ultimately engaging multiple neurotransmitter systems. Accordingly, the specific cellular and synaptic processes contributing to sex-dependent stress reactivity and resilience are promising avenues for identifying therapeutic targets.

The current study identified a cortical node capable of integrating cardiovascular outcomes. Moreover, activity in this vmPFC cell population produced sex-specific effects on physiological stress responses. In addition to highlighting the necessity of sex-based investigation, these data point to a neurochemical basis for sex differences in stress-related health determinants. Ultimately, further investigation of brain-body interactions in the face of prolonged stress may provide a better understating of disease risk and resilience factors.

References

Adhikari, A., Lerner, T. N., Finkelstein, J., Pak, S., Jennings, J. H., Davidson, T. J., Ferenczi, E., Gunaydin, L. A., Mirzabekov, J. J., Ye, L., Kim, S. Y., Lei, A., & Deisseroth, K. (2015). Basomedial amygdala mediates top-down control of anxiety and fear. *Nature*, *527*(7577), 179–185. https://doi.org/10.1038/nature15698

Alexander, L., Gaskin, P. L. R., Sawiak, S. J., Fryer, T. D., Hong, Y. T., Cockcroft, G. J., Clarke, H. F., & Roberts, A. C. (2019). Fractionating Blunted Reward Processing Characteristic of Anhedonia by Over-Activating Primate Subgenual Anterior Cingulate Cortex. *Neuron*, *101*(2), 307-320.e6. https://doi.org/10.1016/j.neuron.2018.11.021

Alexander, L., Wood, C. M., Gaskin, P. L. R., Sawiak, S. J., Fryer, T. D., Hong, Y. T., McIver, L., Clarke, H. F., & Roberts, A. C. (2020). Over-activation of primate subgenual cingulate cortex enhances the cardiovascular, behavioral and neural responses to threat. *Nature Communications*, *11*(1), 1–14. https://doi.org/10.1038/s41467-020-19167-0

Almey, A., Cannell, E., Bertram, K., Filardo, E., Milner, T. A., & Brake, W. G. (2014). Medial prefrontal cortical estradiol rapidly alters memory system bias in female rats: Ultrastructural analysis reveals membrane-associated estrogen receptors as potential mediators. *Endocrinology*, *155*(11), 4422–4432. https://doi.org/10.1210/en.2014-1463

Andrade, S., Arbo, B. D., Batista, B. A. M., Neves, A. M., Branchini, G., Brum, I. S., Barros, H. M. T., Gomez, R., & Ribeiro, M. F. M. (2012). Effect of progesterone on the expression of GABA $_{A}$ receptor subunits in the prefrontal cortex of rats: implications of sex differences and brain hemisphere. *Cell Biochemistry and Function*, *30*(8), 696–700. https://doi.org/10.1002/cbf.2854

Aubele, T., & Kritzer, M. F. (2012). Androgen influence on prefrontal dopamine systems in adult male rats: Localization of cognate intracellular receptors in medial prefrontal projections to the ventral tegmental area and effects of gonadectomy and hormone replacement on glutamate-stimulated. *Cerebral Cortex*, *22*(8), 1799–1812.

https://doi.org/10.1093/cercor/bhr258

Beckmann, M., Johansen-Berg, H., & Rushworth, M. F. S. (2009). Connectivity-based parcellation of human cingulate cortex and its relation to functional specialization. *Journal of Neuroscience*, *29*(4), 1175–1190. https://doi.org/10.1523/JNEUROSCI.3328-08.2009

Beissner, F., Meissner, K., Bär, K. J., & Napadow, V. (2013). The autonomic brain: An activation likelihood estimation meta-analysis for central processing of autonomic function. *Journal of Neuroscience*, *33*(25), 10503–10511. https://doi.org/10.1523/JNEUROSCI.1103-13.2013

Binder, E. B., & Nemeroff, C. B. (2010). The CRF system, stress, depression and anxietyinsights from human genetic studies. In *Molecular Psychiatry* (Vol. 15, Issue 6, pp. 574–588). Nature Publishing Group. https://doi.org/10.1038/mp.2009.141

Chicco, A. J., McCune, S. A., Emter, C. A., Sparagna, G. C., Rees, M. L., Bolden, D. A., Marshall, K. D., Murphy, R. C., & Moore, R. L. (2008). Low-intensity exercise training delays heart failure and improves survival in female hypertensive heart failure rats. *Hypertension*, *51*(4 PART 2 SUPPL.), 1096–1102. https://doi.org/10.1161/HYPERTENSIONAHA.107.107078

Cora, M. C., Kooistra, L., & Travlos, G. (2015). Vaginal Cytology of the Laboratory Rat and Mouse:Review and Criteria for the Staging of the Estrous Cycle Using Stained Vaginal Smears. *Toxicologic Pathology*, *43*(6), 776–793. https://doi.org/10.1177/0192623315570339

Diorio, D., Viau, V., & Meaney, M. J. (1993). The Role of the Medial Prefrontal Cortex (Cingulate Gyrus) in the Regulation of Hypothalamic-Pituitary-Adrenal Responses to Stress. In *The Journal of Neuroscience* (Vol. 13, Issue g).

Drevets, W. C., Price, J. L., Simpson, J. R., Todd, R. D., Reich, T., Vannier, M., & Raichle, M. E. (1997). Subgenual prefrontal cortex abnormalities in mood disorders. *Nature*, *386*(6627), 824–827. https://doi.org/10.1038/386824a0

Drevets, W. C., Savitz, J., & Trimble, M. (2008). The subgenual anterior cingulate cortex in

mood disorders. *CNS Spectrums*, *13*(8), 663–681. https://doi.org/10.1017/S1092852900013754

Dum, R. P., Levinthal, D. J., & Strick, P. L. (2019). The mind-body problem: Circuits that link the cerebral cortex to the adrenal medulla. *Proceedings of the National Academy of Sciences of the United States of America*, *116*(52), 26321–26328. https://doi.org/10.1073/pnas.1902297116

Electrophysiology, T. F. of the E. S. (1996). Heart Rate Variability. *Circulation*, *93*(5), 1043–1065. https://doi.org/10.1161/01.CIR.93.5.1043

Ferenczi, E. A., Zalocusky, K. A., Liston, C., Grosenick, L., Warden, M. R., Amatya, D., Katovich, K., Mehta, H., Patenaude, B., Ramakrishnan, C., Kalanithi, P., Etkin, A., Knutson, B., Glover, G. H., & Deisseroth, K. (2016). Prefrontal cortical regulation of brainwide circuit dynamics and reward-related behavior. *Science*, *351*(6268). https://doi.org/10.1126/science.aac9698

Figueiredo, H. F., Bruestle, A., Bodie, B., Dolgas, C. M., & Herman, J. P. (2003). The medial prefrontal cortex differentially regulates stress-induced c-fos expression in the forebrain depending on type of stressor. *European Journal of Neuroscience*, *18*(8), 2357–2364. https://doi.org/10.1046/j.1460-9568.2003.02932.x

Finley, S. K., & Kritzer, M. F. (1999). Immunoreactivity for intracellular androgen receptors in identified subpopulations of neurons, astrocytes and oligodendrocytes in primate prefrontal cortex. *Journal of Neurobiology*, *40*(4), 446–457. https://doi.org/10.1002/(SICI)1097-4695(19990915)40:4<446::AID-NEU3>3.0.CO;2-J

Flak, J. N., Jankord, R., Solomon, M. B., Krause, E. G., & Herman, J. P. (2011). Opposing effects of chronic stress and weight restriction on cardiovascular, neuroendocrine and metabolic function. *Physiology and Behavior*, *104*(2), 228–234. https://doi.org/10.1016/j.physbeh.2011.03.002

Fuchikami, M., Thomas, A., Liu, R., Wohleb, E. S., Land, B. B., DiLeone, R. J., Aghajanian, G.

K., & Duman, R. S. (2015). Optogenetic stimulation of infralimbic PFC reproduces ketamine's rapid and sustained antidepressant actions. *Proceedings of the National Academy of Sciences of the United States of America*, *112*(26), 8106–8111. https://doi.org/10.1073/pnas.1414728112

Gabbott, P. L. A., Warner, T. A., Jays, P. R. L., Salway, P., & Busby, S. J. (2005). Prefrontal cortex in the rat: Projections to subcortical autonomic, motor, and limbic centers. *The Journal of Comparative Neurology*, *492*(2), 145–177. https://doi.org/10.1002/cne.20738

Galvin, C., & Ninan, I. (2014). Regulation of the mouse medial prefrontal cortical synapses by endogenous estradiol. *Neuropsychopharmacology*, *39*(9), 2086–2094. https://doi.org/10.1038/npp.2014.56

Gianaros, P. J., & Sheu, L. K. (2009). A review of neuroimaging studies of stressor-evoked blood pressure reactivity: Emerging evidence for a brain-body pathway to coronary heart disease risk. In *NeuroImage* (Vol. 47, Issue 3, pp. 922–936). https://doi.org/10.1016/j.neuroimage.2009.04.073

Gianaros, P. J., & Wager, T. D. (2015). Brain-Body Pathways Linking Psychological Stress and Physical Health. *Current Directions in Psychological Science*, *24*(4), 313–321. https://doi.org/10.1177/0963721415581476

Goldstein, J. M., Hale, T., Foster, S. L., Tobet, S. A., & Handa, R. J. (2019). Sex differences in major depression and comorbidity of cardiometabolic disorders: impact of prenatal stress and immune exposures. In *Neuropsychopharmacology* (Vol. 44, Issue 1, pp. 59–70). Nature Publishing Group. https://doi.org/10.1038/s41386-018-0146-1

Goodson, M. L., Packard, A. E. B., Buesing, D. R., Maney, M., Myers, B., Fang, Y., Basford, J. E., Hui, D. Y., Ulrich-Lai, Y. M., Herman, J. P., & Ryan, K. K. (2017). Chronic stress and Rosiglitazone increase indices of vascular stiffness in male rats. *Physiology and Behavior*, *172*, 16–23. https://doi.org/10.1016/j.physbeh.2016.03.031

Grippo, A. J., & Johnson, A. K. (2009). Stress, depression and cardiovascular dysregulation: A

review of neurobiological mechanisms and the integration of research from preclinical disease models. In *Stress* (Vol. 12, Issue 1, pp. 1–21). https://doi.org/10.1080/10253890802046281

Guerra-Araiza, C., Villamar-Cruz, O., González-Arenas, A., Chavira, R., & Camacho-Arroyo, I. (2003). Changes in progestrone receptor isoforms content in the rat brain during the oestrous cycle and after oestradiol and progesterone treatments. *Journal of Neuroendocrinology*, *15*(10), 984–990. https://doi.org/10.1046/j.1365-2826.2003.01088.x

Hamani, C., Mayberg, H., Stone, S., Laxton, A., Haber, S., & Lozano, A. M. (2011). The Subcallosal Cingulate Gyrus in the Context of Major Depression. *BPS*, *69*, 301–308. https://doi.org/10.1016/j.biopsych.2010.09.034

Handa, R. J., Hejna, G. M., & Lorens, S. A. (1997). Androgen inhibits neurotransmitter turnover in the medial prefrontal cortex of the rat following exposure to a novel environment. *Brain Research*, *751*(1), 131–138. https://doi.org/10.1016/S0006-8993(96)01394-7

Hao, J., Rapp, P. R., Leffler, A. E., Leffler, S. R., Janssen, W. G. M., Lou, W., McKay, H., Roberts, J. A., Wearne, S. L., Hof, P. R., & Morrison, J. H. (2006). Estrogen alters spine number and morphology in prefrontal cortex of aged female rhesus monkeys. *Journal of Neuroscience*, *26*(9), 2571–2578. https://doi.org/10.1523/JNEUROSCI.3440-05.2006

Hara, Y., Crimins, J. L., Puri, R., Wang, A. C. J., Motley, S. E., Yuk, F., Ramos, T. M., Janssen, W. G. M., Rapp, P. R., & Morrison, J. H. (2018). Estrogen Alters the Synaptic Distribution of Phospho-GluN2B in the Dorsolateral Prefrontal Cortex While Promoting Working Memory in Aged Rhesus Monkeys. *Neuroscience*, *394*, 303–315. https://doi.org/10.1016/j.neuroscience.2018.09.021

Homayoun, H., & Moghaddam, B. (2007). NMDA receptor hypofunction produces opposite effects on prefrontal cortex interneurons and pyramidal neurons. *Journal of Neuroscience*, *27*(43), 11496–11500. https://doi.org/10.1523/JNEUROSCI.2213-07.2007

Ji, G., & Neugebauer, V. (2012). Modulation of medial prefrontal cortical activity using in vivo

recordings and optogenetics. *Molecular Brain*, *5*, 36. https://doi.org/10.1186/1756-6606-5-36

Lacuey, N., Hampson, J. P., Theeranaew, W., Zonjy, B., Vithala, A., Hupp, N. J., Loparo, K. A., Miller, J. P., & Lhatoo, S. D. (2018). Cortical structures associated with human blood pressure control. *JAMA Neurology*, *75*(2), 194–202. https://doi.org/10.1001/jamaneurol.2017.3344

Le, C. H., Mulligan, C. M., Routh, M. A., Bouma, G. J., Frye, M. A., Jeckel, K. M., Sparagna, G. C., Lynch, J. M., Moore, R. L., McCune, S. A., Bristow, M., Zarini, S., Murphy, R. C., & Chicco, A. J. (2014). Delta-6-desaturase links polyunsaturated fatty acid metabolism with phospholipid remodeling and disease progression in heart failure. *Circulation: Heart Failure*, *7*(1), 172–183. https://doi.org/10.1161/CIRCHEARTFAILURE.113.000744

Liotti, M., Mayberg, H. S., Brannan, S. K., McGinnis, S., Jerabek, P., & Fox, P. T. (2000). Differential limbic-cortical correlates of sadness and anxiety in healthy subjects: Implications for affective disorders. *Biological Psychiatry*, *48*(1), 30–42. https://doi.org/10.1016/S0006-3223(00)00874-X

Mayberg, H. S., Lozano, A. M., Voon, V., McNeely, H. E., Seminowicz, D., Hamani, C., Schwalb, J. M., & Kennedy, S. H. (2005). Deep brain stimulation for treatment-resistant depression. *Neuron*, *45*(5), 651–660. https://doi.org/10.1016/j.neuron.2005.02.014

McKlveen, J. M., Myers, B., & Herman, J. P. (2015). The Medial Prefrontal Cortex: Coordinator of Autonomic, Neuroendocrine and Behavioural Responses to Stress. In *Journal of Neuroendocrinology* (Vol. 27, Issue 6, pp. 446–456). Blackwell Publishing Ltd. https://doi.org/10.1111/jne.12272

McKlveen, Jessica M., Moloney, R. D., Scheimann, J. R., Myers, B., & Herman, J. P. (2019). “Braking” the Prefrontal Cortex: The Role of Glucocorticoids and Interneurons in Stress Adaptation and Pathology. *Biological Psychiatry*, *86*(9), 669–681. https://doi.org/10.1016/j.biopsych.2019.04.032

McKlveen, Jessica M, Morano, R. L., Fitzgerald, M., Zoubovsky, S., Cassella, S. N., Scheimann, J. R., Ghosal, S., Mahbod, P., Packard, B. A., Myers, B., Baccei, M. L., & Herman, J. P. (2016). Chronic Stress Increases Prefrontal Inhibition: A Mechanism for Stress-Induced Prefrontal Dysfunction. *Biological Psychiatry*, *80*(10), 754–764. https://doi.org/10.1016/j.biopsych.2016.03.2101

Moda-Sava, R. N., Murdock, M. H., Parekh, P. K., Fetcho, R. N., Huang, B. S., Huynh, T. N., Witztum, J., Shaver, D. C., Rosenthal, D. L., Alway, E. J., Lopez, K., Meng, Y., Nellissen, L., Grosenick, L., Milner, T. A., Deisseroth, K., Bito, H., Kasai, H., & Liston, C. (2019). Sustained rescue of prefrontal circuit dysfunction by antidepressant-induced spine formation. *Science*, *364*(6436). https://doi.org/10.1126/science.aat8078

Möller-Leimkühler, A. M. (2007). Gender differences in cardiovascular disease and comorbid depression. *Dialogues in Clinical Neuroscience*, *9*(1), 71–83.

Montague, D., Weickert, C. S., Tomaskovic-Crook, E., Rothmond, D. A., Kleinman, J. E., & Rubinow, D. R. (2008). Oestrogen receptor α localisation in the prefrontal cortex of three mammalian species. *Journal of Neuroendocrinology*, *20*(7), 893–903. https://doi.org/10.1111/j.1365-2826.2008.01743.x

Müller-Ribeiro, F. C. de F., Zaretsky, D. V., Zaretskaia, M. V., Santos, R. A. S., DiMicco, J. A., & Fontes, M. A. P. (2012). Contribution of infralimbic cortex in the cardiovascular response to acute stress. *American Journal of Physiology-Regulatory, Integrative and Comparative Physiology*, *303*(6), R639–R650. https://doi.org/10.1152/ajpregu.00573.2011

Myers-Schulz, B., & Koenigs, M. (2012). Functional anatomy of ventromedial prefrontal cortex: Implications for mood and anxiety disorders. In *Molecular Psychiatry* (Vol. 17, Issue 2, pp. 132–141). https://doi.org/10.1038/mp.2011.88

Myers, B. (2016). Corticolimbic regulation of cardiovascular responses to stress. *Physiology & Behavior*, *172*, 49–59. https://doi.org/10.1016/j.physbeh.2016.10.015

Myers, B., Carvalho-Netto, E., Wick-Carlson, D., Wu, C., Naser, S., Solomon, M. B., Ulrich-Lai,

Y. M., & Herman, J. P. (2016). GABAergic Signaling within a Limbic-Hypothalamic Circuit Integrates Social and Anxiety-Like Behavior with Stress Reactivity. *Neuropsychopharmacology : Official Publication of the American College of Neuropsychopharmacology*, *41*(6), 1530–1539. https://doi.org/10.1038/npp.2015.311

Myers, B., Mark Dolgas, C., Kasckow, J., Cullinan, W. E., & Herman, J. P. (2014). Central stress-integrative circuits: Forebrain glutamatergic and GABAergic projections to the dorsomedial hypothalamus, medial preoptic area, and bed nucleus of the stria terminalis. *Brain Structure and Function*, *219*(4). https://doi.org/10.1007/s00429-013-0566-y

Myers, B., McKlveen, J. M., & Herman, J. P. (2014). Glucocorticoid actions on synapses, circuits, and behavior: Implications for the energetics of stress. In *Frontiers in Neuroendocrinology* (Vol. 35, Issue 2, pp. 180–196). Academic Press Inc. https://doi.org/10.1016/j.yfrne.2013.12.003

Myers, B., McKlveen, J. M., Morano, R., Ulrich-Lai, Y. M., Solomon, M. B., Wilson, S. P., & Herman, J. P. (2017). Vesicular Glutamate Transporter 1 Knockdown in Infralimbic Prefrontal Cortex Augments Neuroendocrine Responses to Chronic Stress in Male Rats. *Endocrinology*, *158*(10), 3579–3591. https://doi.org/10.1210/en.2017-00426

Naqvi, T. Z., Naqvi, S. S. A., & Merz, C. N. B. (2005). Gender differences in the link between depression and cardiovascular disease. In *Psychosomatic Medicine* (Vol. 67, Issue SUPPL. 1). Psychosom Med. https://doi.org/10.1097/01.psy.0000164013.55453.05

Öngür, D., Ferry, A. T., & Price, J. L. (2003). Architectonic subdivision of the human orbital and medial prefrontal cortex. *Journal of Comparative Neurology*, *460*(3), 425–449. https://doi.org/10.1002/cne.10609

Radley, J. J., Arias, C. M., & Sawchenko, P. E. (2006). Regional differentiation of the medial prefrontal cortex in regulating adaptive responses to acute emotional stress. *Journal of Neuroscience*, *26*(50), 12967–12976. https://doi.org/10.1523/JNEUROSCI.4297-06.2006

Radley, J. J., Rocher, A. B., Rodriguez, A., Ehlenberger, D. B., Dammann, M., Mcewen, B. S.,

Morrison, J. H., Wearne, S. L., & Hof, P. R. (2008). Repeated stress alters dendritic spine morphology in the rat medial prefrontal cortex. *Journal of Comparative Neurology*, *507*(1), 1141–1150. https://doi.org/10.1002/cne.21588

Rau, A. R., & Hentges, S. T. (2017). The relevance of AgRP neuron-derived GABA inputs to POMC neurons differs for spontaneous and evoked release. *Journal of Neuroscience*, *37*(31), 7362–7372. https://doi.org/10.1523/JNEUROSCI.0647-17.2017

Roberts, A. C., & Clarke, H. F. (2019). Why we need nonhuman primates to study the role of ventromedial prefrontal cortex in the regulation of threat- And reward-elicited responses. *Proceedings of the National Academy of Sciences of the United States of America*, *116*(52), 26297–26304. https://doi.org/10.1073/pnas.1902288116

Sankar, T., Chakravarty, M. M., Jawa, N., Li, S. X., Giacobbe, P., Kennedy, S. H., Rizvi, S. J., Mayberg, H. S., Hamani, C., & Lozano, A. M. (2019). Neuroanatomical predictors of response to subcallosal cingulate deep brain stimulation for treatment-resistant depression. *Journal of Psychiatry & Neuroscience : JPN*, *44*(6), 1–10. https://doi.org/10.1503/jpn.180207

Schaeuble, D., Packard, A. E. B., McKlveen, J. M., Morano, R., Fourman, S., Smith, B. L., Scheimann, J. R., Packard, B. A., Wilson, S. P., James, J., Hui, D. Y., Ulrich-Lai, Y. M., Herman, J. P., & Myers, B. (2019). Prefrontal Cortex Regulates Chronic Stress-Induced Cardiovascular Susceptibility. *Journal of the American Heart Association*, *8*(24), e014451. https://doi.org/10.1161/JAHA.119.014451

Sgoifo, A., Carnevali, L., Pico Alfonso, M. D. L. A., & Amore, M. (2015). Autonomic dysfunction and heart rate variability in depression. *Stress*, *18*(3), 343–352. https://doi.org/10.3109/10253890.2015.1045868

Shansky, R. M., Hamo, C., Hof, P. R., Lou, W., McEwen, B. S., & Morrison, J. H. (2010). Estrogen promotes stress sensitivity in a prefrontal cortex-amygdala pathway. *Cerebral Cortex*, *20*(11), 2560–2567. https://doi.org/10.1093/cercor/bhq003

Shansky, R. M., Hamo, C., Hof, P. R., McEwen, B. S., & Morrison, J. H. (2009). Stress-induced dendritic remodeling in the prefrontal cortex is circuit specific. *Cerebral Cortex*, *19*(10), 2479–2484. https://doi.org/10.1093/cercor/bhp003

Shoemaker, J. K., Badrov, M. B., Al-Khazraji, B. K., & Jackson, D. N. (2016). Neural control of vascular function in skeletal muscle. *Comprehensive Physiology*, *6*(1), 303–329. https://doi.org/10.1002/cphy.c150004

Sierra-Mercado, D., Padilla-Coreano, N., & Quirk, G. J. (2011). Dissociable roles of prelimbic and infralimbic cortices, ventral hippocampus, and basolateral amygdala in the expression and extinction of conditioned fear. *Neuropsychopharmacology*, *36*(2), 529–538. https://doi.org/10.1038/npp.2010.184

Smith, B. L., Morano, R. L., Ulrich-Lai, Y. M., Myers, B., Solomon, M. B., & Herman, J. P. (2018). Adolescent environmental enrichment prevents behavioral and physiological sequelae of adolescent chronic stress in female (but not male) rats. *Stress (Amsterdam, Netherlands)*, *21*(5), 464–473. https://doi.org/10.1080/10253890.2017.1402883

Solomon, M. B., Loftspring, M., De Kloet, A. D., Ghosal, S., Jankord, R., Flak, J. N., Wulsin, A. C., Krause, E. G., Zhang, R., Rice, T., McKlveen, J., Myers, B., Tasker, J. G., & Herman, J. P. (2015). Neuroendocrine function after hypothalamic depletion of glucocorticoid receptors in male and female mice. *Endocrinology*, *156*(8), 2843–2853. https://doi.org/10.1210/en.2015-1276

Tavares, R. F., Corrêa, F. M. A., & Resstel, L. B. M. (2009). Opposite role of infralimbic and prelimbic cortex in the tachycardiac response evoked by acute restraint stress in rats. *Journal of Neuroscience Research*, *87*(11), 2601–2607. https://doi.org/10.1002/jnr.22070

Thayer, J. F., Åhs, F., Fredrikson, M., Sollers, J. J., & Wager, T. D. (2012). A meta-analysis of heart rate variability and neuroimaging studies: Implications for heart rate variability as a marker of stress and health. In *Neuroscience and Biobehavioral Reviews* (Vol. 36, Issue 2, pp. 747–756). https://doi.org/10.1016/j.neubiorev.2011.11.009

Uylings, H. B. M., Groenewegen, H. J., & Kolb, B. (2003). Do rats have a prefrontal cortex? In *Behavioural Brain Research* (Vol. 146, Issues 1–2, pp. 3–17). Elsevier. https://doi.org/10.1016/j.bbr.2003.09.028

Vahl, T. P., Ulrich-Lai, Y. M., Ostrander, M. M., Dolgas, C. M., Elfers, E. E., Seeley, R. J., D'Alessio, D. A., & Herman, J. P. (2005). Comparative analysis of ACTH and corticosterone sampling methods in rats. *American Journal of Physiology. Endocrinology and Metabolism*, *289*(5), E823-8. https://doi.org/10.1152/ajpendo.00122.2005

Vertes, R. P. (2004). Differential Projections of the Infralimbic and Prelimbic Cortex in the Rat. *Synapse (New York, N.Y.)*, *51*(1), 32–58. https://doi.org/10.1002/syn.10279

Vijayakumar, N., Cheng, T. W., & Pfeifer, J. H. (2017). Neural correlates of social exclusion across ages: A coordinate-based meta-analysis of functional MRI studies. In *NeuroImage* (Vol. 153, pp. 359–368). Academic Press Inc. https://doi.org/10.1016/j.neuroimage.2017.02.050

Wei, J., Yuen, E. Y., Liu, W., Li, X., Zhong, P., Karatsoreos, I. N., McEwen, B. S., & Yan, Z. (2014). Estrogen protects against the detrimental effects of repeated stress on glutamatergic transmission and cognition. *Molecular Psychiatry*, *19*(5), 588–598. https://doi.org/10.1038/mp.2013.83

Wood, J. N., & Grafman, J. (2003). Human prefrontal cortex: Processing and representational perspectives. *Nature Reviews Neuroscience*, *4*(2), 139–147. https://doi.org/10.1038/nrn1033

Wood, M., Adil, O., Wallace, T., Fourman, S., Wilson, S. P., Herman, J. P., & Myers, B. (2018). Infralimbic prefrontal cortex structural and functional connectivity with the limbic forebrain: a combined viral genetic and optogenetic analysis. *Brain Structure and Function*, 1–25. https://doi.org/10.1007/s00429-018-1762-6

Wulsin, L. R., Horn, P. S., Perry, J. L., Massaro, J. M., & D'Agostino, R. B. (2015). Autonomic Imbalance as a Predictor of Metabolic Risks, Cardiovascular Disease, Diabetes, and

Mortality. *The Journal of Clinical Endocrinology & Metabolism*, *100*(6), 2443–2448. https://doi.org/10.1210/jc.2015-1748

Yuen, E. Y., Wei, J., & Yan, Z. (2016). Estrogen in prefrontal cortex blocks stress-induced cognitive impairments in female rats. In *Journal of Steroid Biochemistry and Molecular Biology* (Vol. 160, pp. 221–226). Elsevier Ltd. https://doi.org/10.1016/j.jsbmb.2015.08.028

CHAPTER 4: SEX DIFFERENCES IN PREFRONTAL-HYPOTHALAMIC CONTROL OF BEHAVIOR AND STRESS RESPONDING[1]

Overview

Depression and cardiovascular disease are both augmented by daily life stress. Yet, the biological mechanisms that translate psychological stress to affective and physiological outcomes are unknown. Previously, we demonstrated that stimulation of the stress-responsive ventral medial prefrontal cortex (vmPFC) has sexually divergent outcomes on behavior and physiology. Importantly, the vmPFC does not innervate brain regions directly responsible for initiating autonomic or neuroendocrine stress responses; thus, we hypothesize that intermediate synapses integrate cortical information to initiate stress responding. The posterior hypothalamus (PH) directly innervates stress-effector regions and receives substantial innervation from the vmPFC. In the current study, we use circuit-specific approaches to examine whether vmPFC synapses in the PH coordinate stress responding. Here we examine the effects of optogenetic vmPFC-circuit stimulation in males and females on behavior and stress responding. Additionally, we use an intersectional genetic approach to knock down synaptobrevin in PH-projecting vmPFC neurons. Our collective results show that male vmPFC-PH circuitry promotes positive valence and is both sufficient and necessary to reduce sympathetic-mediated stress responses. In females, the vmPFC-PH circuit does not affect behavior but is sufficient to elevate neuroendocrine stress responses. Altogether, these data suggest cortical regulation of stress-reactivity is regulated by hypothalamic projections in a sex-specific manner.

Introduction

[1] The following material is prepared to be submitted for publication under the title, “Sex differences in prefrontal-hypothalamic control of behavior and stress responding”.
Funding: This work was supported by NIH grants R00 HL122454 awarded to BM and AHA Predoctoral Fellowship 827519 awarded to DS.

Prolonged or repeated stress exposure burdens mental and physical health. Epidemiological evidence reveals that stress predisposes individuals to poor health outcomes including, but not limited to, major depressive disorder (MDD) and cardiovascular disease (CVD). Even though the prevalence and comorbidity of MDD and CVD are well-documented, their burden remains unchecked. Additionally, the female prevalence of mood disorders and heart disease are more than double the rates of MDD in males creating substantial comorbidity (Goldstein et al., 2018; Möller-Leimkühler, 2007; Wake & Yoshiyama, 2009). These data highlight the importance of studying stress as a risk factor for mood and cardiometabolic disease and emphasize the need to progress the understanding of biological sex as a variable for disease. To address this health issue, we need a fundamental understanding of how stress affects the brain's ability to integrate affective and physiological systems. In this series of experiments, we examine neural circuit regulation of behavior(?) and stress physiology to elucidate mechanisms potentially underlying pathology.

Human neuroimaging and basic research have implicated the ventral medial prefrontal cortex (vmPFC) in MDD symptoms. The vmPFC processes emotional stimuli and social exclusion making it a key region to study to better understand mood disorders (Beckmann et al., 2009; Vijayakumar et al., 2017). Likewise, the putative anatomical homolog of the vmPFC in rodents is implicated in depressive-like behavior and promotes behavioral adaptations to stress (Hamani et al., 2012; J. M. McKlveen et al., 2015). The vmPFC is composed primarily of glutamatergic projection neurons with output regulated by a population of GABAergic interneurons (J. M. McKlveen et al., 2015). Chronic stress affects the excitatory/inhibitory balance of the vmPFC, affecting the output of the region (Page & Coutellier, 2019). Previously, we found in male rats that output from vmPFC glutamate neurons is necessary for coordinating neuroendocrine stress responses and sufficient to reduce neuroendocrine and autonomic stress reactivity (Myers et al., 2017; Schaeuble et al., 2019; Wallace et al., 2021). Importantly, stimulation of vmPFC glutamate protects against harmful cardiovascular remodeling and

increased vascular stiffness caused by stress-induced elevation of sympathetic nervous system activity to the heart. Conversely, the study found vmPFC output has no effect on social-motivated behavior yet augments sympatho-excitation in females resulting in increased blood glucose and heart rate reactivity to acute stress exposure. These data suggest the vmPFC is capable of modulating stress responding, however, the vmPFC does not directly innervate brain regions that initiate sympathetic or neuroendocrine responses to stress. However, the posterior hypothalamus (PH) receives vmPFC input and innervates neuroendocrine and autonomic effector regions suggesting the PH has an extensive role in stress integration (Schaeuble & Myers, 2022). While the density of vmPFC projections to the PH has been reported (Wood et al., 2019), little was known about whether or how these projections translate vmPFC output to behavioral or physiological outcomes. Based on evidence that the PH facilitates avoidance behaviors, as well as HPA axis and autonomic stress responses (DiMicco et al., 1986; Myers et al., 2016; Nyhuis et al., 2016), we hypothesize the PH serves as an integrator of cortical information to trans-synaptically influence behavior and regulate neuroendocrine and autonomic stress responses.

To test whether vmPFC innervation of the PH coordinates behavior and physiological stress responses, we used a combination of circuit-specific approaches to stimulate or inhibit vmPFC axons terminals in the PH. PH-projecting vmPFC neuron stimulation was achieved with an optogenetic approach in the PH to open light-activated cation channels selectively expressed in the axon terminals of vmPFC projecting neurons. We stimulated this circuit to observe whether the PH serves as an intermediate synapse for sympathetic and neuroendocrine-mediated stresses responses and behavior. Additionally, we used an intersectional genetic approach to inhibit PH-projecting vmPFC neurons. This experiment tested the necessity of the vmPFC-PH circuit for appropriate stress responding in both sexes. Ultimately, these data provide evidence that stress responses initiated by the vmPFC are sexually divergent and the

PH is a key region in coordinating cortical information to engage physiological responses to stress.

Methods

2.1 Experimental design

The data in this publication are from two experiments. A timeline for experiment 1 is outlined in figure 4.1A. The first experiment comprised of 2 cohorts of male rats to yield 17 YFP and 16 ChR2 on-target injections and cannula placements. A parallel group of male rats (n = 6) were used for slice electrophysiology. The experiment also used 1 cohort of female rats which yielded 12 on-target YFP and ChR2 injections and cannulae. Throughout the experiments, both male and female rats received the same stimulation and were subjected to real-time place-preference and social-interaction tests before acute restraint stress. At the end of experiments, brain tissue was collected to validate our approach. Experiment 2 comprised of 2 cohorts of males to yield 9 GFP and 8 TeNT rats. A separate female cohort yielded 8 GFP and 6 TeNT rats. All rats were injected and allowed to recover for 6 weeks before restraint and tissue collection. The experiments were comprised of male (n = 9/GFP, 8/TeNT) and female (n = 8/GFP, 6/TeNT) rats that were run in separate cohorts.

2.2 Animals

Age-matched adult male and female Sprague-Dawley rats were obtained from Envigo (Denver, CO) with male rat weight ranging from 250-300g and female from 150-200g. After stereotaxic surgery, rats were individually housed in shoebox cages with cardboard tube enrichment. All rats were housed in temperature- and humidity-controlled room with a 12-hour light-dark cycle (lights on at 07:00h, off at 19:00h) and food and water *ad libitum*. In accordance with ARRIVE guidelines, all treatments were randomized, and experimenters blinded. All procedures and protocols were approved by the Colorado State University Institutional Animal Care and Use Committee (protocol: 1321) and complied with the National Institutes of Health

Guidelines for the Care and Use of Laboratory Animals. Signs of poor health and/or weight loss ≥ 20% of pre-surgical weight were *a priori* exclusion criteria.

2.3 Microinjections

For experiment 1, rats were anesthetized with isoflurane (1-5%) followed by analgesic (0.6 mg/kg buprenorphine-SR, subcutaneous) administration. Rats received bilateral microinjections (1 µL) of adeno-associated virus (AAV) into the IL (males: 2.7 mm anterior to bregma, 0.6 mm lateral to midline, and 4.0 mm ventral from dura, females: 2.45 mm anterior to bregma, 0.5 mm lateral to midline, and 4.0 mm ventral from dura). AAV5-packaged constructs (University of North Carolina Vector Core, Chapel Hill, NC) either expressed yellow fluorescent protein (YFP) or ChR2 conjugated to YFP under a synapsin promoter to allow for axon terminal expression in projection neurons (Wood et al., 2019). All microinjections were carried out with a 25-gauge, 2-µL microsyringe (Hamilton, Reno, NV) using a microinjection unit (Kopf, Tujunga, CA) at a rate of 5 minutes/µL. The needle was left in place for 5 minutes before and after injections to reduce tissue damage and allow diffusion. Skin was closed with wound clips that were removed 2 weeks after injections and prior to fiber optic surgery described below. Animals were allowed at least 6 weeks for recovery and ChR2 expression.

For experiment 2, a Cre-dependent approach was used to selectively express tetanus toxin (TeNT) in PH-projecting vmPFC neurons to inhibit neurotransmitter release (Link et al., 1992; McMahon et al., 1993; Sando et al., 2017; Xu & Südhof, 2013). Using the same surgical procedures as previously described, rats were anesthetized and bilaterally injected with 0.75 µL of a retrograde AAV-packaged construct expressing Cre into the PH and either 0.75 µL Cre-dependent (DIO) green fluorescent protein (GFP) or Cre-dependent TeNT into the vmPFC. The TeNT virus was obtained from Stanford Gene Vector and Virus Core while the DIO GFP (50457-AAV5) and retrograde Cre (114472-AAVrg) were obtained from Addgene. After injection, rats were allowed 6 weeks for recovery and TeNT expression.

2.4 Electrophysiology

Adult male rats (n = 6) were injected with AAV constructs as described above and, after 8 to 12 weeks, anesthetized with 5% isoflurane prior to decapitation and brain removal as previously described (Rau & Hentges, 2017; Wallace et al., 2021). Detailed methods are provided in the supplement.

2.5 Fiber optic cannulae

For experiment 1, rats were anesthetized (isoflurane 1-5%) followed by analgesic (0.6 mg/kg buprenorphine-SR, subcutaneous) and antibiotic (5mg/kg gentamicin, intramuscular) administration before bilateral implantation of fiber-optic cannulas. Cannulas (flat tip 400/430 µm, NA = 0.66, 1.1 mm pitch with 7.5 mm length; Doric Lenses, Québec, Canada) were targeted to the PH (males and females: 4.0 mm posterior to bregma, 0.5 mm lateral to midline, and 7.5 mm ventral from dura) and lowered into place. Cannulas were secured to the skull with metal screws (Plastics One) and dental cement (Stoelting, Wood Dale, IL) before skin was sutured. Following 1 week of recovery, rats were handled daily and acclimated to the stimulation procedure for another week before experiments began. Rat handling and cannula habituation continued daily throughout experiments.

2.6 Optogenetic stimulation

In experiment 1, light pulses (8 mW, 5 ms pulses, 10 Hz) were delivered through a fiber-optic patch cord (240 µm core diameter, NA = 0.63; Doric Lenses) connected to a 473 nm LED driver (Doric Lenses).

2.7 Estrous cycle cytology

Following each assessment, vaginal cytology was examined to approximate the estrous cycle stage. A damp (deionized water) cotton swab was used to collect cells from the vaginal canal and roll them onto a glass slide. Dried slides were viewed under a 10x objective light microscope by a minimum of two blind observers and were categorized as proestrus, estrus, metestrus, or diestrus (Cora et al., 2015; Smith et al., 2018; Solomon et al., 2015).

2.9 Restraint stress

Restraint was used to examine neuroendocrine responses to acute stress. Blood glucose and plasma corticosterone were measured as indicators of sympathetic and HPA-axis stress responses, respectively. For experiment 1, rats were placed in plastic decapicones (Braintree Scientific, Braintree, MA) and connected to fiber-optic patch cords for optic stimulation throughout the 30 min restraint, as previously described. Once restrained, the distal tail was clipped and blood samples (approximately 250 µL) were collected at the initiation of restraint with additional samples taken 15 and 30 min after (Vahl et al., 2005). After 30 minutes, patch cords were disconnected, and rats were returned to their homecage with additional blood samples collected at 60 and 90-minute recovery timepoints after the initiation of restraint. Blood glucose was determined with Contour Next EZ glucometers (Bayer, Parsippany, NJ) and 2 independent readings for each time point were averaged. This same protocol was used for the circuit inhibition experiment, but those rats did not require fiber optic cable attachment. Blood samples were centrifuged at 2500 X gravity for 15 min at 4˚C and plasma was stored at −20˚C until measured for corticosterone concentration with Enzo Life Sciences Corticosterone ELISA kit (Catalog No. ADI-900-097).

2.10 Non-invasive heart rate and blood pressure recordings

Heart rate and blood pressure recordings were examined whether acute stimulation of PH vmPFC axon terminals affects cardiovascular activity. Rats were lightly anesthetized with 2% isoflurane then placed prone on a heating pad with low anesthesia maintained via nose cone. Internal body temperature was monitored with a rectal probe and kept at 37°C. A fiber optic patch cord was attached to the cannula before non-invasive blood pressure cuff was slid onto the base of the tail to record heart rate and blood pressure. Using the CODA® monitor (Kent Scientific), heart rate and blood pressure were recorded for 3 minutes before the LED turned on to emit blue light (473 mm) in the PH for 6 minutes. For analysis, data was gathered into three bins (3 mins of no-stimulation, first 3 mins of stimulation, second 3 mins of stimulation).

2.11 Tissue collection

At the conclusion of experiments, brain tissue was collected for technique validation and immunohistology experiments. Prior to euthanasia, a subset of rats were tethered to a fiber optic patch cord for optogenetic stimulation (8 mW, 5 ms pulses, 10 Hz) 90 minutes prior to tissue collection to examine immediate-early gene (c-Fos) expression. After, rats were injected with an overdose of sodium pentobarbital and perfused transcardially with 0.9% saline followed by 4.0% paraformaldehyde in 0.1 M phosphate buffer solution (PBS). Brains were removed and post-fixed in 4.0% paraformaldehyde for 24 h at room temperature, followed by storage in 30% sucrose in PBS at 4˚C. Coronal sections were made on a freezing microtome at 30 µm thickness and then stored in cryoprotectant solution at -20˚C.

2.12 Immunohistochemistry and microscopy

To verify injection and cannula placement in experiment 1, coronal brain sections were imaged with a Zeiss Axio Imager Z2 microscope using a 10x objective. For quantification of the number of fluorescent c-Fos positive cells in the PH, cells were hand-counted by a treatment-blind observer over 10 20x-tiled micrographs adjacent to cannula tracts. GABA was imaged to qualitatively examine if the c-Fos-positive PH cells contained GABA.

For fluorescent labeling of c-Fos and gamma-aminobutyric acid (GABA), coronal brain sections were removed from cryoprotectant and rinsed at room temperature in 1X PBS (5 x 5 min). Sections were then submerged into blocking solution (1X PBS, 0.1% bovine serum albumin, and 0.2% Triton X-100) for 1 hour. Then, sections were incubated in polyclonal guinea pig anti-c-Fos primary antibody (Synaptic Systems; 226-005) (1:1000 in 1X PBS) overnight. The next day, another PBS wash (5 x 5 min) was done before the tissue was incubated in Cy5 donkey anti-guinea pig secondary antibody (Jackson Immuno Research; 706-175-148) (1:1000 in 1X PBS) for 1 hour. Following a PBS wash, the tissue was placed into blocking solution (1X PBS, 6% bovine serum albumin, 8% normal goat serum, 2% normal donkey serum, and 0.4% Triton X-100) for 4 hours. The tissue was next incubated in rabbit anti-GABA primary antibody

(Sigma; MFCD00162297)(1:250 in blocking solution) for 60 hours at 4˚C. After, the tissue was washed in PBS and incubated in biotinylated secondary antibody goat anti-rabbit (Vector Laboratories; BA-100) (1:500 in 1X PBS) for 2 hours. Another PBS wash was conducted before the tissue was incubated in Avidin-Biotin Complex (Vector Laboratories; Vectastain ABC Kit PK-4000) (1:500 in 1X PBS) for 1 hour. The tissue was washed in PBS again before incubation in Cy3-Streptavidin (Jackson Immuno Research; 016-160-084) (1:500 in PBS) for 1 hour. Finally, the tissue was washed in PBS mounted and cover slipped.

To verify inhibition of the vmPFC to PH circuit in experiment 2, immunohistochemistry was utilized to quantify the percent of synpatobrevin-2 protein in PH-targeted vmPFC axons in both the GFP and TeNT treatment groups. Synaptobrevin-2 was labeled in addition to GFP fluorescence amplification to assure robust labeling of vmPFC axons in the PH (Sando et al., 2017). For labeling, tissue was removed from cryoprotectant and washed in PBS (5 x 5 mins) before submerged in blocking solution (1X PBS + 0.1% BSA + 0.2% Triton X-100) for 2 hours. After, the tissue was incubated in rabbit anti-GFP primary antibody (Invitrogen; A11122) (1:1000 in blocking solution) overnight. The next morning the tissue was washed in PBS and incubated in A488 goat anti-rabbit secondary antibody (Invitrogen, A11008) (1:500 in 1X PBS) for 30 mins. Following a PBS wash, tissue was submerged in another blocking solution (4% BSA, 3% donkey serum, 0.1% Triton) for 1 hour before incubated in Synaptobrevin-2 primary antibody (Synaptic Systems; 104 211C3) (1:200 in blocking solution) overnight. On the final day, the tissue was washed in PBS and incubated in Cy5 donkey anti-mouse secondary (Jackson Immuno Research; 715-175-150) (1:500 in PBS) for 2 hours. Tissue was then washed in PBS and mounted for quantification.

2.13 Quantification of Synaptobrevin-2 and GFP colocalization

Slides were imaged with a Zeiss Axio Imager Z2 microscope. On average, 6 images of PH-projecting vmPFC axons were taken per rat. 5-image z-stacks, spanning 2.5 μm, were taken using a 63X objective with apotome processing. Using Zeiss colocalization tool (Zeiss Blue

edition version Zen 2.6 pro), a blinded observer applied a colocalization threshold to individual axons in the PH to calculate the percentage of the GFP axon colocalized with Cy5 fluorescence labeling synaptobrevin-2 protein.

2.14 Data analysis

For both experiments, data are expressed as mean ± standard error of the mean. Data were analyzed using Prism 9.3.1 (GraphPad, San Diego, CA), with statistical significance set at $p < 0.05$ for rejection of null hypotheses. Stimulation induced c-Fos was analyzed with a nonparametric Mann-Whitney unpaired t-test comparing virus groups. In the case of significant main or interaction effects, Sidak's multiple comparisons were run to determine group differences. Stress responses over time (corticosterone, glucose) (and non-invasive blood pressure readings) were analyzed using mixed-effects analysis with virus and time (repeated) as factors, followed by Fisher's post-hoc if significant main or interaction effects were present.

1. Results

3.1 Optogenetic stimulation of PH targeted vmPFC terminals

AAV viral vectors were injected into the vmPFC to express cytosolic YFP or membrane-localized ChR2-YFP in vmPFC neurons under the synapsin promoter. A timeline of optogenetic circuit stimulation experiments is illustrated in figure 1A. Representation of viral spread (Fig. 4.1B) shows injection spread in the PFC with similar spread profiles in both sexes and mapped fiber optic cannula placements show cannulae were targeted to the PH to selectively stimulate vmPFC terminals (Fig. 4.1C). Representative micrographs confirmed virus injection in the vmPFC and bilateral cannulae placement in the PH (Fig. 4.1D&E). To validate the approach, whole-cell patch-clamp recordings in slice demonstrated light-evoked depolarizing current in male vmPFC neurons expressing ChR2 in the PH (Fig. 4.1F). Stimulation increased expression of immediate-early gene, c-Fos, approximately 2-fold in both ChR2 males (Fig. 4.1G Males: n = 8-9/group, unpaired T-test, $p < 0.0001$) and females (Fig. 4.1H Females: n = 7-8/group, unpaired T-test $p < 0.5$) compared to YFP controls further validating the approach. Additionally,

immunohistochemistry representation shows that a portion of the c-Fos positive cells contain GABA neurotransmitter (Fig. 4.1I).

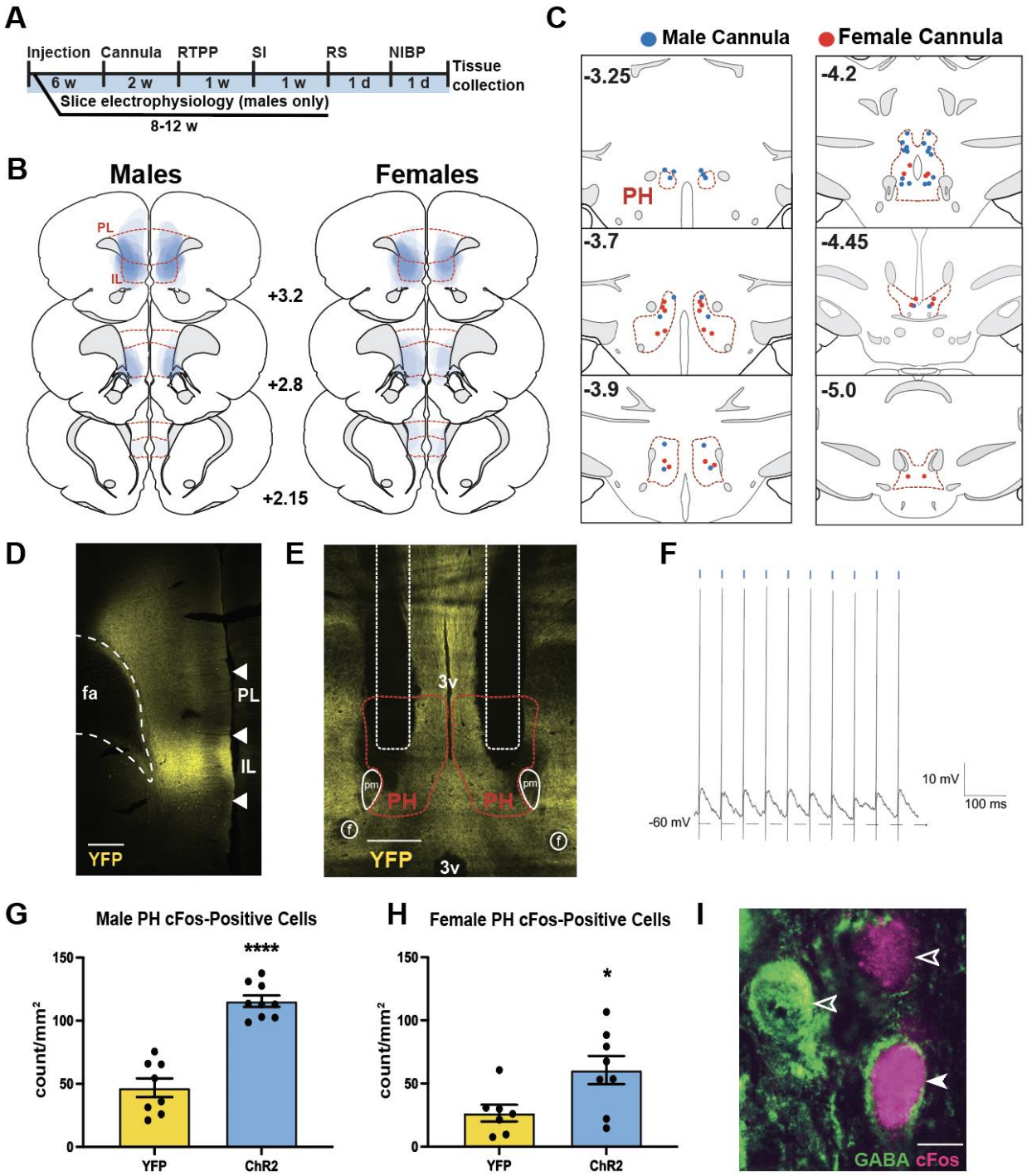

Figure 4.1: Experimental design and validation for vmPFC neuron terminal stimulation in the PH. (A) Experimental timeline. w: week, d: day, RTPP: real-time place preference, SI: social interaction, RS: restraint stress, NIBP: non-invasive heart rate and blood pressure recording. (B) AAV injection spread mapped in blue. Red dotted lines indicate the border of the infralimbic (IL) and prelimbic (PL) cortices. Numbers indicate the distance in millimeters of the tissue

sections rostral to bregma. (C) On-target bilateral cannula placements (Male: blue dots, Female: red dots) of ChR2 rats mapped within the PH (red outline). Coronal sections adapted from Swanson Rat Brain Atlas (3rd edition). Numbers indicate the distance in millimeters of the tissue sections caudal to bregma. (D) Photomicrograph representative image of virus spread in the vmPFC 2.8 millimeters rostral to bregma. Yellow fluorescent protein (YFP) indicates a ventromedial prefrontal cortex injection of AAV-packaged constructs that led to the expression of cytosolic YFP or membrane-targeted ChR2-YFP under the synapsin promoter. Scale bar indicates 500 μm. (E) Photomicrograph of representative posterior hypothalamus (PH) fiber optic cannula placement. White dotted lines outline borders of the fiber optics. Red dotted lines outline the borders of the PH 4.2 millimeters caudal to bregma. Solid white lines outline the borders of the principal mammillary tract (pm) and fornix (f). 3v; third ventricle. Scale bar indicates 1000 μm. (F) Current-clamp recordings found stimulation-locked spiking with 10 Hz stimulation (1.1 mW, 5 ms pulse). (G) Stimulation increased the number of c-Fos positive cells 2-fold in the male PH (n = 8-9/group). (H) Stimulation increased the number of c-Fos positive cells in the female PH (n = 7-8/group). * $p < 0.05$, **** $p < 0.0001$ vs. YFP. (I) Representative image of cells in the PH expressing c-Fos (magenta) and/or containing gamma-aminobutyric acid (GABA) (green). Blank arrows indicate c-Fos or GABA neurons, and white-filled arrows indicate neurons with c-Fos and GABA. Scale bar indicates 20μm.

3.2 Endocrine reactivity

To determine the sufficiency of PH-targeted vmPFC axon terminals for altering sympathetic and HPA axis responses, blood glucose and plasma corticosterone were analyzed during restraint stress, respectively. Optic stimulation decreased blood glucose (Fig. 4.2A; n = 16-17/group, mixed-effects: time $F(4,119) = 34.59$, $p < 0.0001$, ChR2 $F(1,31) = 1.349$, $p = 0.2544$, time x ChR2 $F(4,119) = 1.161$, $p = 0.3315$) during restraint in males (15 min, $p = 0.0214$), but did not affect blood glucose levels during restraint stress in females (Fig. 4.2B; n = 12/group, mixed-effects: time $F(4,78) = 24.63$, $p < 0.00001$, ChR2 $F(1,21) = 0.1839$, $p = 0.6724$, time x ChR2 $F(4,78) = 0.4490$, $p = 0.7728$.). Stimulation had no effect on male plasma corticosterone (Fig. 4.2C; n = 16-17/group, mixed effects: time $F(4,114) = 74.15$, $p < 0.0001$, ChR2 $F(1,31) = 0.4775$, $p = 0.4947$, Time x ChR2 $F(4,114) = 0.4223$, $p = 0.7923$), but stimulation increased plasma CORT in female rats at the 60 and 90-minute recovery timepoints (Fig. 4.2D; n = 12/group, mixed effects: time $F(4,99) = 23.91$, $p < 0.0001$, ChR2 $F(1,99) = 3.491$, $p = 0.0647$, Time x ChR2 $F(4,99) = 2.323$, $p = 0.0619$, 60-minutes $p = 0.0049$, 90-minutes $p = 0.0346$). Collectively, these results suggest that PH-targeted vmPFC neurotransmitter release in males reduces sympathetic activity but does not alter HPA axis corticosterone secretion. In

females, stimulation of this circuit does not alter glucose mobilization but increases HPA axis activity.

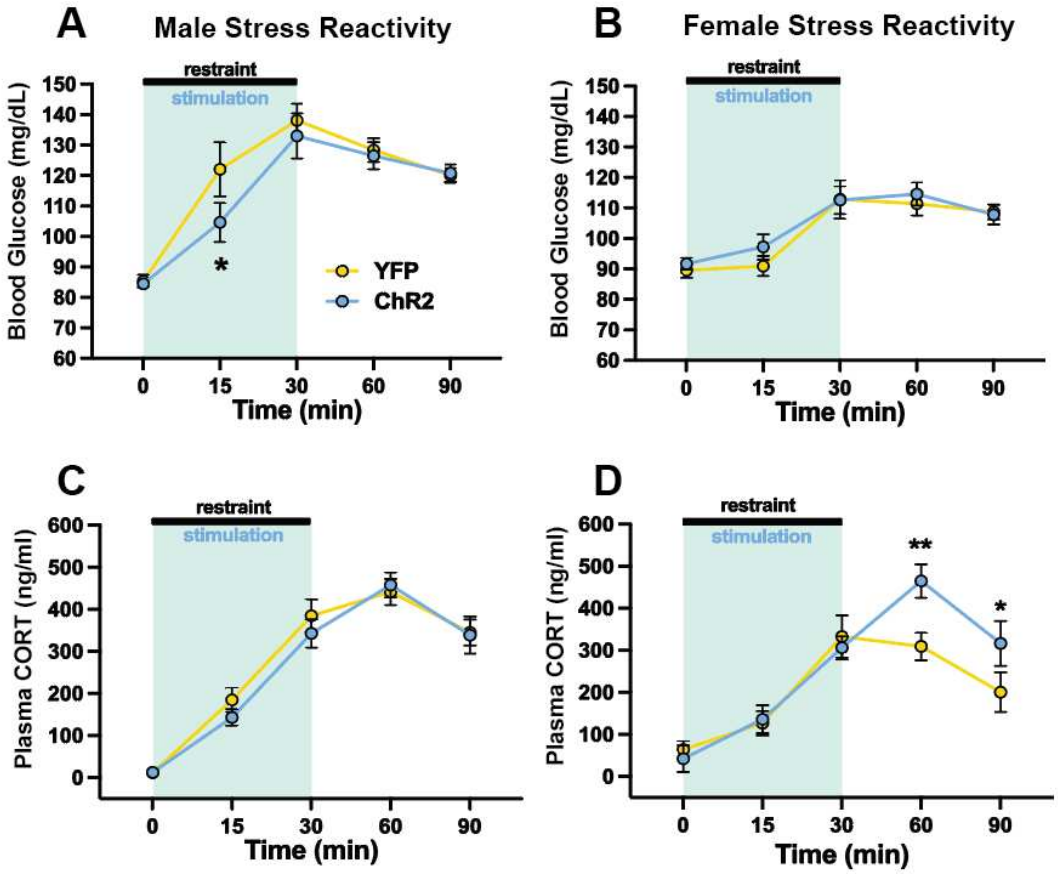

Figure 4.2: Stimulation of PH-targeted vmPFC projections reduces male glucose response but increases female corticosterone response to novel restraint stress. (A) Blue light stimulation decreased blood glucose in ChR2 males compared to YFP controls during restraint. (B) Stimulation had no effect on blood glucose in females. (C) Stimulation did not affect plasma corticosterone (CORT) in males but increased CORT responses in females (D) following restraint. n = 10-17/group, * $p < 0.05$, ** $p < 0.01$ vs. YFP.

3.3 Hemodynamic activity

To determine whether PH targeted vmPFC axons terminals acutely influence cardiovascular activity, a non-invasive tail cuff was used to measure heart rate (HR) and mean arterial pressure (MAP) during optic stimulation. In males, acute stimulation had no effect on heart rate (Fig. 4.3A; n = 5-6/group, mixed-effects: time $F(2,16) = 0.2428$, $p = 0.7873$, ChR2 $F(1,9) = 0.6553$, $p = 0.4391$, time x ChR2 $F(2,16) = 0.005515$, $p = 0.9945$). In females,

stimulation increased heart rate (Fig. 4.3B; n = 7-10/group, mixed effects: time F(2,20) = 0.6655, p = 0.5250, ChR2 F(1,15) = 6.639, p = 0.0211, time x ChR2 F(2,20) = 3.753, p = 0.0413) during the first 3 minutes of stimulation (3 minutes, p = 0.0090, 6 minutes, p = 0.053). Stimulation had no effects on male (Fig. 4.3C; n = 7-8/group, mixed effects: time F(2,18) = 13.56, p < 0.001,ChR2 F(1,13) = 3.157, p = 0.0990, time x ChR2 F(2,18) = 0.8222, p = 0.4553) or female MAP (Fig. 4.3D; n = 9-12/group, mixed effects: time F(2,25) = 8.991, p < 0.01,ChR2 F(1,19) = 0.09478, p = 0.7615, time x ChR2 F(2,25) = 0.1097, p = 0.8965). Collectively, hemodynamic recordings from non-invasive tail cuff show that stimulation of PH targeted vmPFC axon terminals does not affect hemodynamic activity in males but elevates heart rate in females.

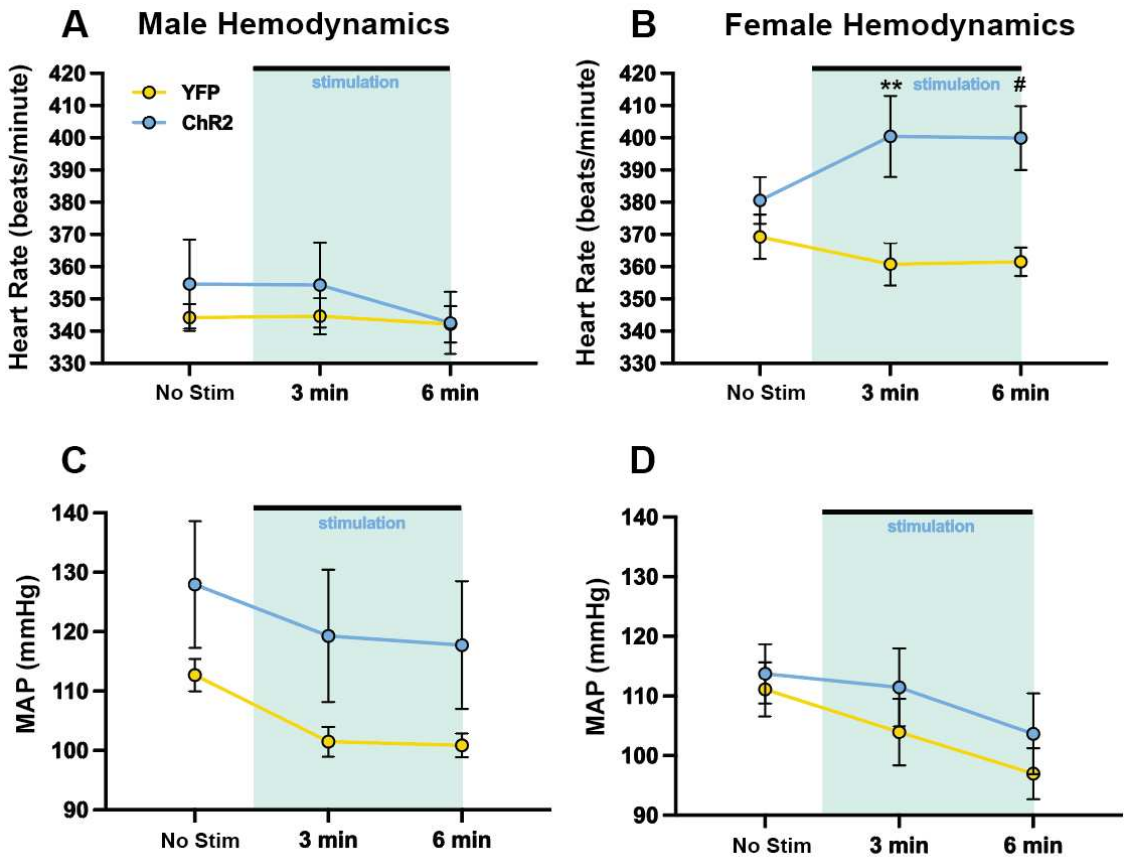

Figure 4.3: Acute stimulation of PH-targeted vmPFC projections does not affect blood pressure but elevates heart rate in females (A) Stimulation (blue shading) during non-invasive tail cuff recordings had no effect no heart rate in males. (B) Stimulation elevated heart rate in females compared to YFP controls. Stimulation had no effect on blood pressure in males (C) or females (D). bpm: beats per minute. n = 5-8/group, ** p < 0.01, # p = 0.053 vs. GFP.

3.4 Inhibition of PH-projecting vmPFC neurons

Intersectional genetics was used to identify the necessity of the ventral medial prefrontal cortex (vmPFC) to posterior hypothalamus (PH) circuit for sympathetic and HPA-axis responses to acute stress. Placement of PH-targeted microinjections of the retrograde Cre-AAV are depicted on modified coronal sections adapted from (Swanson, 2004) (Fig. 4.4A). A representative micrograph (Fig. 4.4B) shows Cre-dependent GFP-labeled cells in the vmPFC, thus confirming on-target vmPFC and PH injections. Representative micrographs show the synaptobrevin-2 colocalization on GFP axons in both GFP (Fig. 4.4C) and TeNT (Fig. 4.4D) injected female rats. Quantification shows that TeNT significantly reduces the percentage of synaptobrevin-2 protein over 3-fold in GFP axons in both males (Fig. 4.4E) (n = 6-7/group, Mann-Whitney unpaired t-test: TeNT vs GFP, $p = 0.0012$) and females (Fig. 4.4F) (n = 7/group, Mann-Whitney unpaired t-test: TeNT vs GFP, $p = 0.0003$).

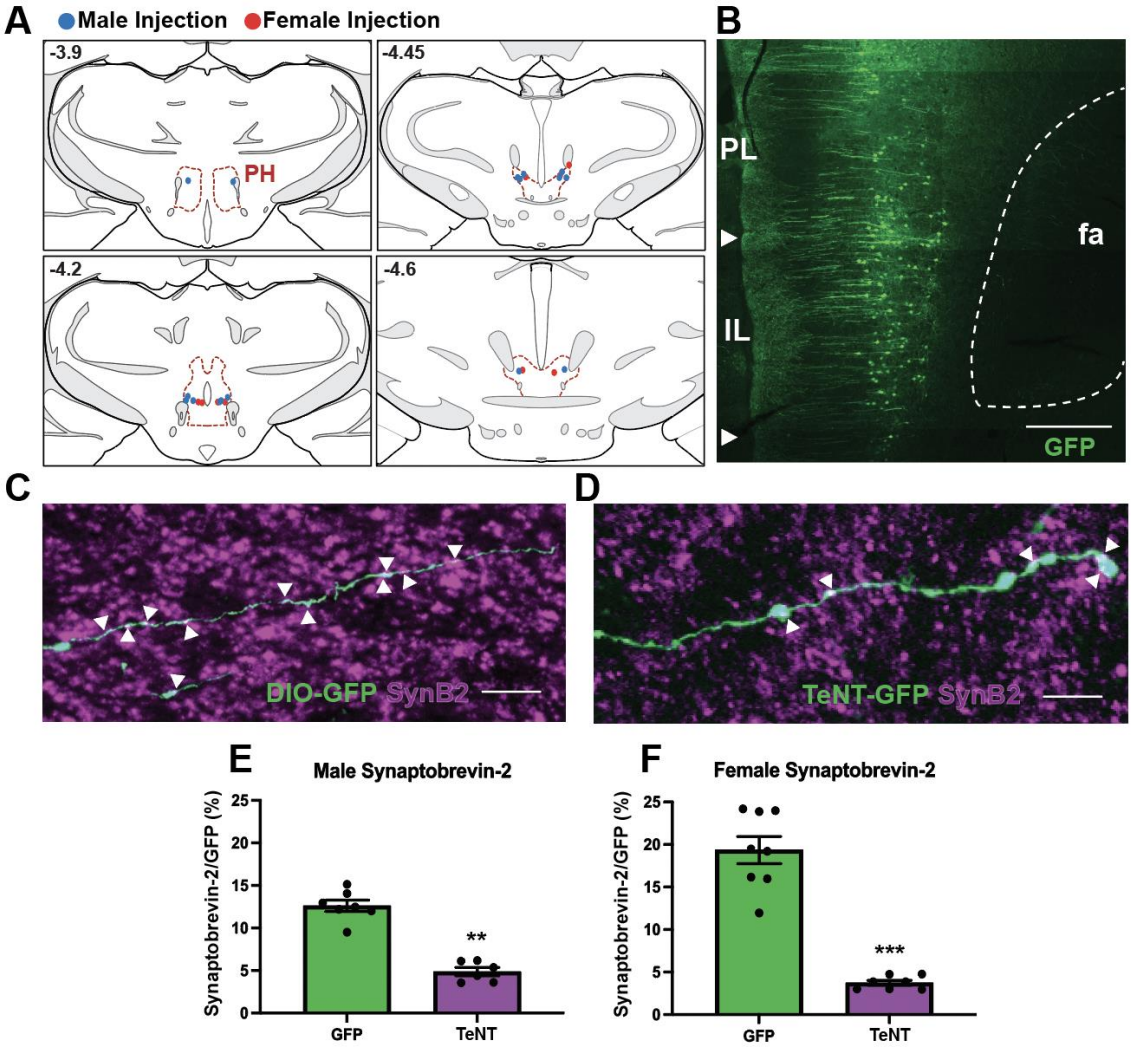

Figure 4.4: Experimental design and validation for vmPFC-PH circuit inhibition
(A) On-target bilateral injections of retrograde CRE-AAV of the TeNT treatment group. Coronal sections adapted from the 3rd Swanson Rat Brain Atlas (Swanson, 2004). Numbers indicate the distance in millimeters of the tissue sections caudal to bregma. (B) A representative micrograph demonstrates injection of CRE-dependent DIO-GFP targeted at the IL with minimal spread to the PL. IL: infralimbic cortex, PL: prelimbic cortex, fa: anterior forceps of the corpus callosum. Representative micrographs used to quantify synaptobrevin-2 protein colocalizing (white) on GFP-expressing vmPFC axons in the PH of female GFP (C) and TeNT (D) rats. Scale bar indicates 20μm. Synaptobrevin-2 protein is decreased in both male (E) and female (F) TeNT compared to GFP controls. n = 6-8/group, ** $p < 0.01$, *** $p < 0.001$ vs GFP.

3.5 *vmPFC-PH inhibition effects on endocrine reactivity*

To test the necessity of PH-projecting vmPFC neurons for mediating acute sympathetic and HPA axis stress responses, blood samples were taken during restraint and recovery to measure circulating blood glucose and plasma corticosterone. TeNT vmPFC-PH circuit

inhibition elevated blood glucose mobilization in males (Fig. 4.5A; n = 9/group, mixed effects: Time $F(4,64) = 20.90$, $p < 0.0001$, Virus $F(1,16) = 2.793$, $p = 0.1141$, Time x Virus $F(4,64) = 3.487$, $p = 0.0122$; 15-min, $p = 0.0225$; 30-min, $p = 0.0020$) but not females (Fig. 4.5B; n = 6-8/group, mixed effects: Time $F(4,46) = 8.906$, $p < 0.0001$, Virus $F(1,12) = 1.096$, $p = 0.3157$, Time x Virus $F(4,46) = 0.4552$, $p = 0.7681$). In males, TeNT reduced plasma CORT (Fig. 4.5C; n = 8/group, mixed effects: Time $F(4,23) = 13.40$, $p < 0.0001$, Virus $F(1,14) = 3.519$, $p = 0.0817$, Time x Virus $F(4,23) = 1.603$, $p = 0.2073$; 60-min, $p = 0.0038$) but had no effect on female HPA-axis reactivity (Fig. 4.5D; n = 6-7/group, mixed effects: Time $F(4,42) = 8.824$, $p < 0.0001$, Virus $F(1,11) = 0.00145$, $p = 0.9703$, Time x Virus $F(4,42) = 0.2218$, $p = 0.2218$). Altogether, TeNT vmPFC-PH circuit inhibition in males enhanced blood glucose during acute restraint yet attenuated plasma corticosterone. Interestingly, vmPFC-PH circuit inhibition did not affect blood glucose or plasma corticosterone responses to acute stress in females.

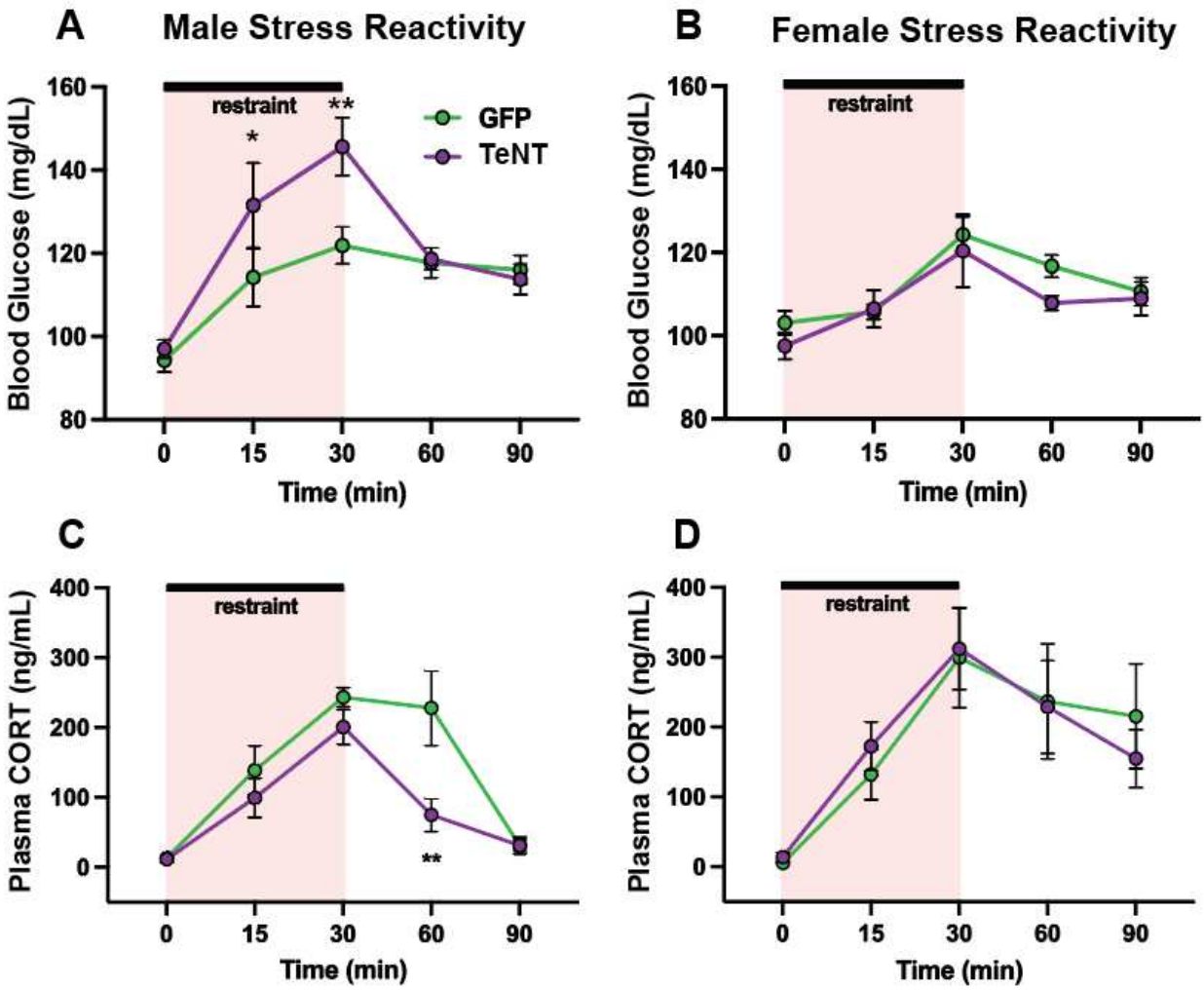

Figure 4.5: Inhibition of PH-targeted vmPFC projections increases glucose and decreases corticosterone responses to novel restraint stress in males but has no effect in females. TeNT IL-PH circuit inhibition elevated blood glucose mobilization at the in males (A), but not in females (B). Circuit inhibition also decreased plasma corticosterone responses in males (C) but there was no effect in females (D). n = 6-8/group, * $p < 0.05$, ** $p < 0.01$ vs. GFP.

3.6 Estrous cycle cytology

After all experiments where data was collected, each random-cycling female rat was swabbed and vaginal cytology was assessed to determine estrous stage. Results for the distribution of rats in each estrous phase can be seen in supplementary table 4.1 and supplementary table 2. Because rats in each cohort were in multiple phases of the estrous cycle for every experiment, sample size for each stage was underpowered for statistical analysis.

Table 4.1. Percent of rats in each estrus cycle stage during experiments

Estrous cycle stages during PH terminal stimulation experiments
During timepoints where data was collected, vaginal cytology was used to identify estrous cycle stage in random-cycling rats. RTPP: real-time place preference, S-I: social-interaction, c-Fos: Stimulation c-Fos from Figure 2F. n = 12/group

Group	*Phase*	*RTPP*	*S-I*	*Restraint*	*c-Fos*
YFP	Diestrus	33.33%	25.00%	33.33%	25.00%
	Proestrus	16.67%	33.33%	33.33%	58.33%
	Estrus	0.00%	16.67%	0.00%	0.00%
	Metestrus	50.00%	25.00%	33.33%	16.67%
ChR2	Diestrus	41.67%	25.00%	33.33%	25.00%
	Proestrus	25.00%	33.33%	41.67%	41.67%
	Estrus	0.00%	16.67%	8.33%	8.33%
	Metestrus	33.33%	25.00%	16.67%	25.00%

.

Table 4.2. Percent of rats in each estrus cycle phase during restraint

Estrous cycle stages during TeNT acute restraint experiment
During timepoints where data was collected, vaginal cytology was used to identify estrous cycle stage in random-cycling rats. n = 6-8/group.

Group	*Phase*	*Restraint*
GFP	Diestrus	0.00%
	Proestrus	50.00%
	Estrus	0.00%
	Metestrus	50.00%
TeNT	Diestrus	0.00%
	Proestrus	50.00%
	Estrus	16.67%
	Metestrus	33.33%

Discussion

Previously, our group demonstrated the role of the vmPFC glutamate neurons in behavioral, neuroendocrine, and cardiovascular reactivity to stress in both male and female rats (Myers et al., 2017; Schaeuble et al., 2019; Wallace et al., 2021). In the current study, we used circuit-specific approaches to examine whether activity of PH-targeted vmPFC neurons is sufficient or necessary to affect behavior, stress reactivity, and cardiovascular activity in either male or female rats. Stimulation of vmPFC-PH terminals was associated with positive valence and decreased sympathetic-mediated blood glucose reactivity to acute stress in males. These results were also observed with soma stimulation of vmPFC glutamate neurons demonstrating that this specific circuit mediates those previously reported responses. Meanwhile, social motivation, hemodynamics, and HPA-axis-mediated plasma corticosterone responses to acute stress appear to not be affected by acute PH stimulation of this circuit suggesting that vmPFC

glutamate neurons initiate these processes through alternate synapses. Furthermore, inhibition of PH targeted-vmPFC neurons in males identified the necessity of this circuit to maintain appropriate blood glucose and corticosterone responses to acute stress. In females, stimulation of the vmPFC-PH circuit had no effects on place preference or behavior which is consistent with vmPFC soma stimulation. Although the context of hemodynamic recordings was different from previous experiments, stimulation of PH-targeted vmPFC neurons elevated heart rate as observed previously. On the contrary, activity of the vmPFC-PH circuit is not sufficient or necessary to affect sympathetic-mediated blood glucose reactivity to acute stress, but stimulating the circuit is sufficient to elevate plasma corticosterone following acute stress exposure. Collectively, vmPFC-PH circuit-specific stimulation demonstrates vmPFC output is sexually divergent and PH-targeted vmPFC neurons are sufficient to influence behavior and sympathetic-mediated stress responses in males and heart rate in females. Additionally, vmPFC-PH inhibition experiments demonstrated that this circuit is necessary for appropriate acute stress responding males but not in females.

Stress is a mutual risk factor for mood disorders and cardiovascular disease, so understanding how activity of the vmPFC coordinates stress responding may contribute to insight on the comorbidity of these diseases. Although ties between psychosocial stress, mood disorders, and cardiovascular health have been established (Sgoifo et al., 2014), we are only beginning to discover the foundation of these diseases. The vmPFC presents as a unique target because of its role in depression and ability to coordinate visceral responses to environmental stimuli (Drevets et al., 2008, 1997; Lacuey et al., 2018; Mayberg et al., 2005). Rodent models demonstrate that the male vmPFC is necessary for regulating the HPA axis (McKlveen et al., 2013; Radley et al., 2006) and stimulating the vmPFC is sufficient to mitigate autonomic cardiovascular responses to stress (Camargos et al., 2012). Furthermore, vmPFC pyramidal glutamate neuron activity is necessary for limiting acute cardiovascular reactivity (Schaeuble et al., 2019) and optogenetically stimulating these neurons is sufficient to mitigate chronic stress-

induced susceptibility to cardiovascular disease in male rats (Wallace et al., 2021). Interestingly, vmPFC projection neurons are known to synapse onto GABAergic neurons in the PH and decreased $GABA_A$-mediated neurotransmission in PH decreases, neuroendocrine responses, heart rate reactivity (Myers et al., 2016a; Shekhar et al., 1990). While the phenotype of the cells containing $GABA_A$ receptors is unknown, vmPFC projection neurons may be necessary to elicit a tonic level of GABA-mediated inhibition with the PH to retrain exaggerated stress responding. It is shown that the PH projects to neuroendocrine and autonomic effector regions (Nyhuis et al., 2016) so a shift in tonic inhibition may lead to exaggerated stress responding predisposing individuals to disease risk. While the vmPFC axons in the PH did not appear to affect male cardiovascular measures in this experiment, other groups have demonstrated that the PH may be involved more so in the chronic regulation of heart rate and blood pressure reactivity. For example, aberrant synaptic function within the PH is shown to inhibit habituation to repeated stress exposure (Nyhuis et al., 2016). Further experiments are required to investigate how chronic stress affects the PH and the phenotype of PH neurons innervated by the vmPFC.

An interesting conclusion from this study is that stimulation of this vmPFC-PH circuit is sufficient to produce sexually divergent responses to stress. While it is unknown why this occurs, there could be a few explanations. The projection neurons from the vmPFC to the PH are primarily glutamatergic (Myers et al., 2014), but we do not know the profile of the cells they synapse onto in the PH. PH output is regulated by a strong network of GABA-mediated inhibition and here we show vmPFC PH terminal stimulation led to elevated c-Fos expression in the PH in both GABA cells and non-GABA cells. Because driving this circuit induced sexually divergent outcomes, we speculate that biological sex influences either the proportion of GABAergic cells innervated by the vmPFC, or the phenotype cells involved in stress responding. Second, there may be sex differences in PH output. The PH is predominantly composed of glutamate neurons and is interconnected with many surrounding hypothalamic nuclei, cortical limbic systems, and behavioral and endocrine-effector regions (Abrahamson and

Moore, 2001; Schaeuble and Myers, 2022; Ulrich-Lai et al., 2011; Ziegler et al., 2002). We know that the PH innervates downstream stress-regulatory regions (Nyhuis et al., 2016) demonstrating that the PH is an important hub for stress integration. Unfortunately, all the knowledge of PH circuitry and output is exclusively in male rodents, so it is unknown if PH output is also necessary for stress reactivity in females. This leads to our third hypothesis, that sex hormones modulate neural activity of the vmPFC and PH. Estrogen receptors α,β (ERα and ERβ), and G-protein coupled estrogen receptor (GPER) are present throughout the vmPFC (Almey et al., 2014; Montague et al., 2008). ER mRNA and protein expression are abundant in the hypothalamus and ER signaling modulates HPA axis activity through ERβ (Kudwa et al., 2014; Laflamme et al., 1998; Simerly et al., 1990). Given the robust bi-directional innervation between the PH and PVN, is it reasonable that the PH activity can be affected by ER signaling. Estradiol also modulates the excitability of vmPFC neurons to influence behavior and to have anti-depressant-like effects (Almey et al., 2014; Dossat et al., 2018; Yousuf et al., 2019). Conversely, studies indicate that androgens, and not exclusively estrogen, modulate neuronal function and may account differences in stress responding (Handa et al., 1994). Testosterone upregulates corticotropic releasing hormone mRNA upstream of the paraventricular nucleus of the hypothalamus and is shown to regulate HPA axis activity (Viau et al., 2001). Additionally, androgens and estrogens have contrasting effects on neurotransmitters in the vmPFC following acute stress (Handa et al., 1997). Another consideration is aromatase, an enzyme that converts testosterone into estradiol. Aromatase is located throughout the cortex and hypothalamus and its activity can result in elevated levels of estradiol potentiating neural effects mentioned above in regards to stress responding (Lu et al., 2019; Wei et al., 2014). Unfortunately, it is unclear how sex hormones affect this circuit, but it is evident they influence neural activity in stress-reactive circuits. To summarize, vmPFC-PH circuit experiments demonstrate biological sex may affect cell phenotype innervated by the vmPFC, output from the PH, and/or sex hormone modulation of neuron function.

Considerations and limitations

While these experiments identify a novel cortical to hypothalamic pathway for stress responding, there are some considerations worth discussing. For this study, AAV injections were targeted at the infralimbic cortex (IL), the ventral subregion of the vmPFC, to gauge whether sympathetic and neuroendocrine effects of IL soma stimulation were mediated through the PH. Because of sparse, dorsal viral spread into the prelimbic cortex (PL), we accurately termed this circuit vmPFC to PH for clarity. While it is true that IL and PL activity may have opposing effects on stress reactivity (Radley et al., 2006; Tavares et al., 2009), stimulation of PH-targeted vmPFC terminals did not conflict with results from IL soma stimulation leading us to believe the PL may have little or no influence over results. Additionally, PL anatomical innervation of the PH has been reported, and it appears to be less dense and less stress reactive than IL innervation(Abrahamson & Moore, 2001; Myers et al., 2016; Vertes, 2004).

In experiment 2, inhibition of the vmPFC-PH circuit demonstrated the circuit was necessary for appropriate acute stress reactivity in males but not females. While the extent of the inhibition of neurotransmitter release from PH-projecting vmPFC neurons was not quantified, the TeNT inhibition reduced synaptobrevin-2 protein in both males and females suggesting that the protein was cleaved thus inhibiting vesicle fusion to the presynaptic membrane. Furthermore, it has been thoroughly demonstrated that this approach causes a TeNT-dependent loss of synaptobrevin-2 in excitatory synapses (Sando et al., 2017).

Another limitation is the use of anesthesia during non-invasive hemodynamic recordings. To apply the tail cuff and attach the fiber optics, the rat had to be maintained under light anesthesia. Anesthesia may have masked heart rate and blood pressure responses to stimulation, but a stimulation-induced elevated heart rate was observed in females which aligns with radiotelemetry-derived data obtained previously (Wallace et al., 2021). In future experiments, we look to implement radiotelemetry to study how stress circuitry controls hemodynamic activity real-time in a stressful context.

Lastly, data presented here aligns with our last paper to show that stimulating vmPFC glutamate neurons during acute restraint reduced stress reactivity in males yet had no effect on female corticosterone. Stimulation elevated corticosterone in females, while the mechanism for this is not clear, the HPA axis is a tightly-regulated pathway and any perturbation such as optogenetic stimulation or inhibition may affect adrenal responsivity to stress. Also, it is important to consider the specificity of the approaches used in each experiment that could affect the results. In experiment 1, the sufficiency of the vmPFC-PH to influence behavior and stress responding was tested with an optogenetic approach. Because channelrhodopsin expression was under a synapsin promoter, blue light delivery via optic cannula in the PH allowed for circuit-specific examination of the vmPFC-PH. In experiment 2, an intersectional genetic approach was used to test the necessity of the vmPFC-PH circuit for sympathetic and neuroendocrine-mediated stress reactivity. While this experiment knocked down synaptobrevin-2 in PH-projecting vmPFC neurons, there is the potential that axon collaterals of these neurons could also be inhibited. This could lead to inhibition of neurotransmitter release from vmPFC neurons in other regions. Yet, the collective data indicate sex specific necessity and sufficiency of the circuit for controlling stress responses

In conclusion, data presented here align with our prior experiment to demonstrate the importance of the vmPFC activity as a node for behavior and stress reactivity.
We identified that stimulating vmPFC output yields sexually divergent outcomes in terms of behavior and stress responding providing us with insight to how stress may yield sex differences in disease risk for depressive disorders and cardiovascular disease. Moreover, activity of vmPFC synapses in the PH yields sexually-divergent results but reveals the PH serves as an important region for integrating cortical output for stress responding. In conclusion, identifying activity of neurons in the PH may explain sex-based differences in stress reactivity and disease susceptibility.

References

Abrahamson, E. E., & Moore, R. Y. (2001). The posterior hypothalamic area: chemoarchitecture and afferent connections. In *Brain Research* (Vol. 889). www.elsevier.com/locate/bres

Almey, A., Cannell, E., Bertram, K., Filardo, E., Milner, T. A., & Brake, W. G. (2014). Medial Prefrontal Cortical Estradiol Rapidly Alters Memory System Bias in Female Rats: Ultrastructural Analysis Reveals Membrane-Associated Estrogen Receptors as Potential Mediators. *Endocrinology*, *155*(11), 4422–4432. https://doi.org/10.1210/EN.2014-1463

Beckmann, M., Johansen-Berg, H., & Rushworth, M. F. S. (2009). Connectivity-based parcellation of human cingulate cortex and its relation to functional specialization. *Journal of Neuroscience*, *29*(4), 1175–1190. https://doi.org/10.1523/JNEUROSCI.3328-08.2009

Camargos, F., Müller-Ribeiro, F., Zaretsky, D. V, Zaretskaia, M. V, Santos, R. A. S., Dimicco, J. A., Antônio, M., & Fontes, P. (2012). Contribution of infralimbic cortex in the cardiovascular response to acute stress. *Am J Physiol Regul Integr Comp Physiol*, *303*, 639–650. https://doi.org/10.1152/ajpregu.00573.2011.-The

Cora, M. C., Kooistra, L., & Travlos, G. (2015). Vaginal Cytology of the Laboratory Rat and Mouse: Review and Criteria for the Staging of the Estrous Cycle Using Stained Vaginal Smears. *Toxicologic Pathology*, *43*(6), 776–793. https://doi.org/10.1177/0192623315570339

DiMicco, J. A., Abshire, V. M., Hankins, K. D., Sample, R. H. B., & Wible, J. H. (1986). Microinjection of GABA antagonists into posterior hypothalamus elevates heart rate in anesthetizes rats. *Neuropharmacology*, *25*(9), 1063–1066. https://doi.org/10.1016/0028-3908(86)90203-0

Dossat, A. M., Wright, K. N., Strong, C. E., & Kabbaj, M. (2018). Behavioral and biochemical sensitivity to low doses of ketamine: Influence of estrous cycle in C57BL/6 mice. *Neuropharmacology*, *130*, 30–41. https://doi.org/10.1016/J.NEUROPHARM.2017.11.022

Drevets, W. C., Price, J. L., Simpson, J. R., Todd, R. D., Reich, T., Vannier, M., & Raichle, M. E.

(1997). Subgenual prefrontal cortex abnormalities in mood disorders. *Nature*, *386*(6627), 824–827. https://doi.org/10.1038/386824a0

Drevets, W. C., Savitz, J., & Trimble, M. (2008). The Subgenual Anterior Cingulate Cortex in Mood Disorders. *CNS Spectrums*, *13*(8), 663. /pmc/articles/PMC2729429/

Felix-Ortiz, A. C., & Tye, K. M. (2014). Amygdala inputs to the ventral hippocampus bidirectionally modulate social behavior. *Journal of Neuroscience*, *34*(2), 586–595. https://doi.org/10.1523/JNEUROSCI.4257-13.2014

Goldstein, J. M., Hale, T., Foster, S. L., Tobet, S. A., & Handa, R. J. (2018). Sex differences in major depression and comorbidity of cardiometabolic disorders: impact of prenatal stress and immune exposures. *Neuropsychopharmacology 2018 44:1*, *44*(1), 59–70. https://doi.org/10.1038/s41386-018-0146-1

Hamani, C., MacHado, D. C., Hipólide, D. C., Dubiela, F. P., Suchecki, D., MacEdo, C. E., Tescarollo, F., Martins, U., Covolan, L., & Nobrega, J. N. (2012). Deep Brain Stimulation Reverses Anhedonic-Like Behavior in a Chronic Model of Depression: Role of Serotonin and Brain Derived Neurotrophic Factor. *Biological Psychiatry*, *71*(1), 30. https://doi.org/10.1016/J.BIOPSYCH.2011.08.025

Handa, R. J., Hejna, G. M., & Lorens, S. A. (1997). Androgen inhibits neurotransmitter turnover in the medial prefrontal cortex of the rat following exposure to a novel environment. *Brain Research*, *751*(1), 131–138. https://doi.org/10.1016/S0006-8993(96)01394-7

Handa, R. J., Nunley, K. M., Lorens, S. A., Louie, J. P., McGivern, R. F., & Bollnow, M. R. (1994). Androgen regulation of adrenocorticotropin and corticosterone secretion in the male rat following novelty and foot shock stressors. *Physiology & Behavior*, *55*(1), 117–124. https://doi.org/10.1016/0031-9384(94)90018-3

Kudwa, A. E., McGivern, R. F., & Handa, R. J. (2014). Estrogen receptor β and oxytocin interact to modulate anxiety-like behavior and neuroendocrine stress reactivity in adult male and female rats. *Physiology and Behavior*, *129*, 287–296.

https://doi.org/10.1016/j.physbeh.2014.03.004

Lacuey, N., Hampson, J. P., Theeranaew, W., Zonjy, B., Vithala, A., Hupp, N. J., Loparo, K. A., Miller, J. P., & Lhatoo, S. D. (2018). Cortical structures associated with human blood pressure control. *JAMA Neurology*, *75*(2), 194–202. https://doi.org/10.1001/jamaneurol.2017.3344

Laflamme, N., Nappi, R. E., Drolet, G., Labrie, C., & Rivest, S. (1998). Expression and neuropeptidergic characterization of estrogen receptors (ERα and ERβ) throughout the rat brain: Anatomical evidence of distinct roles of each subtype. *Journal of Neurobiology*, *36*(3), 357–378. https://doi.org/10.1002/(SICI)1097-4695(19980905)36:3<357::AID-NEU5>3.0.CO;2-V

Link, E., Edelmann, L., Chou, J. H., Binz, T., Yamasaki, S., Eisel, U., Baumert, M., Südhof, T. C., Niemann, H., & Jahn, R. (1992). Tetanus toxin action: Inhibition of neurotransmitter release linked to synaptobrevin proteolysis. *Biochemical and Biophysical Research Communications*, *189*(2), 1017–1023. https://doi.org/10.1016/0006-291X(92)92305-H

Lu, Y., Sareddy, G. R., Wang, J., Wang, R., Li, Y., Dong, Y., Zhang, Q., Liu, J., O'Connor, J. C., Xu, J., Vadlamudi, R. K., & Brann, D. W. (2019). Neuron-derived estrogen regulates synaptic plasticity and memory. *Jour1. Lu Y, Sareddy GR, Wang J, Wang R, Li Y, Dong Y, Zhang Q, Liu J, O'Connor JC, Xu J, Vadlamudi RK, Brann DW. Neuron-Derived Estrogen Regulates Synaptic Plasticity and Memory. J Neurosci. 2019;39:2792–2809.Nal of Neuroscience*, *39*(15), 2792–2809. https://doi.org/10.1523/JNEUROSCI.1970-18.2019

Mayberg, H. S., Lozano, A. M., Voon, V., McNeely, H. E., Seminowicz, D., Hamani, C., Schwalb, J. M., & Kennedy, S. H. (2005). Deep Brain Stimulation for Treatment-Resistant Depression. *Neuron*, *45*(5), 651–660. https://doi.org/10.1016/J.NEURON.2005.02.014

McKlveen, J. M., Myers, B., & Herman, J. P. (2015). The Medial Prefrontal Cortex: Coordinator of Autonomic, Neuroendocrine and Behavioural Responses to Stress. *Journal of Neuroendocrinology*, *27*(6), 446–456. https://doi.org/10.1111/jne.12272

McKlveen, Jessica M., Myers, B., Flak, J. N., Bundzikova, J., Solomon, M. B., Seroogy, K. B., & Herman, J. P. (2013). Role of Prefrontal Cortex Glucocorticoid Receptors in Stress and Emotion. *Biological Psychiatry*, *74*(9), 672–679. https://doi.org/10.1016/J.BIOPSYCH.2013.03.024

McMahon, H. T., Ushkaryov, Y. A., Edelmann, L., Link, E., Binz, T., Niemann, H., Jahn, R., & Südhof, T. C. (1993). Cellubrevin is a ubiquitous tetanus-toxin substrate homologous to a putative synaptic vesicle fusion protein. *Nature*, *364*(6435), 346–349. https://doi.org/10.1038/364346a0

Möller-Leimkühler, A. M. (2007). Gender differences in cardiovascular disease and comorbid depression. *Dialogues in Clinical Neuroscience*, *9*(1), 71–83. http://www.ncbi.nlm.nih.gov/pubmed/17506227

Montague, D., Weickert, C. S., Tomaskovic-Crook, E., Rothmond, D. A., Kleinman, J. E., & Rubinow, D. R. (2008). Oestrogen Receptor α Localisation in the Prefrontal Cortex of Three Mammalian Species. *Journal of Neuroendocrinology*, *20*(7), 893–903. https://doi.org/10.1111/J.1365-2826.2008.01743.X

Myers, B., Carvalho-Netto, E., Wick-Carlson, D., Wu, C., Naser, S., Solomon, M. B., Ulrich-Lai, Y. M., & Herman, J. P. (2016). GABAergic signaling within a limbic-hypothalamic circuit integrates social and anxiety-like behavior with stress reactivity. *Neuropsychopharmacology*, *41*(6), 1530–1539. https://doi.org/10.1038/npp.2015.311

Myers, B., McKlveen, J. M., & Herman, J. P. (2014). Glucocorticoid actions on synapses, circuits, and behavior: Implications for the energetics of stress. *Frontiers in Neuroendocrinology*, *35*(2), 180–196. https://doi.org/10.1016/J.YFRNE.2013.12.003

Myers, B., McKlveen, J. M., Morano, R., Ulrich-Lai, Y. M., Solomon, M. B., Wilson, S. P., & Herman, J. P. (2017). Vesicular Glutamate Transporter 1 Knockdown in Infralimbic Prefrontal Cortex Augments Neuroendocrine Responses to Chronic Stress in Male Rats. *Endocrinology*, *158*(10), 3579–3591. https://doi.org/10.1210/en.2017-00426

Nyhuis, T. J., Masini, C. V, Day, H. E. W., & Campeau, S. (2016). Evidence for the Integration of Stress-Related Signals by the Rostral Posterior Hypothalamic Nucleus in the Regulation of Acute and Repeated Stress-Evoked Hypothalamo-Pituitary-Adrenal Response in Rat. *The Journal of Neuroscience*, *36*(3), 795 LP – 805. http://www.jneurosci.org/content/36/3/795.abstract

Page, C. E., & Coutellier, L. (2019). Prefrontal excitatory/inhibitory balance in stress and emotional disorders: Evidence for over-inhibition. *Neuroscience & Biobehavioral Reviews*, *105*, 39–51. https://doi.org/10.1016/J.NEUBIOREV.2019.07.024

Radley, J. J., Arias, C. M., & Sawchenko, P. E. (2006). Regional Differentiation of the Medial Prefrontal Cortex in Regulating Adaptive Responses to Acute Emotional Stress. *The Journal of Neuroscience*, *26*(50), 12967. https://doi.org/10.1523/JNEUROSCI.4297-06.2006

Rau, A. R., & Hentges, S. T. (2017). The relevance of AgRP neuron-derived GABA inputs to POMC neurons differs for spontaneous and evoked release. *Journal of Neuroscience*, *37*(31), 7362–7372. https://doi.org/10.1523/JNEUROSCI.0647-17.2017

Sando, R., Bushong, E., Zhu, Y., Huang, M., Considine, C., Phan, S., Ju, S., Uytiepo, M., Ellisman, M., & Maximov, A. (2017). Assembly of excitatory synapses in the absence of glutamatergic neurotransmission. *Neuron*, *94*(2), 312. https://doi.org/10.1016/J.NEURON.2017.03.047

Schaeuble, D., & Myers, B. (2022). Cortical–Hypothalamic Integration of Autonomic and Endocrine Stress Responses. *Frontiers in Physiology*, *13*, 820398. https://doi.org/10.3389/FPHYS.2022.820398

Schaeuble, D., Packard, A. E. B., McKlveen, J. M., Morano, R., Fourman, S., Smith, B. L., Scheimann, J. R., Packard, B. A., Wilson, S. P., James, J., Hui, D. Y., Ulrich-Lai, Y. M., Herman, J. P., & Myers, B. (2019). Prefrontal Cortex Regulates Chronic Stress-Induced Cardiovascular Susceptibility. *Journal of the American Heart Association*, *8*(24), e014451.

https://doi.org/10.1161/JAHA.119.014451

Sgoifo, A., Carnevali, L., & Grippo, A. J. (2014). The socially stressed heart. Insights from studies in rodents. *Neuroscience and Biobehavioral Reviews*, *39*, 51–60. https://doi.org/10.1016/J.NEUBIOREV.2013.12.005

Shekhar, A., Hingtgen, J. N., & DiMicco, J. A. (1990). GABA receptors in the posterior hypothalamus regulate experimental anxiety in rats. *Brain Research*, *512*(1), 81–88. https://doi.org/10.1016/0006-8993(90)91173-E

Simerly, R. B., Swanson, L. W., Chang, C., & Muramatsu, M. (1990). Distribution of androgen and estrogen receptor mRNA-containing cells in the rat brain: An in situ hybridization study. *Journal of Comparative Neurology*, *294*(1), 76–95. https://doi.org/10.1002/CNE.902940107

Smith, B. L., Morano, R. L., Ulrich-Lai, Y. M., Myers, B., Solomon, M. B., & Herman, J. P. (2018). Adolescent environmental enrichment prevents behavioral and physiological sequelae of adolescent chronic stress in female (but not male) rats. *Stress (Amsterdam, Netherlands)*, *21*(5), 464–473. https://doi.org/10.1080/10253890.2017.1402883

Solomon, M. B., Loftspring, M., De Kloet, A. D., Ghosal, S., Jankord, R., Flak, J. N., Wulsin, A. C., Krause, E. G., Zhang, R., Rice, T., McKlveen, J., Myers, B., Tasker, J. G., & Herman, J. P. (2015). Neuroendocrine function after hypothalamic depletion of glucocorticoid receptors in male and female mice. *Endocrinology*, *156*(8), 2843–2853. https://doi.org/10.1210/en.2015-1276

Swanson, L. W. (2004). *Brain Maps: Structure of the Rat Brain* (Third Ed.). Academic Press.

Tavares, R. F., Corrêa, F. M. A., & Resstel, L. B. M. (2009). Opposite role of infralimbic and prelimbic cortex in the tachycardiac response evoked by acute restraint stress in rats. *Journal of Neuroscience Research*, *87*(11), 2601–2607. https://doi.org/10.1002/jnr.22070

Ulrich-Lai, Y. M., Jones, K. R., Ziegler, D. R., Cullinan, W. E., & Herman, J. P. (2011). Forebrain Origins of Glutamatergic Innervation to the Rat Paraventricular Nucleus of the Hypothalamus: Differential Inputs to the Anterior Versus Posterior Subregions NIH Public

Access. *J Comp Neurol*, *519*(7), 1301–1319. https://doi.org/10.1002/cne.22571

Vertes, R. P. (2004). Differential projections of the infralimbic and prelimbic cortex in the rat. *Synapse*, *51*(1), 32–58. https://doi.org/10.1002/syn.10279

Viau, V., Soriano, L., & Dallman, M. F. (2001). Androgens alter corticotropin releasing hormone and arginine vasopressin mRNA within forebrain sites known to regulate activity in the hypothalamic-pituitary-adrenal axis. *Journal of Neuroendocrinology*, *13*(5), 442–452. https://doi.org/10.1046/J.1365-2826.2001.00653.X

Vijayakumar, N., Cheng, T. W., & Pfeifer, J. H. (2017). Neural correlates of social exclusion across ages: a coordinate-based meta-analysis of functional MRI studies. *NeuroImage*, *153*, 359. https://doi.org/10.1016/J.NEUROIMAGE.2017.02.050

Wake, R., & Yoshiyama, M. (2009). Gender Differences in Ischemic Heart Disease. *Recent Patents on Cardiovascular Drug Discovery*, *4*, 234–240.

Wallace, T., Schaeuble, D., Pace, S. A., Schackmuth, M. K., Hentges, S. T., Chicco, A. J., & Myers, B. (2021). Sexually divergent cortical control of affective-autonomic integration. *Psychoneuroendocrinology*, *129*, 105238. https://doi.org/10.1016/j.psyneuen.2021.105238

Wei, J., Yuen, E. Y., Liu, W., Li, X., Zhong, P., Karatsoreos, I. N., McEwen, B. S., & Yan, Z. (2014). Estrogen protects against the detrimental effects of repeated stress on glutamatergic transmission and cognition. *Molecular Psychiatry*, *19*(5), 588–598. https://doi.org/10.1038/mp.2013.83

Wood, M., Adil, O., Wallace, T., Fourman, S., Wilson, S. P., Herman, J. P., & Myers, B. (2019). Infralimbic prefrontal cortex structural and functional connectivity with the limbic forebrain: a combined viral genetic and optogenetic analysis. *Brain Structure & Function*, *224*(1), 73–97. https://doi.org/10.1007/s00429-018-1762-6

Xu, W., & Südhof, T. C. (2013). A Neural Circuit for Memory Specificity and Generalization. *Science (New York, N.Y.)*, *339*(6125), 1290. https://doi.org/10.1126/SCIENCE.1229534

Yousuf, H., Smies, C. W., Hafenbreidel, M., Tuscher, J. J., Fortress, A. M., Frick, K. M., &

Mueller, D. (2019). Infralimbic Estradiol Enhances Neuronal Excitability and Facilitates Extinction of Cocaine Seeking in Female Rats via a BDNF/TrkB Mechanism. *Frontiers in Behavioral Neuroscience*, *13*, 168. https://doi.org/10.3389/FNBEH.2019.00168/BIBTEX

Ziegler, D. R., Cullinan, W. E., & Herman, J. P. (2002). Distribution of vesicular glutamate transporter mRNA in rat hypothalamus. *The Journal of Comparative Neurology*, *448*(3), 217–229. https://doi.org/10.1002/cne.10257

CHAPTER 5: ROLE OF VMPFC-PH CIRCUIT IN CARDIOVASCULAR SUSCEPTIBILITY TO CHRONIC STRESS EXPOSURE[1]

Overview

Chronic life stress increases the risk of cardiovascular susceptibility reducing quality of life and increasing mortality risk. These conditions commonly co-occur with sex-based differences in incidence and severity. However, the biological mechanisms linking the stress to cardiovascular dysfunction are poorly understood. To address this, we used a circuit-specific approach to investigate how chronic stress impacts a known cardio-regulatory cortical-hypothalamic circuit in each sex. Previously, activity of ventral medial prefrontal cortex (vmPFC) neurons projecting to the posterior hypothalamus (PH) has demonstrated sexually divergent outcomes in terms of endocrine and cardiovascular reactivity to stress, but here we observe this circuit serves a role in coordinating stress responses following chronic stress exposure. Altogether, these data suggest chronic stress impacts cortical-hypothalamic regulation of stress-reactivity.

Introduction

Major depressive disorder (MDD) and cardiovascular disease (CVD) are both augmented by chronic stress exposure; however, a neurobiological mechanism for this association is unknown. The ventral medial prefrontal cortex (vmPFC) is important for translating stress appraisal into adaptive behavioral and physiological responses through descending multi-synaptic circuits that target autonomic and HPA axis effectors. Chronic life stress impacts the activity of the vmPFC (Fogaça & Duman, 2019; McKlveen et al., 2019), consequently, altering vmPFC output to descending brain regions that may impair the ability of an organism to generate adaptive physiological responses to stress exposure. The vmPFC sends projections to multiple stress-regulatory hypothalamic nuclei; however, innervation of the posterior hypothalamus (PH) is the densest (Wood et al., 2019). The PH has excitatory output

[1]The following is preliminary material from a recently completed experiment.

that can increase neuroendocrine and sympathetic-mediated cardiovascular activity (DiMicco et al., 1986; DiMicco & Abshire, 1987; Myers et al., 2016; Nyhuis et al., 2016; Ulrich-Lai et al., 2011), but prior to this dissertation it was not known if vmPFC inputs into the PH mediated these effects. In the previous chapter, we found vmPFC-projecting PH neurons to be both sufficient and necessary to control stress reactivity in male rats but optogenetic stimulation of this circuit was only sufficient to increase neuroendocrine and heart rate responses in females. Evidence suggests that the PH is important for coordinating physiological stress responses in the response to chronic stress (Myers et al., 2016; Nyhuis et al., 2016), but all this research has been done in male rats exclusively. Data on how female rats respond to chronic stress has been unknown until recently and we discovered that females are less susceptible to chronic stress-induced cardiac pathology than males and this may be due to differences in vmPFC output (Wallace et al., 2021). Because we observed sexually divergent outcomes in the vmPFC-PH circuit's role in acute stress responding, we wanted to examine whether this circuit may contribute to sex differences in chronic stress susceptibility. To address this question, we examined whether vmPFC neurons projecting to the PH are necessary to maintain hemodynamic control and proper acute stress reactivity following chronic stress.

Methods

Experimental Design

A timeline for this experiment can be found in figure 5.1. The data in this chapter are from one experiment that was composed of 4 cohorts of rats (2 cohorts of each sex). Each cohort had 4 treatment groups of rats: rats were injected with a virus-packaged Cre-dependent green fluorescent protein (GFP) or a Cre-dependent tetanus toxin (TeNT). Within each virus group, half of the rats were subjected to a chronic variable stress (CVS) paradigm and the other half were not exposed to stressors. In total, the male rats consisted of 7-9/group and the females 10-11/group of on-target injections. All rats were injected and allowed 2 weeks of

recovery prior to radiotelemetry device implantation and 2 more weeks of recovery before data collection. Rats with injections outside of the PH were removed from the study.

Animals

4 cohorts of age-matched adult male and female Sprague-Dawley rats were used for these experiments (2 cohorts/sex). The 4 cohorts of rats were obtained from Charles River. Male rats weight ranged from 215-300 and females from 175-275 g. After stereotaxic surgery, rats were individually housed in shoebox cages with cardboard tube enrichment. All rats were housed in temperature and humidity-controlled rooms with a 12-hour light-dark cycle (lights on at 06:00h, off at 18:00h) and food and water *ad libitum*. All procedures and protocols were approved by the Colorado State University Institutional Animal Care and Use Committee (protocol: 1321) and complied with the National Institutes of Health Guidelines for the Care and Use of Laboratory Animals. Signs of poor health and/or weight loss ≥ 20% of pre-surgical weight were *a priori* exclusion criteria.

Microinjections

A CRE-dependent approach was used to selectively express tetanus toxin (TeNT) in PH-projecting vmPFC neurons to inhibit neurotransmitter release (Link et al., 1992; McMahon et al., 1993; Sando et al., 2017; Xu & Südhof, 2013). Rats were anesthetized with isoflurane (1-5%) followed by analgesic (0.6 mg/kg buprenorphine-SR, subcutaneous) administration. Rats received bilateral microinjections (0.75 µL). Using the same surgical procedures as previously described, rats were anesthetized and bilaterally injected with 0.75 µL of retrograde Cre-AAV into the PH followed by either 0.75 µL Cre-dependent GFP or Cre-dependent TeNT into the vmPFC. The TeNT virus was obtained from Stanford Gene Vector and Virus Core while the DIO GFP (50457-AAV5) and retrograde Cre-AAV (114472-AAVrg) were obtained from Addgene. Injection coordinates for the vmPFC and PH in both males and females are identical to those reported in Chapter 4 experiment 2.

Telemetry Surgery

2 weeks following injections, abdominal surgery was performed to implant radiotelemetry devices as described in Chapters 2 and 3.

Chronic Variable Stress

After recovery from telemetry surgery, 2 weeks of chronic variable stress (CVS) were performed as described in Chapters 2 and 3.

Weight Matching

No CVS rats were food restricted to match the weights of CVS and non-CVS animals to assure body weight did not affect cardiovascular structure or function. Weight matching protocol is similar as described chapter 2 in (Flak et al., 2011).

Novel Environment

Rats were then exposed to a 30-minute novel environment stressor to assess acute cardiovascular reactivity. For the novel environment test, rats were placed into a brightly-lit semi-transparent arena that was on top of 4 radiotelemetry receiver pads (Data Sciences International, St. Paul, MN). Heart rate (HR), arterial pressure (MAP), temperature, and activity were collected during the stressor in 1-minute bins and analyzed with Ponemah software (Version:6.4x Data Sciences International).

Acute Restraint Stress

Restraint was used to examine neuroendocrine responses to acute stress as described previously in chapter 4. Blood glucose and plasma corticosterone were measured as indicators of sympathetic and HPA-axis stress responses, respectively. As described previously, rats were placed in plastic decapicones (Braintree Scientific, Braintree, MA) and the distal tail was clipped and blood samples (approximately 250 µL) were collected at the initiation of restraint with additional samples taken 15 and 30 min after (Vahl et al., 2005). After 30 minutes, the rats were returned to their homecage with additional blood samples collected at 60 and 90-minute recovery time points after the initiation of restraint. Blood glucose was quantified with Contour Next EZ glucometers (Bayer, Parsippany, NJ) and 2 independent readings for each time point

were averaged. Blood samples were centrifuged at 2500 X gravity for 15 min at 4˚C and plasma was stored at −20˚C until measured for corticosterone concentration with Enzo Life Sciences Corticosterone ELISA kit (Catalog No. ADI-900-097).

Tissue Collection

At the conclusion of the experiments, brain tissue was collected for technique validation. For euthanization, rats were injected with an overdose of sodium pentobarbital and perfused transcardially with 0.9% saline followed by 4.0% paraformaldehyde in 0.1 M phosphate buffer solution (PBS). Brains were removed and post-fixed in 4.0% paraformaldehyde for 24 h at room temperature, followed by storage in 30% sucrose in PBS at 4˚C. Coronal sections were made on a freezing microtome at 20μm thickness and then stored in cryoprotectant solution at -20˚C.

Microscopy

To verify injection and cannula placement in experiment 1, coronal brain sections were imaged with a Zeiss Axio Imager Z2 microscope using a 10x objective.

Data Analysis

For these series of experiments, data are expressed as mean ± standard error of the mean. Hemodynamic data collected from the radiotelemetry devices were analyzed with Ponemah v6 (Data Sciences International, MN). Baseline data in Ponemah were collected before the start of CVS during a similar timepoint as when data for experiments were obtained. Baseline data were analyzed using Prism 9.5 (GraphPad, San Diego, CA), with statistical significance set at $p < 0.05$ for rejection of null hypotheses. Stress responses over time (MAP, HR, glucose, CORT) were analyzed using mixed-effects analysis with CVS, virus, and time (repeated) as factors, followed by Fisher's post-hoc if significant main or interaction effects were present. Baseline MAP and HR were analyzed with a nonparametric Mann-Whitney t Test to compare GFP and TeNT.

Results

Injections Figure 5.1B shows a representative map of PH-targeted retrograde AAV injections of rats injected with Cre-dependent TeNT into the vmPFC. PH injections were all between -3.9 and -4.45 mm caudal from bregma according to Swanson Rat Brain Atlas (Swanson, 2004). Data from off-target injected rats were removed from all analyses after injections were mapped.

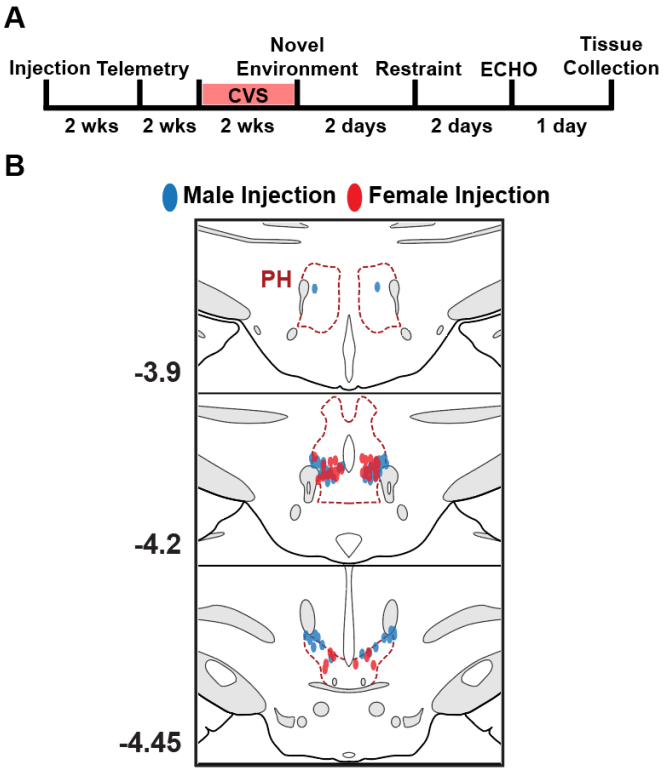

Figure 5.1. Experimental design and posterior hypothalamus injections. (A) Experimental timeline. wks: weeks, CVS: chronic variable stress, ECHO: echocardiography. (B) On-target injection placements within the posterior hypothalamus (PH). The red dotted line represents the border of the PH. Numbers on the left indicate the location of the coronal section according to Swanson Brain Atlas (3rd edition). Blue ovals represent male injections. Red ovals represent female injections.

Novel Environment hemodynamic activity

During novel environment exposure, blood pressure and heart rate were recorded to examine the role of the vmPFC-PH circuit in hemodynamic control during acute stress. All values are shown as a change from baseline values which are displayed in bar graphs adjected to each respective figure. During the novel environment, male CVS TeNT MAP is decreased at the 1 (1 p = 0.0167) and 2-minute (2 p = 0.0431) timepoint compared to the No CVS GFP group

(Fig. 2A mixed-effects (n = 6-7/group): Time F(30,659) = 39.81, p < 0.0001). In Females (Fig. 5.2B Mann-Whitney GFP vs. TeNT, p = 0.0342, mixed-effects (n = 7-11/group): Time F(30,1020) = 72.82, p < 0.0001), CVS TeNT MAP was decreased from No CVS GFP (3 p = 0.0470, 4 p = 0.0075, 5 p = 0.0315, 6 p = 0.0150, 7 p = 0.0130, 8 p = 0.0256, 9 p = 0.0125, 10 p = 0.0119, 11 p = 0.0226, 12 p = 0.0097, 29 p = 0.0316), No CVS TeNT (2 p = 0.0196), and CVS GFP (3 p = 0.0229, 4 p = 0.0124, 5 p = 0.0321, 6 p = 0.0475, 10 p = 0.0415, 23 p = 0.0297). Additionally, the No CVS TeNT MAP was decreased from No CVS GFP at the 21-minute time point (21 p = 0.0328). Male CVS TeNT heart rate reactivity (Fig. 5.2C mixed-effects (n = 10-11/group): Time F(30,682) = 35.41, p < 0.0001) was decreased from the No CVS GFP (2 p = 0.0441, 6 p = 0.0035), No CVS TeNT (6 p = 0.0432), and CVS GFP (10 p = 0.0280,11 p = 0.0321,16 p = 0.4250, 20 p = 0.0340) at multiple timepoints during the novel environment. Interestingly, there were no differences in female heart rate reactivity (Fig. 5.2D). Collectively, these data show that inhibited vmPFC neurotransmitter release to the PH in chronically stressed males decreased pressor and heart rate responses to acute stress. In females, only pressor responses to acute stress were attenuated.

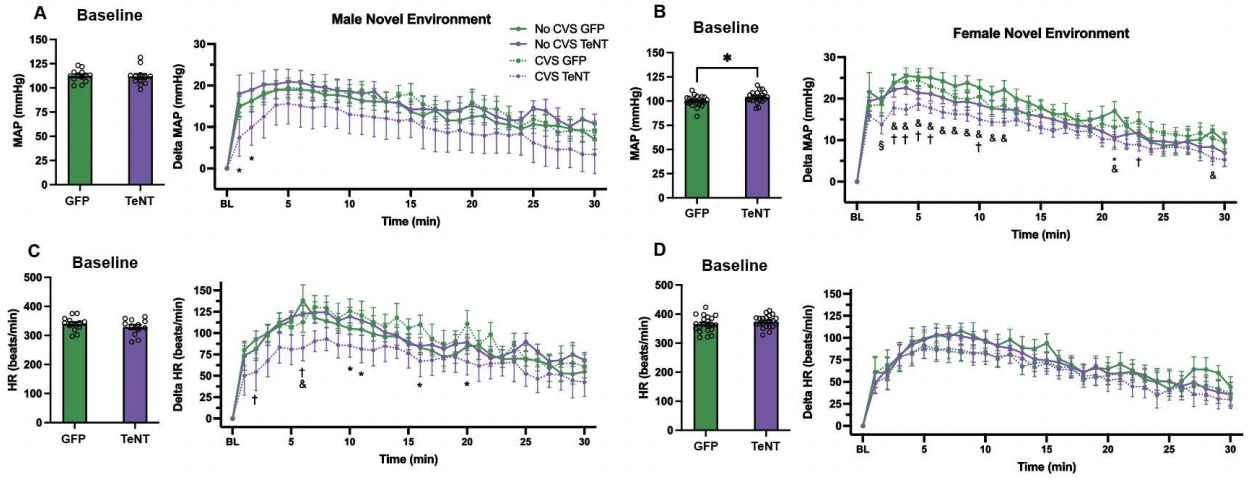

Figure 5.2. Effects of chronic variable stress and vmPFC-PH circuit inhibition on hemodynamic reactivity to novel environment stress. In males, CVS and TeNT interaction decreased MAP compared to non-stressed controls. * CVS TeNT vs. No CVS GFP (A). TeNT and CVS-TeNT interaction decreased MAP reactivity in females. Baseline * p < 0.5 GFP vs. TeNT, * No CVS TeNT vs. No CVS GFP, † CVS TeNT vs. CVS GFP, & CVS TeNT vs. No CVS GFP, § CVS

TeNT vs. No CVS TeNT (B). CVS and TeNT interact to decrease male HR reactivity. * CVS TeNT vs. CVS GFP, † CVS TeNT vs. No CVS GFP, & CVS TeNT vs. No CVS TeNT (C). Multiple comparisons showed no groups differences female HR reactivity to acute novel environment stress (D). MAP: mean arterial pressure, HR: heart rate. CVS: chronic variable stress, GFP: green fluorescent protein, TeNT: tetanus toxin. All statistical markers indicate $p < 0.5$.

Acute Restraint Endocrine Reactivity

Blood glucose and corticosterone (CORT) were measured to examine acute stress responses following CVS. During restraint, male glucose reactivity in the No CVS TeNT group was decreased from the No CVS GFP at the 15 (15 $p = 0.0243$) and 30-minute (30 $p = 0.0012$) time points (Fig. 3A mixed-effects (n = 8-9/group): Time $F(4,109) = 19.20$, $p < 0.0001$, TeNT $F(1,29) = 7.450$, $p < 0.0107$). The CVS TeNT group also decreased from the No CVS GFP group at the 0 (0 $p = 0.0460$) and 15-minute (15 $p= 0.0027$) time points. Additionally, the CVS GFP group was elevated from the No CVS TeNT group at 30 minutes (30 $p = 0.0212$). There were no TeNT or stress effects on female blood glucose at any timepoint throughout restraint (Fig. 3B mixed-effects (n = 10-11/group): Time $F(4,145) = 2.56$, $p = 0.0410$). In males, the No CVS TeNT CORT response was decreased from the No CVS GFP group at the 30-minute time point (Fig. 3 C mixed effects (n = 7-9/group): $F(4,103) = 40.58$, $p < 0.0001$, 30 $p = 0.0196$). The CVS GFP ($p = 0.0061$) and CVS TeNT ($p = 0.0021$) groups also both decreased from the No CVS GFP group at the 60-minute time point. Female CORT responses were decreased in the CVS GFP from the No CVS GFP group ($p = 0.0414$) and No CVS TeNT ($p= 0.0036$) at the 30-minute time point (Fig. 3D Time $F(4,103) = 37.49$, $p < 0.0001$, CVS $F(1,34) = 6.504$, $p = 0.0154$). Likewise, the CVS TeNT group was decreased from No CVS GFP at 30 (30 $p = 0.0282$) and 60 minutes (60 $p = 0.0016$) and No CVS TeNT at the 30-minute ($p = 0.0026$) timepoint. Lastly, the No CVS TeNT was decreased from No CVS GFP at 60 minutes ($p = 0.0140$). In males, these data show that inhibited vmPFC-PH circuit interacted with CVS and decreased sympathetic and HPA axis-mediated responses to acute restraint stress. In females, CVS TeNT decreased only HPA axis-mediated responses.

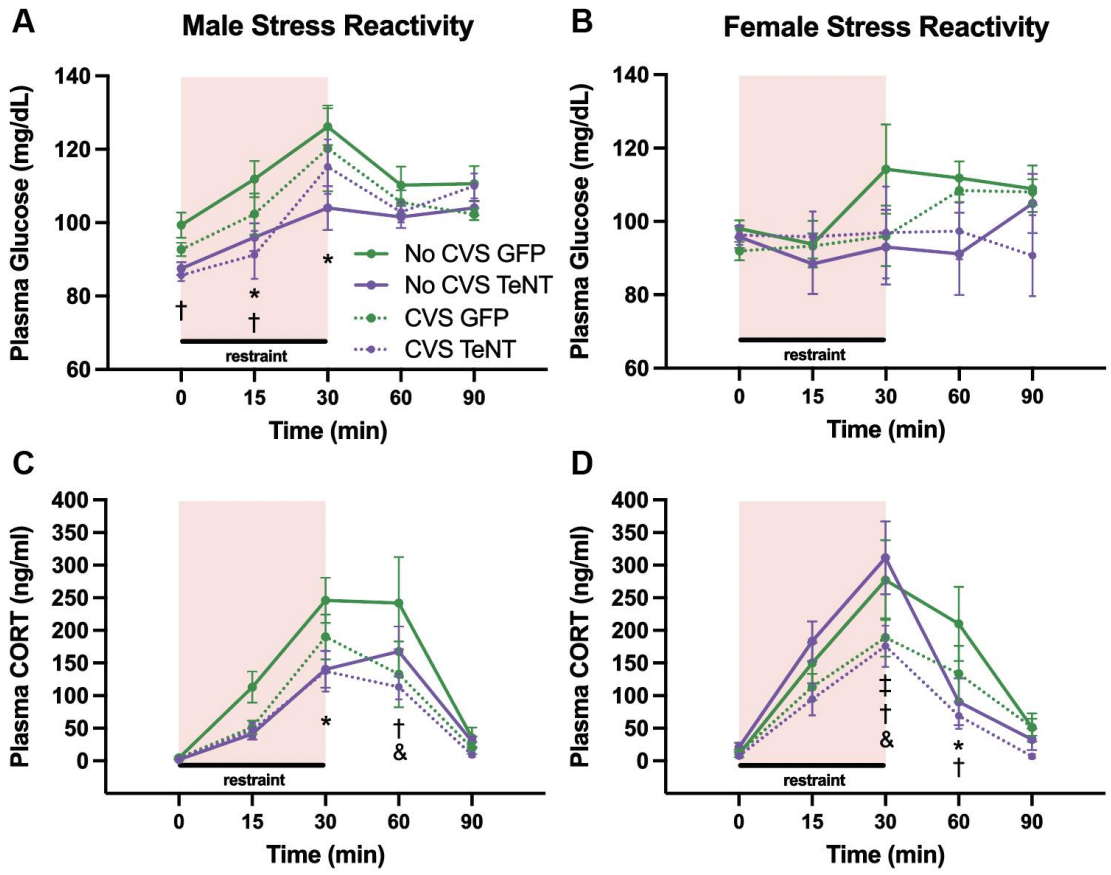

Figure 5.3. Effects of chronic variable stress and vmPFC-PH circuit inhibition on sympathetic and neuroendocrine reactivity to acute restraint stress. TeNT decreased male glucose reactivity to acute restraint. * No CVS TeNT vs. No CVS GFP, † CVS TeNT vs. No CVS GFP (A). Females showed no group difference in plasma glucose (B). Stress, TeNT, and Stress-TeNT interaction decrease plasma CORT in males during restraint. * No CVS TeNT vs. No CVS GFP, † CVS GFP vs. No CVS GFP, & CVS TeNT vs. No CVS GFP (C). Stress and TeNT alone decreased CORT responses in both the GFP and TeNT treated females. * No CVS TeNT vs. No CVS GFP, † CVS GFP vs. No CVS GFP, & CVS TeNT vs. No CVS TeNT, ‡ CVS GFP vs. No CVS GFP (D). CORT: corticosterone, CVS: chronic variable stress, GFP: green fluorescent protein, TeNT: tetanus toxin. All statistical markers indicate $p < 0.5$.

Discussion

Previously we discovered that the vmPFC-PH circuit in males is sufficient to decrease blood glucose and necessary for appropriate glucose and corticosterone responding during acute restraint stress. In females, stimulation of vmPFC neuron terminals in the PH was sufficient to elevate corticosterone following acute restraint and heart rate during anesthesia. Interestingly, the vmPFC-PH circuit was not necessary for mediating corticosterone or glucose reactivity in females or hemodynamic activity in anesthetized males. While these data provided

insight into the function of the vmPFC-PH circuit during acute stress, previous literature has suggested that the PH is a key region for regulating habituation to repeated stress (Nyhuis et al., 2016). To address this, we performed a study to determine whether the vmPFC-PH circuit is necessary for autonomic, neuroendocrine, and cardiovascular control following chronic variable stress exposure.

Following CVS, two separate acute stress assays tested whether chronic stress and vmPFC-PH circuit inhibition altered the ability of male and female rats to mount neuroendocrine, autonomic, and cardiovascular stress responses. During acute novel stress, TeNT circuit inhibition interacted with CVS to decrease MAP reactivity in both sexes. Also, males in the CVS TeNT group had decreased heart rate reactivity. During restraint, both TeNT and CVS interacting with TeNT decreased blood glucose and plasma corticosterone in males. In females, CVS alone and CVS plus TeNT reduced corticosterone reactivity and there were no effects on blood glucose. This suggests that female corticosterone reactivity following stress may be mediate through another circuit. Together these data suggest that the vmPFC-PH circuit is necessary for stress reactivity following long-term stress exposure. This coincides with data that showed disruption of normal male PH activity with a $GABA_A$ agonist inhibited the ability to habituate corticosterone responses to repeated stress (Nyhuis et al., 2016) and the PH serves as an important stress-regulatory region (Myers et al., 2016).

We demonstrated that the vmPFC-PH circuit may be stress inhibitory in males and stress excitatory in females, but here when challenged with chronic stress, circuit knockdown, and food restriction, the circuit decreases cardiovascular and endocrine reactivity in both sexes. While an explanation for why this occurs is unknown, there could be a few reasons. In chapter 4 and in (Myers et al., 2017), it has been demonstrated that vmPFC project to both GABA and non-GABA cells in the PH. Because the activity of GABA cells in the PH is shown to be important for controlling PH excitatory output (DiMicco et al., 1986), the vmPFC projections are likely very important for delivering contextual information and influencing activity in the PH.

Here, stress and loss of vmPFC inputs could combine to change local activity within the PH. This is important because the PH is known to project to preganglionic and neurosecretory cells so it is logical that disrupting PH signaling could decrease stress responses(Nyhuis et al., 2016). It is of note that some autonomic-mediated stress responses such as glucose and heart rate in females were not affected in this experiment. As mentioned in the previous chapter, this could be a result of sex hormones or sex differences in cell types innervated in the vmPFC-PH circuit. In the future, a detailed look of vmPFC innervation of the PH and how stress effects the transcriptional regulation of PH glutamate and GABA receptors in each sex would provide us valuable information on how this circuit may be sexually divergent.

Considerations

First, technical limitations of the intersectional genetic approach have been explained in detail in the discussion of chapter 4. The technique is circuit specific, and we demonstrated that PH-projecting vmPFC neurons have decreased synaptobrevin protein, but the extent of the neurotransmitter release inhibition is unknown.

A second consideration is the male glucose responses to acute restraint in figure 3. Here we showed TeNT decreased glucose reactivity compared to the No CVS GFP group which is contradictory to the data in figure 6 of chapter 4 where TeNT increased glucose reactivity compared to GFP controls (those rats did not experience CVS). TeNT and CVS interacted to decrease blood glucose at the 0-minute time point which could have contributed to a lower blood glucose throughout the restraint. While there is no clear explanation, this may be a result of the food restriction. This would imply that the vmPFC-PH circuit in males may play an important role in meeting metabolic demand depending on environmental context.

One other consideration that needs to be addressed is the heart rate variability (HRV) analysis. Because chronic stress and circuit inhibition appeared to inhibit male glucose responses, investigating changes autonomic balance over the course of CVS may help us understand current results. HRV is a reliable indicator of overall cardiovascular health and well-

being. Other groups have explained how mood, which is affected by vmPFC activity, can lead to a shift in heart rate variability and poor cardiovascular outcomes and have outlined methods for performing the analysis. However, many studies using HRV collect data from relatively short periods and not over the course of weeks. While our data lines up with our own and others' work, we needed to consider different approaches for visualizing the data before publication. Furthermore, upcoming estrous stage, echocardiography, aortic pulse wave velocity, resting hemodynamic activity, body temperature, and activity data may all provide more valuable information on the importance of a functioning vmPFC-PH circuit during chronic stress exposure in each sex.

Altogether, data shown here indicates that the vmPFC-PH circuit is important for coordinating acute stress reactivity after chronic stress exposure. This experiment provides a neural mechanism by how dysfunction of a brain region capable of controlling mood and stress reactivity can contribute to stress-induced cardiovascular susceptibility.

References

DiMicco, J. A., & Abshire, V. M. (1987). Evidence for GABAergic inhibition of a hypothalamic sympathoexcitatory mechanism in anesthetized rats. *Brain Research*, *402*(1), 1–10. https://doi.org/10.1016/0006-8993(87)91041-9

DiMicco, J. A., Abshire, V. M., Hankins, K. D., Sample, R. H. B., & Wible, J. H. (1986). Microinjection of GABA antagonists into posterior hypothalamus elevates heart rate in anesthetizes rats. *Neuropharmacology*, *25*(9), 1063–1066. https://doi.org/10.1016/0028-3908(86)90203-0

Flak, J. N., Jankord, R., Solomon, M. B., Krause, E. G., & Herman, J. P. (2011). Opposing effects of chronic stress and weight restriction on cardiovascular, neuroendocrine and metabolic function. *Physiology and Behavior*, *104*(2), 228–234. https://doi.org/10.1016/j.physbeh.2011.03.002

Fogaça, M. V., & Duman, R. S. (2019). Cortical GABAergic dysfunction in stress and depression: New insights for therapeutic interventions. *Frontiers in Cellular Neuroscience*, *13*. https://doi.org/10.3389/fncel.2019.00087

Link, E., Edelmann, L., Chou, J. H., Binz, T., Yamasaki, S., Eisel, U., Baumert, M., Südhof, T. C., Niemann, H., & Jahn, R. (1992). Tetanus toxin action: Inhibition of neurotransmitter release linked to synaptobrevin proteolysis. *Biochemical and Biophysical Research Communications*, *189*(2), 1017–1023. https://doi.org/10.1016/0006-291X(92)92305-H

McKlveen, J. M., Moloney, R. D., Scheimann, J. R., Myers, B., & Herman, J. P. (2019). "Braking" the Prefrontal Cortex: The Role of Glucocorticoids and Interneurons in Stress Adaptation and Pathology. *Biological Psychiatry*, *86*(9), 669–681. https://doi.org/10.1016/J.BIOPSYCH.2019.04.032

McMahon, H. T., Ushkaryov, Y. A., Edelmann, L., Link, E., Binz, T., Niemann, H., Jahn, R., & Südhof, T. C. (1993). Cellubrevin is a ubiquitous tetanus-toxin substrate homologous to a putative synaptic vesicle fusion protein. *Nature*, *364*(6435), 346–349.

https://doi.org/10.1038/364346a0

Myers, B., Carvalho-Netto, E., Wick-Carlson, D., Wu, C., Naser, S., Solomon, M. B., Ulrich-Lai, Y. M., & Herman, J. P. (2016). GABAergic signaling within a limbic-hypothalamic circuit integrates social and anxiety-like behavior with stress reactivity. *Neuropsychopharmacology*, *41*(6), 1530–1539. https://doi.org/10.1038/npp.2015.311

Myers, B., McKlveen, J. M., Morano, R., Ulrich-Lai, Y. M., Solomon, M. B., Wilson, S. P., & Herman, J. P. (2017). Vesicular Glutamate Transporter 1 Knockdown in Infralimbic Prefrontal Cortex Augments Neuroendocrine Responses to Chronic Stress in Male Rats. *Endocrinology*, *158*(10), 3579–3591. https://doi.org/10.1210/en.2017-00426

Nyhuis, T. J., Masini, C. V., Day, H. E. W., & Campeau, S. (2016). Evidence for the integration of stress-related signals by the rostral posterior hypothalamic nucleus in the regulation of acute and repeated stress-evoked hypothalamo-pituitary-adrenal response in rat. *Journal of Neuroscience*, *36*(3), 773–784. https://doi.org/10.1523/JNEUROSCI.3413-15.2016

Sando, R., Bushong, E., Zhu, Y., Huang, M., Considine, C., Phan, S., Ju, S., Uytiepo, M., Ellisman, M., & Maximov, A. (2017). Assembly of excitatory synapses in the absence of glutamatergic neurotransmission. *Neuron*, *94*(2), 312. https://doi.org/10.1016/J.NEURON.2017.03.047

Swanson, L. W. (2004). *Brain Maps: Structure of the Rat Brain* (Third Ed.). Academic Press.

Ulrich-Lai, Y. M., Jones, K. R., Ziegler, D. R., Cullinan, W. E., & Herman, J. P. (2011). Forebrain origins of glutamatergic innervation to the rat paraventricular nucleus of the hypothalamus: Differential inputs to the anterior versus posterior subregions. *The Journal of Comparative Neurology*, *519*(7), 1301–1319. https://doi.org/10.1002/cne.22571

Wallace, T., Schaeuble, D., Pace, S. A., Schackmuth, M. K., Hentges, S. T., Chicco, A. J., & Myers, B. (2021). Sexually divergent cortical control of affective-autonomic integration. *Psychoneuroendocrinology*, *129*, 105238. https://doi.org/10.1016/j.psyneuen.2021.105238

Wood, M., Adil, O., Wallace, T., Fourman, S., Wilson, S. P., Herman, J. P., & Myers, B. (2019).

Infralimbic prefrontal cortex structural and functional connectivity with the limbic forebrain: a combined viral genetic and optogenetic analysis. *Brain Structure & Function*, *224*(1), 73–97. https://doi.org/10.1007/s00429-018-1762-6

Xu, W., & Südhof, T. C. (2013). A Neural Circuit for Memory Specificity and Generalization. *Science (New York, N.Y.)*, *339*(6125), 1290. https://doi.org/10.1126/SCIENCE.1229534

CHAPTER 6: CONCLUSION

Over the last few decades, clinical studies have provided an abundance of evidence that activity of a variety of cortical and subcortical brain regions can alter cardiovascular activity. Specifically, there has been a strong correlation between mood and cardiovascular health but no neurological mechanism linking the affective state to cardiovascular activity. Until recently, the complexity of the brain and limited knowledge of neurocircuitry has limited our ability to understand how these brain regions may be responsible for physiological activity such as controlling the cardiac output. Interestingly, brain regions affected by treatment-resistant depression in humans also demonstrate the ability to impact resting cardiovascular activity and engage in stress responses. Stress responding is an evolutionarily conserved mechanism that helps an organism to avoid threats and maintain homeostasis, or an equilibrium of physiological activity that is appropriate for the environmental context.

Depending on the context, the brain engages the autonomic nervous system (ANS) and/or hypothalamic-pituitary-adrenal (HPA) axis to adapt to the environmental challenge. Organisms, such as rodents, are challenged with stressors such as looming predators, injuries, and a low food supply. To survive, the brain must process sensory information from the environment or within the animal and control select physiological processes to adapt to the challenge. Continuing with the rodent example, spotting a predator would engage the autonomic nervous system activating the sympathetic branch or ‘fight or flight’ response and restraining the parasympathetic branch or ‘rest and digest’ response. As a result, the rodent subconsciously elevates the activity of vital organs such as the heart to pump blood and stimulate glucogenic pathways in the liver to elevate blood glucose to provide energy to avoid the threat. Additionally, anticipatory activation of the HPA axis secretes glucocorticoids to increase heart contractility and glucose production in the liver. The ANS and HPA axes require a fine-tuned neuronal activity level to accurately produce stress responses for survival. A tightly regulated stress response is important because elevated sympathetic nervous system (SNS) and HPA axis

activity can harm an organism's long-term health and chances of survival. Chronic stress negatively impacts mood, so daily life stress makes humans susceptible to chronic stress-induced depressive illness. Depression frequently associates with autonomic imbalance characterized by vagal withdrawal and elevated SNS activity which initiates tachycardia and elevates blood pressure predisposing individuals to disease risk. Understanding how chronic stress impacts the brain may provide a connection between mood and cardiovascular health.

It is important to note that women are twice as susceptible to mood disorders and their risk for cardiovascular disease heightens after menopause indicating sex hormones may play a role in stress-induced illness (Goldstein et al., 2018; Newson, 2018). Until now, little is known about sex differences in physiological stress responses, but this dissertation provides the framework for how a specific stress-responsive cortical region is necessary for controlling context-appropriate stress responses in each sex. Recently, it has proven difficult to study the necessity of brain regions to perform certain tasks such as stress responding. Regions such as the vmPFC and PH are comprised of a variety of neuron phenotypes, so while pharmacology can indicate when a brain region may be active or what tasks the activity of the region may perform these methods lack specificity. This dissertation utilizes an array of cell-specific approaches to assess whether vmPFC projection neurons are sufficient and/or necessary to control stress responses and cardiovascular activity in both sexes.

Collectively, chapters 2 and 3 established that male vmPFC glutamate neuron activity is necessary and sufficient to prevent chronic stress-induced cardiovascular susceptibility. These chapters expanded on previous literature by (1) identifying that vmPFC pyramidal glutamate neurons coordinate stress responses and (2) identifying that activity of these vmPFC glutamate neurons has sexually divergent effects on autonomic and neuroendocrine stress reactivity. Previous work in the field demonstrated a strong association between stress and cardiovascular disease even going as far to identify hormones involved (Costoli et al., 2004; Oakley et al., 2019; S. K. Wood et al., 2012), but there was never a neural mechanism established to explain

how corticolimbic brain regions influence cardiovascular activity. Also, broad pharmacological evidence shows that inhibiting and stimulating the vmPFC attenuates decreases heart rate and blood pressure responses to stress, respectively. Here, we demonstrated a coordinated stress response initiated by the vmPFC pyramidal glutamate neurons. These axons send long projections to corticolimbic, subcortical, and even brainstem regions providing a route through how the vmPFC initiates physiological stress responses.

In males, a knockdown of glutamate release from these vmPFC glutamate neurons not only elevated HPA axis activity to acute stress but worsened stress-induced cardiovascular remodeling. The results in this study coincide with previous literature and the idea the vmPFC is an important structure for appraising the environment and maintaining homeostasis. vmPFC glutamate release is necessary for the coordination of the HPA axis in males (Myers et al., 2017), and dysregulated HPA axis during chronic stress predisposes an organism to cardiovascular disease. Interestingly, a follow-up study in males demonstrated that stimulating vmPFC glutamate neurons was sufficient to decrease sympathetic and HPA axis-mediated stress responses and prevent stress-induced left ventricular hypertrophy by decreasing the net sympathetic drive to the heart. Moreover, we discovered that vmPFC female glutamate neuron stimulation increased sympathetic and heart rate reactivity to acute stress. Contractility of the left ventricle of the heart also increased after CVS. Not only was it surprising to find that stimulating these neurons produced sexually divergent results, but chronic stress had an insignificant effect on the adult female net sympathetic drive to the heart or any negative cardiovascular impact. Currently, a mechanism for sexually divergent outcomes is still unknown. We know little about how sex hormones play a role in influencing vmPFC output, but evidence shows estrogen receptors alpha and beta as well as g protein-coupled estrogen receptors are present in both sexes of rats (Almey et al., 2014) and estradiol may increase the activity of the female vmPFC and enhance HPA axis activity in males. Androgen receptors are present in the vmPFC of both sexes with expression being higher in males (DonCarlos et al., 2006).

Conversely, androgens in the male vmPFC are known to decrease CORT responses to a novel environment (Handa et al., 1997). So, it is important to not rule out sex hormones and more studies are necessary to properly understand sex hormone influence over neuroendocrine and autonomic stress reactivity.

Chapters 4 and 5 examined a circuit through which vmPFC pyramidal glutamate neurons alter ANS and HPA axis activity. These chapters progressed the literature by (1) identifying functions of the vmPFC-to-PH circuit and (2) identifying how the vmPFC-PH circuit may coordinate acute and chronic physiological stress responses in both sexes. The PH is known to facilitate HPA axis and sympathetic cardiovascular responses presumably through projections to the paraventricular nucleus of the hypothalamus and raphe pallidus, respectively (Nyhuis et al., 2016). These findings are important because the vmPFC does not densely innervate the neuroendocrine and pre-autonomic regulatory regions, so we speculate that intermediate synapses are important for translating descending corticolimbic information into physiological responses. Recently it was found that the vmPFC sends dense projections to the PH (M. Wood et al., 2019), and the vmPFC neurons synapse non-exclusively on GABAergic neurons (Myers et al., 2016)(also shown in chapter 4). Studies demonstrate that GABAergic disinhibition within the PH elevates cardiovascular output (DiMicco et al., 1986; DiMicco & Abshire, 1987), increases circulating glucocorticoids , and enhanced anxiety-like behavioral responses to acute stress (Myers et al., 2016). Therefore, vmPFC projections to GABAergic PH neurons may provide a route through how vmPFC glutamate output in male rodents decreases physiological stress reactivity.

When examining the functionality of the vmPFC-PH circuit we observed sexually divergent reactivity to acute stress. During acute restraint, the circuit is sufficient to decrease blood glucose reactivity in males yet necessary for preventing exaggerated glucose reactivity. Additionally, the circuit was necessary for CORT reactivity following acute restraint. In females, the circuit is sufficient to increase restraint-induced CORT and anesthetized heart rate, but the

circuit does not appear to be necessary for acute stress reactivity. In comparison to the other dissertation chapters, the sexually divergent outcomes are not surprising, but the lack of blood pressure and heart rate effects with stimulation of the circuit were unanticipated. Other publications have also observed that pharmacologically altering PH activity during a resting state (i.e. no stress and in a home cage) does not alter heart rate or blood pressure (Lisa et al., 1989) which suggests altered input to the PH is needed to observe hemodynamic changes. Thus, implementing radiotelemetry in chapter 5 serves a useful tool to examine how the vmPFC-PH circuit influences cardiovascular output in real-time during a stressful event.

In chapter 5, we addressed whether the vmPFC-PH circuit is necessary for maintaining hemodynamic activity during chronic stress and whether subsequent acute stress responding is affected. While these data are preliminary, there are some clear takeaways. vmPFC-PH circuit inhibition and chronic stress interact to decrease blood pressure reactivity to acute novel environment exposure in both sexes. This finding is particularly interesting because blood pressure reactivity were not sexually divergent, yet the circuit only demonstrated a decrease in heart rate in males. Following CVS, vmPFC-PH circuit inhibition and CVS decreased sympathetic and HPA axis-mediated responses to acute stress. In the same experiment, vmPFC-PH circuit inhibition and CVS decreased HPA axis-mediated responses in females. This coincides with data that showed disruption of normal PH activity with a $GABA_A$ agonist inhibited the ability to habituate CORT responses to repeated stress (Nyhuis et al., 2016) and the PH serves as an important stress-regulatory region (Myers et al., 2016). Together, vmPFC-PH circuit inhibition impairs acute stress reactivity following chronic stress. These stress reactivity data are interesting because they are different from chapter 4 when the animals only experienced novel acute restraint stress. This suggests CVS impacted how the circuit functions and future experiments will investigate how post-synaptic targets of the vmPFC in the PH change following CVS. The impact of CVS on an organisms' ability to mount stress responses is

open to interpretation, but evidence suggests that the vmPFC-PH circuit is needed to engage proper physiological systems to meet environmental challenges.

It is important to mention that multiple molecules, brain regions, and circuits may be simultaneously involved in initiating physiological responses to environmental stimuli. Thus, vmPFC-PH stimulation or inhibition effects observed in these series of experiments are undoubtedly not a result of vmPFC and PH activity alone. While the PH sends glutamate projections to autonomic effector regions such as the intermediolateral cell column in the spinal cord, the vmPFC also projects to the nucleus of the solitary tract which projects to two known parasympathetic regions; the dorsal motor nucleus of the vagus and nucleus ambiguus (Vertes, 2004). Trans-synaptic retrograde tracers injected in the sympathetic ganglia targeting the heart and the adrenal gland show that the amygdala, hippocampus, and vmPFC are all positioned to influence stress reactivity (Westerhaus & Loewy, 2001). Not only can the amygdala influence sympathetic activity through this pathway, but the medial amygdala is also known to influence HR reactivity and sends GABAergic projections to the PH (Fortaleza et al., 2009; Myers et al., 2016). Plus, the insula and bed nucleus of the stria terminalis are other regions capable of exciting and inhibiting autonomic activity following stress, respectively (Myers, 2016). While the vmPFC-PH circuit is shown to be necessary for stress reactivity, collectively, many other corticolimbic regions may also contribute to cardiovascular susceptibility.

In conclusion, proper vmPFC activity is an important node for stress reactivity and glutamatergic projections to the PH circuit have proven to be a novel corticolimbic to hypothalamic pathway to regulate stress responding. Future directions lie in identifying the complete phenotype of PH neurons innervated by the vmPFC in both sexes and how chronic stress impacts each cell type. This may yield important information explaining sex-based differences in stress reactivity and disease susceptibility.

References

Almey, A., Cannell, E., Bertram, K., Filardo, E., Milner, T. A., & Brake, W. G. (2014). Medial Prefrontal Cortical Estradiol Rapidly Alters Memory System Bias in Female Rats: Ultrastructural Analysis Reveals Membrane-Associated Estrogen Receptors as Potential Mediators. *Endocrinology*, *155*(11), 4422–4432. https://doi.org/10.1210/EN.2014-1463

Costoli, T., Bartolomucci, A., Graiani, G., Stilli, D., Laviola, G., & Sgoifo, A. (2004). Effects of chronic psychosocial stress on cardiac autonomic responsiveness and myocardial structure in mice. *American Journal of Physiology - Heart and Circulatory Physiology*, *286*(6 55-6), 2133–2140. https://doi.org/10.1152/AJPHEART.00869.2003/ASSET/IMAGES/LARGE/ZH40060430740003.JPEG

DiMicco, J. A., & Abshire, V. M. (1987). Evidence for GABAergic inhibition of a hypothalamic sympathoexcitatory mechanism in anesthetized rats. *Brain Research*, *402*(1), 1–10. https://doi.org/10.1016/0006-8993(87)91041-9

DiMicco, J. A., Abshire, V. M., Hankins, K. D., Sample, R. H. B., Wible, J. H., JA, D., VM, A., KD, H., RH, S., & JH, W. (1986). Microinjection of GABA antagonists into posterior hypothalamus elevates heart rate in anesthetizes rats. *Neuropharmacology*, *25*(9), 1063–1066. https://doi.org/10.1016/0028-3908(86)90203-0

DonCarlos, L. L., Sarkey, S., Lorenz, B., Azcoitia, I., Garcia-Ovejero, D., Huppenbauer, C., & Garcia-Segura, L. M. (2006). Novel cellular phenotypes and subcellular sites for androgen action in the forebrain. *Neuroscience*, *138*(3), 801–807. https://doi.org/10.1016/J.NEUROSCIENCE.2005.06.020

Fortaleza, E. A. T., Tavares, R. F., & Corrêa, F. M. A. (2009). The medial amygdaloid nucleus modulates cardiovascular responses to acute restraint in rats. *Neuroscience*, *159*(2), 717–726. https://doi.org/10.1016/J.NEUROSCIENCE.2009.01.003

Gao, H. R., Zhuang, Q. X., Li, B., Li, H. Z., Chen, Z. P., Wang, J. J., & Zhu, J. N. (2016).

Corticotropin releasing factor excites neurons of posterior hypothalamic nucleus to produce tachycardia in rats. *Scientific Reports*, *6*. https://doi.org/10.1038/srep20206

Goldstein, J. M., Hale, T., Foster, S. L., Tobet, S. A., & Handa, R. J. (2018). Sex differences in major depression and comorbidity of cardiometabolic disorders: impact of prenatal stress and immune exposures. *Neuropsychopharmacology 2018 44:1*, *44*(1), 59–70. https://doi.org/10.1038/s41386-018-0146-1

Handa, R. J., Hejna, G. M., & Lorens, S. A. (1997). Androgen inhibits neurotransmitter turnover in the medial prefrontal cortex of the rat following exposure to a novel environment. *Brain Research*, *751*(1), 131–138. https://doi.org/10.1016/S0006-8993(96)01394-7

Lisa, M., Marmo, E., Wible, J. H., & DiMicco, J. A. (1989). Injection of muscimol into posterior hypothalamus blocks stress-induced tachycardia. In *American Journal of Physiology - Regulatory Integrative and Comparative Physiology* (Vol. 257, Issue 1). https://doi.org/10.1152/ajpregu.1989.257.1.r246

Myers, B. (2016). Corticolimbic regulation of cardiovascular responses to stress. *Physiology & Behavior*, *172*, 49–59. https://doi.org/10.1016/j.physbeh.2016.10.015

Myers, B., Carvalho-Netto, E., Wick-Carlson, D., Wu, C., Naser, S., Solomon, M. B., Ulrich-Lai, Y. M., & Herman, J. P. (2016). GABAergic Signaling within a Limbic-Hypothalamic Circuit Integrates Social and Anxiety-Like Behavior with Stress Reactivity. *Neuropsychopharmacology*, *41*(6), 1530–1539. https://doi.org/10.1038/npp.2015.311

Myers, B., McKlveen, J. M., Morano, R., Ulrich-Lai, Y. M., Solomon, M. B., Wilson, S. P., & Herman, J. P. (2017). Vesicular Glutamate Transporter 1 Knockdown in Infralimbic Prefrontal Cortex Augments Neuroendocrine Responses to Chronic Stress in Male Rats. *Endocrinology*, *158*(10), 3579–3591. https://doi.org/10.1210/en.2017-00426

Newson, L. (2018). Menopause and cardiovascular disease. *Post Reproductive Health*, *24*(1), 44–49. https://doi.org/10.1177/2053369117749675/ASSET/IMAGES/LARGE/10.1177_205336911

7749675-FIG1.JPEG

Nyhuis, T. J., Masini, C. V., Day, H. E. W., & Campeau, S. (2016). Evidence for the integration of stress-related signals by the rostral posterior hypothalamic nucleus in the regulation of acute and repeated stress-evoked hypothalamo-pituitary-adrenal response in rat. *Journal of Neuroscience*, *36*(3), 773–784. https://doi.org/10.1523/JNEUROSCI.3413-15.2016

Oakley, R. H., Cruz-Topete, D., He, B., Foley, J. F., Myers, P. H., Xu, X., Gomez-Sanchez, C. E., Chambon, P., Willis, M. S., & Cidlowski, J. A. (2019). Cardiomyocyte glucocorticoid and mineralocorticoid receptors directly and antagonistically regulate heart disease in mice. *Science Signaling*, *12*(577), eaau9685. https://doi.org/10.1126/scisignal.aau9685

Saper, C. B., Loewy, A. D., Swanson, L. W., & Cowan, W. M. (1976). Direct hypothalamo-autonomic connections. *Brain Research*, *117*(2), 305–312. https://doi.org/10.1016/0006-8993(76)90738-1

Vertes, R. P. (2004). Differential projections of the infralimbic and prelimbic cortex in the rat. *Synapse*, *51*(1), 32–58. https://doi.org/10.1002/syn.10279

Wallace, T., Schaeuble, D., Pace, S. A., Schackmuth, M. K., Hentges, S. T., Chicco, A. J., & Myers, B. (2021). Sexually divergent cortical control of affective-autonomic integration. *Psychoneuroendocrinology*, *129*, 105238. https://doi.org/10.1016/j.psyneuen.2021.105238

Westerhaus, M. J., & Loewy, A. D. (2001). Central representation of the sympathetic nervous system in the cerebral cortex. *Brain Research*, *903*(1–2), 117–127. https://doi.org/10.1016/S0006-8993(01)02453-2

Wood, M., Adil, O., Wallace, T., Fourman, S., Wilson, S. P., Herman, J. P., & Myers, B. (2019). Infralimbic prefrontal cortex structural and functional connectivity with the limbic forebrain: a combined viral genetic and optogenetic analysis. *Brain Structure & Function*, *224*(1), 73–97. https://doi.org/10.1007/s00429-018-1762-6

Wood, S. K., McFadden, K. V., Grigoriadis, D., Bhatnagar, S., & Valentino, R. J. (2012). Depressive and cardiovascular disease comorbidity in a rat model of social stress: a

putative role for corticotropin-releasing factor. *Psychopharmacology*, *222*(2), 325–336. https://doi.org/10.1007/s00213-012-2648-6